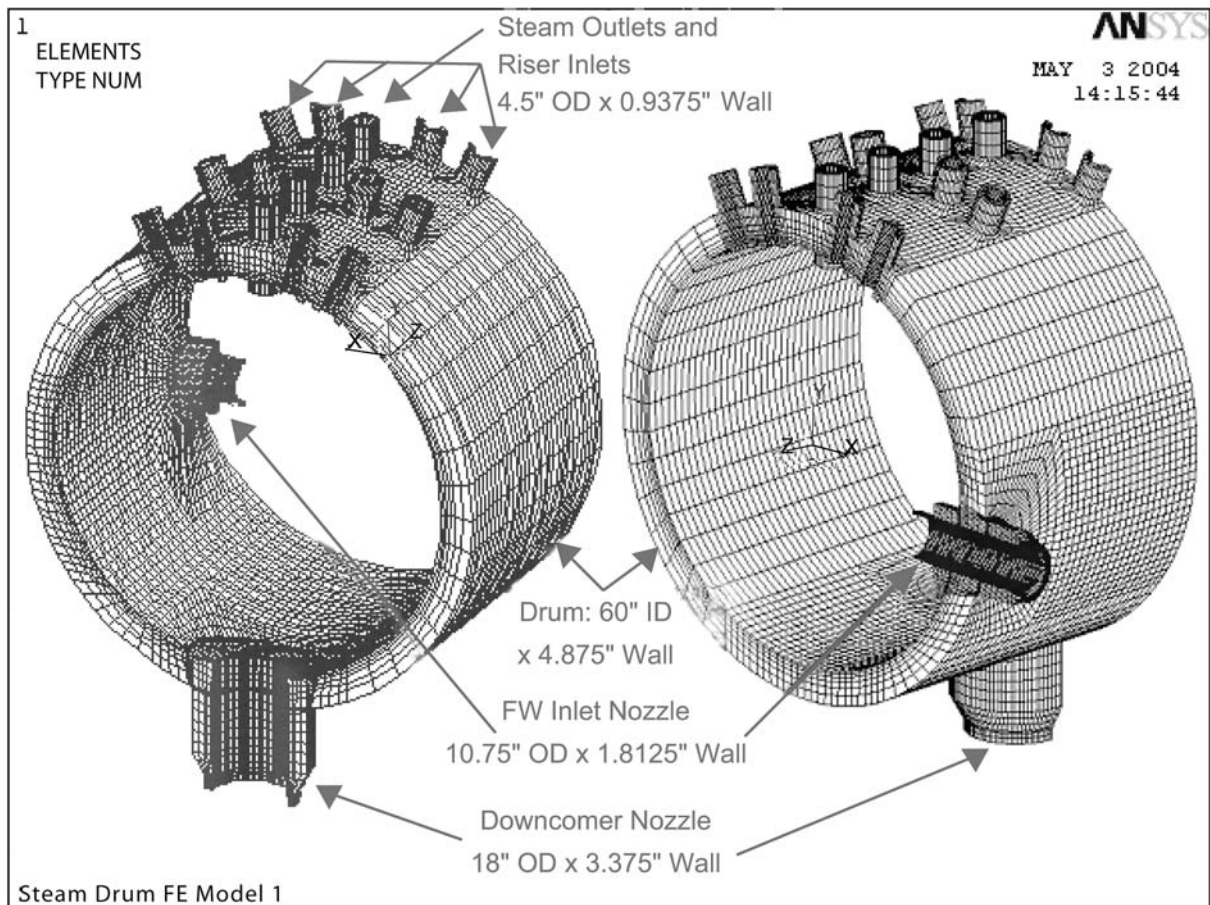


Investigation of Cracking in Fossil Boiler Drums—Finite-Element and Fracture Mechanics Analyses

Technical Report



Investigation of Cracking in Fossil Boiler Drums—Finite-Element and Fracture Mechanics Analyses

1011916

Final Report, October 2005

EPRI Project Manager
K. Coleman

DISCLAIMER OF WARRANTIES AND LIMITATION OF LIABILITIES

THIS DOCUMENT WAS PREPARED BY THE ORGANIZATION(S) NAMED BELOW AS AN ACCOUNT OF WORK SPONSORED OR COSPONSORED BY THE ELECTRIC POWER RESEARCH INSTITUTE, INC. (EPRI). NEITHER EPRI, ANY MEMBER OF EPRI, ANY COSPONSOR, THE ORGANIZATION(S) BELOW, NOR ANY PERSON ACTING ON BEHALF OF ANY OF THEM:

(A) MAKES ANY WARRANTY OR REPRESENTATION WHATSOEVER, EXPRESS OR IMPLIED, (I) WITH RESPECT TO THE USE OF ANY INFORMATION, APPARATUS, METHOD, PROCESS, OR SIMILAR ITEM DISCLOSED IN THIS DOCUMENT, INCLUDING MERCHANTABILITY AND FITNESS FOR A PARTICULAR PURPOSE, OR (II) THAT SUCH USE DOES NOT INFRINGE ON OR INTERFERE WITH PRIVATELY OWNED RIGHTS, INCLUDING ANY PARTY'S INTELLECTUAL PROPERTY, OR (III) THAT THIS DOCUMENT IS SUITABLE TO ANY PARTICULAR USER'S CIRCUMSTANCE; OR

(B) ASSUMES RESPONSIBILITY FOR ANY DAMAGES OR OTHER LIABILITY WHATSOEVER (INCLUDING ANY CONSEQUENTIAL DAMAGES, EVEN IF EPRI OR ANY EPRI REPRESENTATIVE HAS BEEN ADVISED OF THE POSSIBILITY OF SUCH DAMAGES) RESULTING FROM YOUR SELECTION OR USE OF THIS DOCUMENT OR ANY INFORMATION, APPARATUS, METHOD, PROCESS, OR SIMILAR ITEM DISCLOSED IN THIS DOCUMENT.

ORGANIZATION(S) THAT PREPARED THIS DOCUMENT

Structural Integrity Associates, Inc.

B. W. Roberts Engineering Consulting

NOTE

For further information about EPRI, call the EPRI Customer Assistance Center at 800.313.3774 or e-mail askepri@epri.com.

Electric Power Research Institute and EPRI are registered service marks of the Electric Power Research Institute, Inc.

Copyright © 2005 Electric Power Research Institute, Inc. All rights reserved.

CITATIONS

This report was prepared by

Structural Integrity Associates, Inc
3315 Almaden Expressway
Suite 24
San Jose, CA 95118-1557

Principal Authors

D. A. Rosario
R. L. Bax

B. W. Roberts Engineering Consulting
4715 Rocky River Road
Chattanooga, TN 37416

Principal Author

B. W. Roberts

This report describes research sponsored by the Electric Power Research Institute (EPRI).

The report is a corporate document that should be cited in the literature in the following manner:

Investigation of Cracking in Fossil Boiler Drums—Finite-Element Stress and Fracture Mechanics Analyses. EPRI, Palo Alto, CA: 2005. 1011916.

PRODUCT DESCRIPTION

The steam drum is the most expensive of all the boiler components and it is crucial to ensure the drum's integrity. Drums typically operate for the life of the plant with few problems; however, some pressure boundary cracking issues can develop after about 30 years of service. The major concern is that cracking becomes so extensive that it poses a threat to the structural integrity and continued safe operation of the unit. Due to the expense associated with major repairs or replacement, such a major cracking event might force the retirement of the unit.

The boiler drum appears to operate statically. Upon further examination, it is recognized that it receives fluid from two sources—the subcooled feedwater (FW) from the economizer and the saturated steam-water mixture from the waterwalls—and that it discharges fluid to two circuits—dry saturated steam to the superheater inlet header and subcooled water to the waterwall inlet headers. Thus, the drum operates dynamically, especially during periods of thermal transients.

Results and Findings

The project reported earlier in 2005 featured a simplified stress and fracture analysis performed in a global approach. It was recognized that more sophisticated methodology using finite element stress analysis and geometry-specific fracture mechanics analysis should be undertaken using data from operating units that were at least 30 years old. Two projects were initiated on different designed boilers including: a 275 MW Combustion Engineering (CE) controlled circulation; and a 215 MW Babcock & Wilcox (B&W) natural circulation. The results from the CE unit are the subject of this report.

The current project was limited to two types of transients: normal startup/shutdown, and thermal downshocks to the feedwater inlet. The nozzles identified as being most vulnerable to thermal fatigue damage were the feedwater inlet and downcomer nozzles.

The fatigue life for the downcomer nozzle was estimated as 6240 normal startup/shutdown cycles using an ASME design fatigue curve or 395 cycles when adjusted for corrosion fatigue using a pending curve developed by the ASME Subgroup on Fatigue Strength. Relative to normal startup/shutdown, bypassing a string of feedwater heaters reduced cyclic life by a factor of 3.6, and topping off the drum reduced life by a factor of 10.4.

Fracture mechanics analysis validated that the most significant threat to drum integrity is a 1.5X cold hydrostatic test when brittle fracture could occur for a through-wall crack as small as 2.5 in. (6.35 cm). During normal operation when the drum temperature is above 212°F (100°C) and as high as 648°F (342°C), large through-wall cracks greater than 30 in. (76.2 cm) can be tolerated before failure occurs (a leak-before-break scenario). Crack propagation data based on ASME Section XI under-predicts expected crack growth rates; a corrosion fatigue multiplier of 2 to 5 has been suggested as more consistent with experience based on other EPRI studies. Using a

multiplier of 5, a minimum of 1700 normal startup/shutdown cycles was estimated for through-wall propagation of a partial through-wall semi-elliptical crack.

The outcome of the current project was that the pressure stress and environmental influence of corrosion fatigue played the dominant role in drum cracking; thermal stress was secondary.

Challenges and Objectives

This report is mostly focused on boiler steam drums in utility boilers, but the information also applies to chemical recovery, heat recovery, waste heat, and industrial boilers operating at subcritical pressures, using a boiler drum. The report is valuable to those who operate, maintain, assess, and repair boilers.

Applications, Values, and Use

The preceding EPRI project focused on information which established that a case could be made for thermal fatigue as a mechanism for cracking of drum nozzles. This project emphasizes finite element stress analysis and fracture mechanics analysis for an operating unit. The outcome was that the pressure stress and environmental influence of corrosion fatigue was dominant in drum cracking and thermal stress was secondary. This work plus the prior work by EPRI forms the foundation for decision making for utilities that encounter cracking in boiler drum nozzles.

EPRI Perspective

The Materials and Repair Program (M&R) seeks to identify power plant components that pose both short- and long-term threats to the viability of power plants and to provide strategies to deal with those threats. The boiler drum has been a reliable component in the short term with few cracking problems in the first 30 years of operation. With the continued aging of the U.S. fossil fleet and relegation of older units to greater cyclic duty, drum cracking is emerging as a greater threat. This and earlier reports represent several years of systematic EPRI research that will continue through 2006 and perhaps beyond, based on future priorities.

Approach

This research uses analytical tools in finite element stress and fracture mechanics analysis to identify the life-limiting structural components in an operating steam drum and to estimate end-of-life scenarios using those tools. Fatigue life from various operational modes was quantified for both benign and steam-water environments in which the damage is greatly accelerated. Threats to drum integrity from brittle fracture during cold hydrostatic testing and steam leaks during operation were also quantified. The research will continue in 2005 with a second drum having been selected for detailed finite element and fracture mechanics analyses.

Keywords

Boilers
Drums
Fatigue
Corrosion fatigue
Cracking
Cycling

ABSTRACT

Anecdotal information, EPRI-sponsored research, and a survey performed by the EPRI Fossil Repair Applications Center (FRAC) in 2000 provided evidence that utilities have experienced some drum cracking problems, but the cracking is usually not severe. When cracking has been found, there has been no uniform utility practice for mitigation, and approaches have ranged from “do nothing,” to removal by grinding, or removal followed by weld repair. The characteristic time to initial cracking is about 30 years.

In the project preceding the current work and reported earlier in 2005, a simplified stress and fracture analysis was performed in a more global approach to the drum cracking problem. It was recognized in this earlier work that more sophisticated methodology using finite element stress analysis and geometry-specific fracture mechanics analysis should be undertaken using data from operating units that were at least 30 years old. Accordingly, two projects were initiated in pursuing that objective: (a) a 275 MW Combustion Engineering (CE) controlled circulation unit operating at 2000 psig (137.92 bars) turbine throttle pressure that began commercial operation in 1959; and (b) a 215 MW Babcock & Wilcox (B&W) natural circulation unit operating at 2000 psig (137.92 bars) that began commercial operation in 1954. The results from the work on the CE unit are the subject of this report. Results for the B&W unit will be reported in the first quarter of 2006.

The steam drum in the CE unit studied in this project had an inside diameter of 60 in. (1.52 m), a wall thickness of 4.875 in. (12.38 cm), a length of 58.3 ft (17.77 m), and a weight of 260,000 lbs (117,934 kg). At full load, the unit produced 1,960,000 lbs/hr (889,041 kg/hr) of steam. The circulation ratio (ratio of mass flow rate of downcomer to steam output) was about 4.5 to 5.0 at full load and 8.0 to 9.0 at half load. Feedwater entered the drum through four horizontal 10.75 in. (27.31 cm) outer diameter (OD) nozzles oriented just below the centerline. Five 18 in. (45.72 cm) OD downcomer nozzles were positioned directly in the bottom of the drum. The feedwater inlet nozzles and downcomers were attached with full penetration welds. The riser and steam outlet tubes were 4.5 in. OD x 0.938 in. mwt (11.43 cm OD x 2.38 cm mwt) and were attached using partial penetration welds on the OD and inner diameter (ID). These tubes penetrated the drum in five rows bounding a $\pm 24^\circ$ sector at the top of the drum. Of all the nozzles, the analysis showed the feedwater inlet and downcomer to be most critical, and these were the focus of the research. The drum was made entirely from carbon steel, and based on the vintage, it was likely made using coarse grain melting practices, which gives inferior fracture toughness.

While myriad thermal excursions affect the thermal stresses in steam drums, the current project was limited to two types of transients: namely, normal startup/shutdown and thermal downshocks to the feedwater inlet such as those associated with bypassing a string of high-pressure feedwater heaters or topping off a partially full drum shortly following a unit trip.

The two nozzles identified as being most vulnerable to thermal fatigue damage were the feedwater inlet nozzle and the downcomer nozzle, with the latter being more susceptible because of the absence of thermal sleeves as is mandated by the rules of ASME Section I for feedwater inlet nozzles. Thus, in all scenarios examined in this project, the downcomer-to-shell intersection on the ID was the most highly stressed nozzle location.

The fatigue life for the downcomer nozzle was estimated as 6240 normal startup/shutdown cycles using an ASME design fatigue curve or 395 cycles when adjusted for corrosion fatigue using a pending curve developed by the ASME Subgroup on Fatigue Strength. Relative to normal startup/shutdown, bypassing a string of feedwater heaters reduced cyclic life by a factor of 3.6, and topping off the drum reduced life by a factor of 10.4.

The fracture mechanics analysis validated that the most significant threat to drum integrity is a 1.5X cold hydrostatic test when brittle fracture could occur for a through-wall crack as small as 2.5 in. (6.35 cm). During normal operation when the drum temperature is above 212°F (100°C) and as high as 648°F (342°C), large through-wall cracks greater than 30 in. (76.20 cm) can be tolerated before failure occurs (a leak-before-break scenario). Crack propagation data based on ASME Section XI under-predict expected crack growth rates; a corrosion fatigue multiplier of 2 to 5 has been suggested as more consistent with experience based on other EPRI studies. Using a multiplier of 5, a minimum of 1700 normal startup/shutdown cycles was estimated for through-wall propagation of a partial through-wall semi-elliptical crack.

CONTENTS

- 1 INTRODUCTION AND BACKGROUND 1-1**
 - 1.1 Critical Component, Size, Pressures, Fabrication/Erection, Assessment, and Operation 1-1
 - 1.2 Functions of the Drum 1-1
 - 1.2.1 Primary Functions 1-1
 - 1.2.2 Secondary Functions 1-1
 - 1.3 Functional Attributes 1-2
 - 1.4 Drum Penetrations 1-2
 - 1.4.1 Penetrations and Nozzles of Peripheral Interest to This Research 1-2
 - 1.4.2 Penetrations and Nozzles That Are the Focus of This Research 1-3
 - 1.5 Mud Drums 1-3
 - 1.6 Background Leading to the Current Research 1-4
 - 1.7 References 1-5

- 2 DRUM GEOMETRY, OPERATIONAL PARAMETERS, AND MATERIALS 2-1**
 - 2.1 Drum Geometry 2-1
 - 2.2 Operational Parameters 2-6
 - 2.3 Materials 2-7
 - 2.3.1 Plates 2-7
 - 2.3.2 Forgings 2-8
 - 2.4 Mechanical Properties and Chemical Composition 2-9
 - 2.5 References 2-11

- 3 FINITE ELEMENT STRESS ANALYSIS 3-1**
 - 3.1 Finite Element Model 3-1
 - 3.2 Loading and Boundary Conditions 3-4
 - 3.2.1 Loading 3-4
 - 3.2.2 Boundary Conditions 3-5

| | | |
|----------|--|------------|
| 3.3 | Internal Pressure Analysis | 3-6 |
| 3.4 | Thermal Shock Analysis | 3-9 |
| 3.5 | Normal Startup, Steady-State, Shutdown Analysis..... | 3-13 |
| 3.5.1 | Boiler Circulation Study..... | 3-13 |
| 3.5.2 | Operating Data..... | 3-14 |
| 3.5.3 | Startup/Steady-State/Shutdown Stresses..... | 3-23 |
| 3.5.3.1 | Downcomer Nozzle ID | 3-23 |
| 3.5.3.2 | Inlet Nozzle ID..... | 3-23 |
| 3.5.3.3 | Inlet Nozzle OD..... | 3-23 |
| 3.6 | Discussion of Finite Element Stress Analysis | 3-28 |
| 3.7 | References | 3-29 |
| 4 | FATIGUE ANALYSIS | 4-1 |
| 4.1 | Fatigue Life Methodology | 4-1 |
| 4.1.1 | Design Fatigue Curve and Adjustment to Account for Environmental Effects 4-1 | |
| 4.1.2 | Mean Stress Correction | 4-4 |
| 4.2 | Fatigue Life Estimates Based on the FE Stress Analyses..... | 4-5 |
| 4.2.1 | Normal Startup, Steady-State, and Shutdown Fatigue Analysis..... | 4-6 |
| 4.2.2 | Bypassing a String of High-Pressure Feedwater Heaters at Full Load..... | 4-8 |
| 4.2.1 | Topping Off a Partially Full Drum Shortly Following Unit Trip | 4-10 |
| 4.3 | Discussion of Fatigue Analysis | 4-12 |
| 4.4 | References | 4-13 |
| 5 | FRACTURE MECHANICS ANALYSIS | 5-1 |
| 5.1 | Fracture Toughness..... | 5-1 |
| 5.2 | Crack Locations, Crack Models, and Stresses | 5-3 |
| 5.2.1 | Crack Locations | 5-3 |
| 5.2.2 | Crack Models | 5-4 |
| 5.2.2.1 | Part-Through-Wall Cracks | 5-4 |
| 5.2.2.2 | Through-Wall Cracks | 5-5 |
| 5.3 | LEFM Crack Tip Stress Intensity Factors and Critical Size | 5-6 |
| 5.3.1 | Discussion..... | 5-11 |
| 5.4 | Critical Crack Sizes using EPFM | 5-11 |
| 5.4.1 | Crack Model..... | 5-14 |

| | | |
|----------|---|------------|
| 5.5 | Crack Growth | 5-16 |
| 5.5.1 | Corrosion Fatigue Crack Growth Rate | 5-16 |
| 5.5.2 | Crack Growth Results | 5-17 |
| 5.6 | Discussion of Fracture Mechanics Analysis..... | 5-18 |
| 5.7 | References | 5-19 |
| 6 | SUMMARY, CONCLUSIONS, AND FUTURE PLANS | 6-1 |
| 6.1 | Summary and Conclusions | 6-1 |
| 6.1.1 | Finite Element Stress Analysis..... | 6-2 |
| 6.1.2 | Fatigue Analysis..... | 6-3 |
| 6.1.3 | Fracture Mechanics Analysis | 6-4 |
| 6.2 | Future Plans | 6-5 |
| 6.3 | References | 6-5 |

LIST OF FIGURES

| | |
|---|------|
| Figure 2-1 Cross Section of the Drum for the CE 2000 psig (137.93 bars) Unit..... | 2-2 |
| Figure 2-2 Elevation View of the Drum for the CE 2000 psig (137.93 bars) Unit Illustrating the Four Feedwater Nozzles and the Five Downcomers..... | 2-3 |
| Figure 2-3 Detail of Thermal Sleeve Design Utilized for the Feedwater Inlet Nozzle to Minimize Thermal Stresses Arising from Temperature Differentials Between Feedwater Inlet and Drum Saturation Temperatures..... | 2-4 |
| Figure 2-4 Typical Weld Detail for Partial Penetration ID and OD Welds Attaching the Steam Outlet Nozzles and Riser Nozzles to the CE Drum..... | 2-5 |
| Figure 3-1 Drum Elevation Showing Axial Slice Selected for Modeling..... | 3-2 |
| Figure 3-2 3D FE Model of the CE Drum..... | 3-3 |
| Figure 3-3 Close-Up of Inlet Nozzle and Thermal Sleeve Region of the FE Model..... | 3-4 |
| Figure 3-4 Boundary Conditions Imposed on Drum 3D FE Model..... | 3-6 |
| Figure 3-5 2165 psig (149.30 bars) Internal Pressure Loading..... | 3-7 |
| Figure 3-6 First Principal Stresses (psi) due to 2165 psig (149.30 bars) Internal Pressure..... | 3-8 |
| Figure 3-7 Stress Intensities (psi) due to 2165 psig (149.30 bars) Internal Pressure..... | 3-9 |
| Figure 3-8 Transient Stress Response to -100°F (-56°C) Cold Shock at the Drum Inlet..... | 3-11 |
| Figure 3-9 Transient Stress Response at 7 Seconds After the Initial 100°F (-56°C) Cold Shock..... | 3-12 |
| Figure 3-10 Steady-State Stress Response 1 Hour After Initial 100°F (-56°C) Cold Shock.... | 3-13 |
| Figure 3-11 Temperatures, Pressures, Flow Rates, and MW for a Typical Startup..... | 3-19 |
| Figure 3-12 Temperatures, Pressures, Flow Rates, and MW for a Typical Shutdown..... | 3-20 |
| Figure 3-13 Composed Startup/Steady-State/Shutdown Transient for Drum FE Stress Analysis..... | 3-21 |
| Figure 3-14 Maximum Stress at Downcomer Nozzle ID During Startup/Steady- State/Shutdown Transient..... | 3-24 |
| Figure 3-15 Maximum Stress at Inlet Nozzle ID and OD During Startup/Steady- State/Shutdown Transient..... | 3-25 |
| Figure 3-16 Downcomer Nozzle ID Stress Response Versus Time..... | 3-26 |
| Figure 3-17 Inlet Nozzle ID Stress Response Versus Time..... | 3-27 |
| Figure 3-18 Inlet Nozzle OD Stress Response Versus Time..... | 3-28 |
| Figure 4-1 Design Fatigue Curve from ASME Section VIII, Division 2 for Carbon and Low-Alloy Steels and Pending Curve Being Proposed by the Subgroup on Fatigue Strength to Account for Detrimental Effect of Corrosion Fatigue..... | 4-3 |

| | |
|--|------|
| Figure 4-2 Fatigue Life Ratio (Life Reduction Factor) to Account for Corrosion Fatigue (CF) Effects in the Low-Cycle Fatigue Range (<1,000,000 Cycles) | 4-4 |
| Figure 4-3 Fatigue Life Estimates for Normal Startup/Steady-State/Shutdown Cycles Shown on the Design Fatigue Curve and the Pending Corrosion Fatigue Curve | 4-7 |
| Figure 4-4 Fatigue Life Estimates for a -164°F (-91°C) Thermal Downshock from Bypassing the Feedwater Heaters at Full Load Shown on the Design Fatigue Curve and the Pending Corrosion Fatigue Curve | 4-10 |
| Figure 4-5 Fatigue Life Estimates for a -406°F (-226°C) Thermal Downshock from Topping Off a Partially Full Drum Shortly Following Unit Trip Shown on the Design Fatigue Curve and the Pending Corrosion Fatigue Curve | 4-12 |
| Figure 5-1 Inferred Fracture Toughness for Coarse Grain Steel by a +87°F (48°C) Shift in Temperature of the SA-516 Grade 70 Steel with Independent Data for SA-212 Grade B CG Steel | 5-2 |
| Figure 5-2 Crack Locations in Drum Identified for Fracture Mechanics Analysis..... | 5-3 |
| Figure 5-3 Part-Through-Wall Crack Models: (a) Quarter-Elliptical Nozzle Corner Crack, (b) Semi-Elliptical Crack at the ID of a Cylinder | 5-4 |
| Figure 5-4 Stress Gradients for Part-Through-Wall Crack Models | 5-5 |
| Figure 5-5 Through-Wall Axial Crack in a Pressurized Cylinder Model | 5-6 |
| Figure 5-6 Location 1 (Downcomer Axial Crack): K_I versus a Results for a Part-Through-Wall Crack..... | 5-7 |
| Figure 5-7 Location 2 (Downcomer Circ. Crack): K_I versus a Results for a Part-Through-Wall Crack..... | 5-8 |
| Figure 5-8 Location 3 (Inlet Nozzle Axial Crack): K_I versus a Results for a Part-Through-Wall Crack..... | 5-9 |
| Figure 5-9 K_I versus a Results for an Axial Through-Wall Crack in the Drum..... | 5-10 |
| Figure 5-10 Drum Saturation Temperature Versus Operating Pressure..... | 5-12 |
| Figure 5-11 Typical Crack Growth Behavior of Ductile Materials..... | 5-13 |
| Figure 5-12 Tearing Modulus Concept for Stable Crack Growth | 5-13 |
| Figure 5-13 Applied J-integral (J_{app}), Applied Tearing Modulus (T_{app}) and Material Tearing Resistance (T_{mat}) Versus Crack Size for a Through-Wall Axial Crack in a Pipe | 5-15 |
| Figure 5-14 Fatigue Crack Growth Data from ASME Section XI for Carbon and Low-Alloy Ferritic Steels | 5-17 |
| Figure 5-15 Fatigue Crack Growth Data from ASME Section XI for Carbon and Low-Alloy Ferritic Steels | 5-18 |

LIST OF TABLES

| | |
|---|------|
| Table 2-1 Requirements for Mechanical Properties and Chemical Composition for Plates and Nozzles Used in the CE Drum | 2-10 |
| Table 3-1 Data on Cold Shock due to Loss of Feedwater Heaters..... | 3-10 |
| Table 3-2 Data from 1991–1992 Boiler Circulation Study..... | 3-16 |
| Table 3-3 Operating Data Provided by TVA for Two 275 MW CE Drum Units | 3-18 |
| Table 4-1 Estimates of Fatigue Life for Normal Startup, Steady State, and Shutdown | 4-6 |
| Table 4-2 Estimates of Fatigue Life for Bypassing the Feedwater Heaters at Full Load | 4-9 |
| Table 4-3 Estimates of Fatigue Life for Topping Off a Partially Full Drum Shortly Following Unit Trip | 4-11 |
| Table 5-1 Summary of Fracture Toughness Estimates, K_{Ic} , for Coarse Grain Carbon Steels at Room Temperature | 5-1 |
| Table 5-2 Summary of Critical Crack Sizes (Inches) During Normal Operation for Upper-Shelf Fracture Toughness Values Ranging from 100–200 ksi•inch (109–220 MPa√m) | 5-10 |
| Table 5-3 Summary of Critical Crack Sizes (Inches) for a 1.5X Cold Hydro and Room Temperature Fracture Toughness Values Ranging from 45.8–100 ksi•inch (50–109 MPa√m) | 5-11 |
| Table 5-4 Different Categories for a Range of Carbon Steel Base Materials and Welds | 5-14 |

1

INTRODUCTION AND BACKGROUND

1.1 Critical Component, Size, Pressures, Fabrication/Erection, Assessment, and Operation

The steam drum is the most expensive of all the boiler components; thus, it is crucial to ensure the drum's integrity. Drums can be quite large with diameters of 3 to 6 ft (0.91 to 1.83 m), lengths approaching 100 ft (30.48 m), and weights of 400,000 lbs (181,437 kg) [1-1]. For utility use, drums are typically sized to achieve turbine throttle pressures from 1400 to 2800 psig (96.54 to 193.09 bars). Depending on plant design and design margins, drums are typically designed at pressures ranging from 200 to 425 psi (1.38 to 2.93 MPa) above turbine throttle pressure. They are fabricated from thick steel plates rolled into cylinders and capped on the ends with elliptical or hemispherical heads.

During construction, the drum is one of the first pressure parts erected, and because of size and location above the top of the boiler furnace, it is one of the most difficult components to replace. Therefore, long-term plant operation must include strategies to perform condition assessment on the drum and to make any necessary alterations or repairs while the drum is in place. These strategies must also consider plant operation in a manner that will minimize damage to the drum.

1.2 Functions of the Drum

The drum of a subcritical boiler serves two primary functions and several secondary functions.

1.2.1 Primary Functions

The primary functions of the drum are [1-2]:

- To separate the saturated mixture of water and steam discharging into it
- To house the equipment to purify steam after being separated from water before the steam enters the superheater

1.2.2 Secondary Functions

The secondary functions of the drum include the following [1-3]:

- To mix the subcooled feedwater (FW) with the saturated water remaining after separation
- To mix corrosion-control and water-treatment chemicals

- To remove part of the water by blowdown to lower the solids content of the boiler water or lower the water level
- To provide limited water storage to accommodate changes in boiler load

1.3 Functional Attributes

Proper functioning of the steam drum is critical to avoid:

- Carryover of water droplets into the superheater
- Carryunder of steam into the water leaving the drum via the downcomers
- Carryover of solids into the superheater and perhaps ultimately to the turbine [1-3]

Drum internals are used to separate the water from the steam and to distribute the flows of water and steam to establish an acceptable distribution of drum metal temperatures during operation [1-3]. Drum internals typically consist of:

- Baffles that change the direction of flow
- Separators to remove the water from the steam
- Steam purifiers such as washers and screen dryers
- Feedwater and chemical feed distribution headers

1.4 Drum Penetrations

1.4.1 Penetrations and Nozzles of Peripheral Interest to This Research

Many of the drum penetrations are small in size and match the temperature of the drum wall fairly closely during operation so as to produce minimal thermal stresses. These penetrations and associated nozzles have not been particularly important in terms of cracking and failure for the “controlled circulation” designs and are only of peripheral interest in the present research. These controlled circulation units use boiler circulation pumps as the primary means to achieve flow in the waterwalls. Such units typically have fewer riser tubes of smaller diameter and utilize a small number of large-diameter pipes for the downcomer pipes.

Since the focus of the research performed in 2004 and reported here is a drum in a controlled circulation unit, the penetrations and associated nozzles of secondary interest include the following:

- Those that bring the steam-water mixture from the waterwalls to the drums (these are called *risers*)
- Those that route the purified steam from the drum to the superheater
- Those that serve for the injection of chemicals associated with water treatment
- Those that serve to remove fluid during blowdown to either lower the water level in the drum or lower the solids in the boiler water

While detailed consideration was not given to the riser tube-ligament region in this project, it is increasingly evident that this is a vulnerable region in some designs. However, thermal stresses are largely inconsequential in the riser tube-ligament region, and the cracking apparently is not fundamentally due to thermal fatigue. It appears that natural circulation units are most susceptible to such borehole and ligament cracking because more tubes of larger diameter are required in units with these designs, creating far more penetrations in the drum wall. Additionally, rather than a few large-diameter downcomers, some designs utilize a large number of small-diameter penetrations for downcomers, again producing an array of boreholes and ligaments. Finally, instead of welded tubes, rolled riser tubes are more prevalent in natural circulation boilers operating at lower pressures, and this practice may play a role in borehole and ligament cracking. In 2005, a separate project will report on a finite-element-based stress and fracture mechanics analysis for a steam drum in a natural circulation boiler. Future research will be directed toward gaining a better understanding of borehole and ligament cracking for both riser and downcomer areas.

1.4.2 Penetrations and Nozzles That Are the Focus of This Research

The nozzles of particular interest in this research are: 1) the feedwater nozzles that introduce the feedwater into the boiler drum; and 2) the downcomer nozzles that route the subcooled water back down to the waterwalls. These nozzles are of main interest because, during the various operational modes, they have the possibility of having differential temperatures between the adjacent drum wall and the fluids in the nozzles. It is these temperature differentials, which vary with time, that produce the cyclic thermal stresses that lead to cracking. The cracking is often associated with weld heat-affected zones (HAZ), and there is sometimes an exacerbating corrosion aspect from either damaging water chemistry excursions or from selective corrosion attack at the HAZ from overly aggressive chemical cleanings.

1.5 Mud Drums

The preceding discussion in this section has focused on the upper drum. Some configurations also feature a lower drum that can simply act as an intermediate collection point for the subcooled water from the downcomers or can be connected to the top drum by a series of heat absorbing tubes, called the *boiler bank* or *steam-generating bank*. This lower drum is often called the *mud drum* because this is where the sediments found in the boiler water tend to settle and collect. When a mud drum is present, it is typically used for blowdown. Because the temperature differentials and thermal transients for the lower drum are likely to be much less severe than those in the upper drum, the lower drum is of peripheral interest for thermal fatigue in the current research. This is not to say that specific plants have not encountered cracking problems that merit additional investigation to establish the particular circumstances, but thermal fatigue is not expected to be a primary failure driver. An exception can be “stick-through” nozzles, where the portions of the nozzle extending beyond the inside diameter (ID) surface respond faster to temperature excursions than the drum wall, a condition likely to cause toe cracking where the weld joins the drum ID.

1.6 Background Leading to the Current Research

The issue of thermal fatigue in boiler drums was first considered by EPRI Materials & Repair (M&R) subscribers in 2001. In response, an informational survey was sent to all subscribers, but only four surveys were returned [1-4], and the response was judged to be too sparse to validate thermal fatigue as a major utility concern. However, as a part of this initial work, EPRI, along with Structural Integrity Associates and Aptech, became involved in assessing an actual cracking problem in the TransAlta Wabamun Unit 4 downcomer nozzles. The outcome of this initial informational survey and the TransAlta work was as follows [1-4]:

- All four utilities responding to the survey acknowledged some drum cracking problems, but none of the cracking was judged to be severe.
- There was no uniform practice by the four utilities in dealing with cracking, and the approaches ranged from “do nothing” to removal by grinding or removal followed by weld repair.
- Time to initial crack was at least 30 years for all four utilities responding to the survey.
- Efforts for remediation of cracking met limited success with a recurrence of cracking reported in 24 to 48 months.
- For Wabamun Unit 4, two conclusions were drawn from finite element models and fracture mechanics analyses: 1) the cracks were thermally driven and would arrest at a non-threatening depth if left undisturbed, whereas they would reinitiate if removed by grinding; and 2) the cracked drum satisfied a leak-before-break criterion, thus a catastrophic failure was judged to be highly unlikely.

Because of the limited success of the prior effort [1-4], the M&R subscribers again ranked the project on thermal fatigue cracking of boiler drums sufficiently high to gain funding in calendar years 2003–2004. An Interim Report was issued based on the 2003 work [1-5], and the additional work performed in 2004 was integrated into a Final Report [1-6]. The research identified 11 tasks for which results were reported in the two aforementioned reports:

- Task 1 – Drum Geometry
- Task 2 – Drum Materials
- Task 3 – Nozzle and Weld Configuration
- Task 4 – Nozzle Materials
- Task 5 – Design Basis
- Task 6 – Condition Assessment
- Task 7 – Historical Cracking Problems
- Task 8 – Operational Issues
- Task 9 – Simplified Structural Analyses
- Task 11 – Progress Report
- Task 12 – Final Report

It will be noted that Task 10 is omitted from the above listing of tasks. This task was identified as follows:

- Task 10 – Finite Element and Fracture Mechanics Modeling

Because a simplified stress, fatigue, and fracture analysis was utilized in the original project, a more comprehensive and technically sound approach (Task 10) was identified as desirable, but funding was deferred, pending positive results from the initial work. Thus, in 2004 a separate Task 10 project was performed for a Combustion Engineering (CE) drum in a controlled circulation unit, which is the focus of the current report.

In 2005, a project paralleling that for the CE drum will be performed on a Babcock and Wilcox (B&W) drum in a natural circulation boiler.

1.7 References

- 1-1. S. C. Stultz and J. B. Kitto, Eds. *Steam, Its Generation and Uses, 40th Edition*. Babcock & Wilcox Co., Barberton, OH 1992.
- 1-2. Glenn R. Fryling, Ed. *Combustion Engineering, Revised Edition*. Combustion Engineering, Inc., Windsor, CT 1966.
- 1-3. J. G. Singer, Ed. *Combustion Fossil Power, Fourth Edition*. Combustion Engineering, Inc., Windsor, CT 1991.
- 1-4. *Thermal Fatigue Cracking of Boiler Drums*. EPRI, Palo Alto, CA: 2002. 1004614.
- 1-5. *Thermal Fatigue of Fossil Boiler Drum Nozzles*. EPRI, Palo Alto, CA: 2004. 1008039.
- 1-6. *Thermal Fatigue of Fossil Boiler Drum Nozzles*. EPRI, Palo Alto, CA: 2005. 1008070.

2

DRUM GEOMETRY, OPERATIONAL PARAMETERS, AND MATERIALS

In the original project [2-1] data were compiled from 51 drum-type boilers in the fossil fleet of a major southeastern U.S. utility. These units represented a broad cross-section of original equipment manufacturers (OEMs) as follows:

- 25 by Combustion Engineering, Inc. (CE), now Alstom Power, Inc.
- 22 by Babcock & Wilcox Co. (B&W)
- 4 by Foster Wheeler, Inc. (FW)

Among the 51 units, those that were nominally alike fell into 15 distinct groupings. The turbine throttle pressures were 1450, 1800, 2000, and 2400 psig (100, 124.14, 137.93, and 165.52 bars).

For the detailed finite element stress and fracture mechanics analyses which are the focus of this report, two nominally identical CE units from the original project were selected, each rated at 275 MW at main steam turbine throttle conditions of 2000 psig (137.93 bars) pressure and 1050°F (565.56°C) temperature. This selection was not based on a known history of drum cracking. Instead, to more broadly leverage the applicability of the research, the selection was based on:

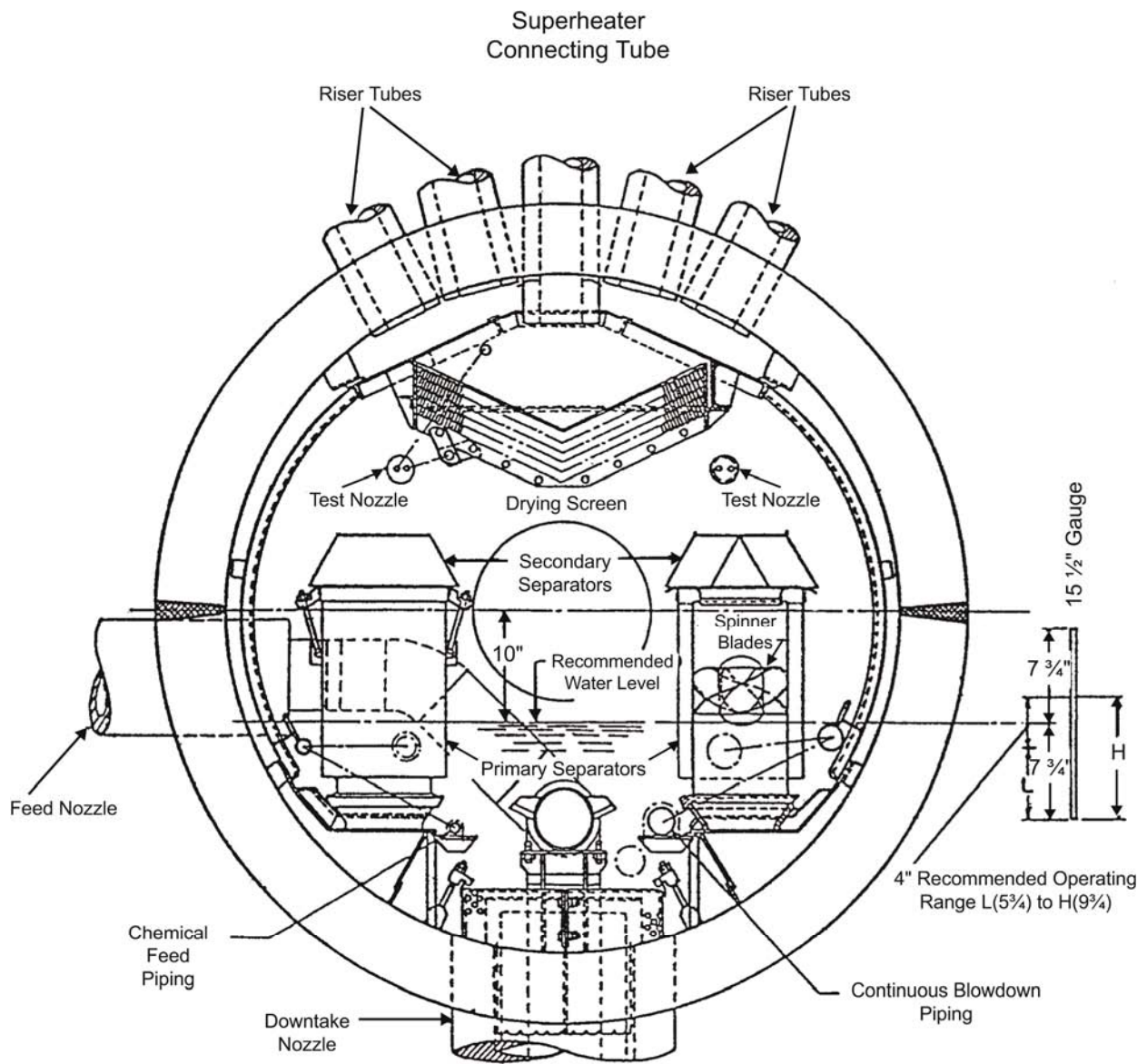
- Convenience in accessing the necessary data to support the project
- Unit size sufficiently large to be a continuing asset to the utility
- Age compatible with the nominal period of 30 years or older reported for drum cracking to develop (the two units went into commercial operation in 1959)
- Drum configuration typical of CE units of the era

2.1 Drum Geometry

The geometric attributes of the drum were as follows:

- Inside diameter of 60 in. (1.52 m)
- Wall thickness of 4.875 in. (12.38 cm)
- Length of 58.3 ft (17.77 m)
- Weight of 260,00 lbs (117,934 kg)

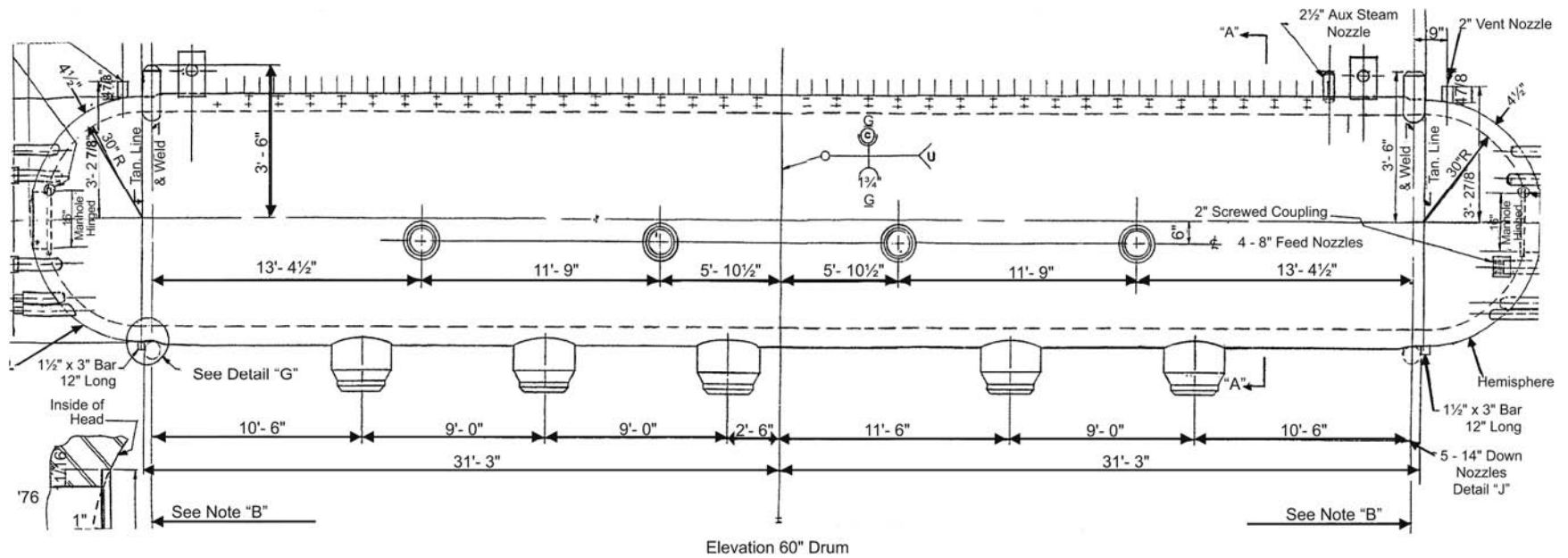
A typical cross section through the drum illustrating the internals is shown in Figure 2-1, and an elevation (side) view is shown in Figure 2-2. The drum has four feedwater nozzles that are oriented horizontally and enter the drum just below the horizontal centerline.



Steam Drum Internals
Typical Arrangement
60 Inch Drum

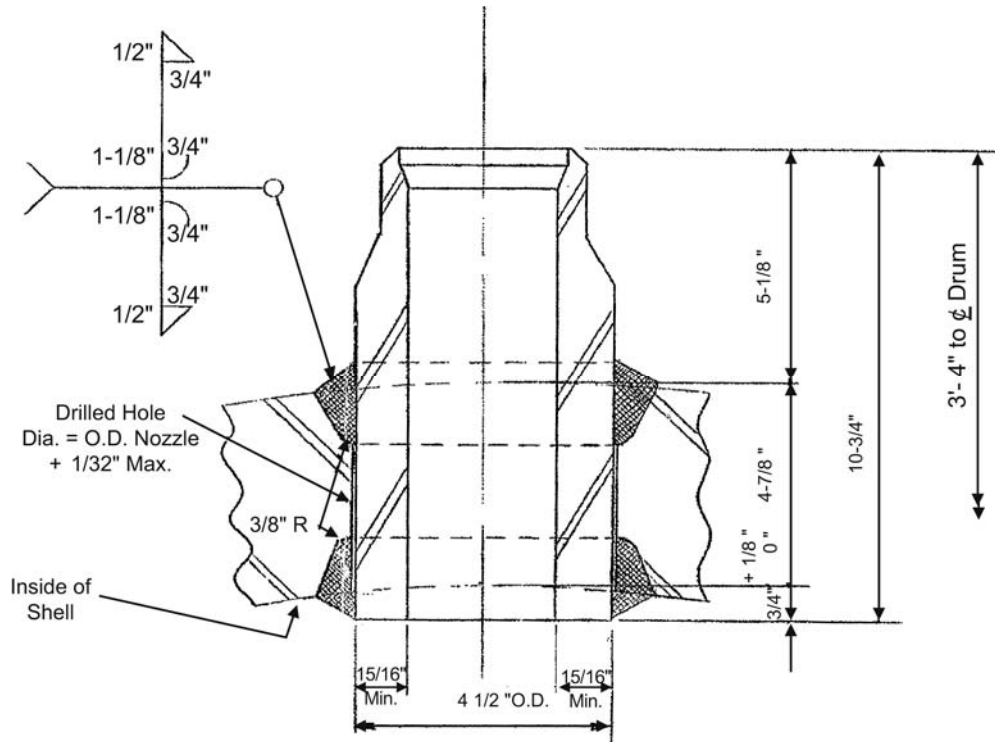
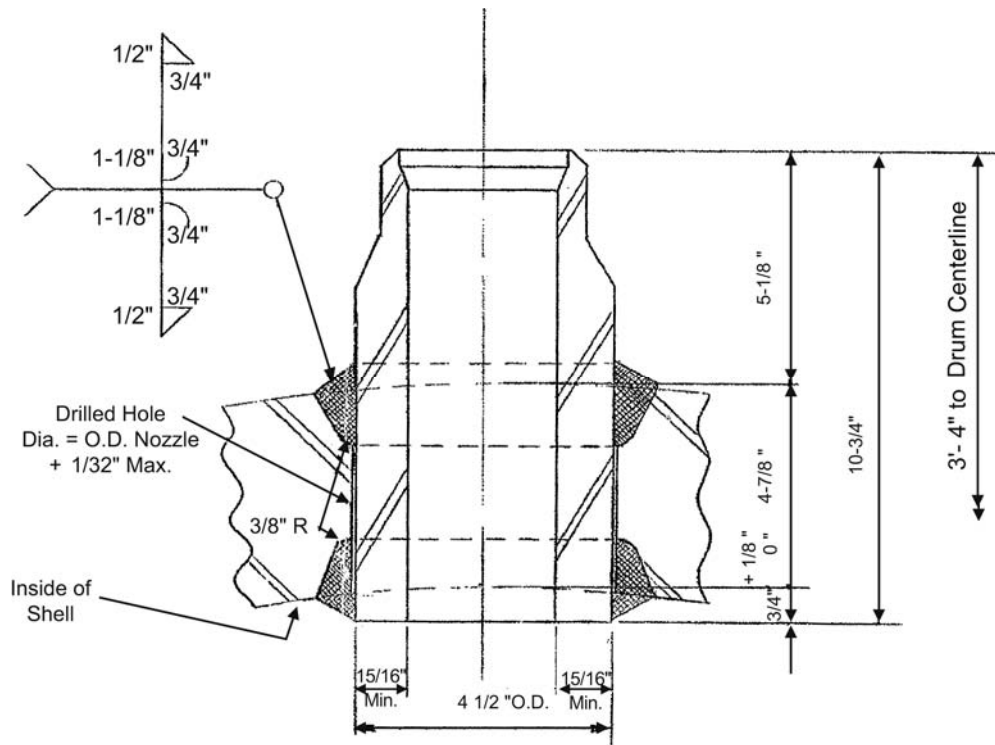
1 in. = 25.4 mm

Figure 2-1
Cross Section of the Drum for the CE 2000 psig (137.93 bars) Unit



1 in. = 25.4 mm

Figure 2-2
Elevation View of the Drum for the CE 2000 psig (137.93 bars) Unit Illustrating the Four Feedwater Nozzles and the Five Downcomers



1 in. = 25.4 mm

Figure 2-4
Typical Weld Detail for Partial Penetration ID and OD Welds Attaching the Steam Outlet Nozzles and Riser Nozzles to the CE Drum

2.2 Operational Parameters

The following operational parameters are applicable to each of the two sister units that are the subject of this report:

- Unit power of 275 megawatts
- Turbine throttle temperature of 1050°F (565.56°C)
- Turbine throttle pressure of 2000 psig (137.92 bars)
- Main steam flow of 1,960,000 pounds/hour (889,041 kg/hour)
- Design pressure of 2275 psig (156.88 bars)
- Drum operating pressure of 2165 psig (149.30 bars)
- Drum saturation temperature at operating pressure of 648°F (342.22°C)
- Four Ingersoll-Rand boiler circulating pumps, each rated at 8800 gpm (33,311.62 liter/min)

Following the 2003 research on the original project [2-1], finite element stress analyses for several operational modes were identified as desirable to assess the cumulative fatigue damage:

- Steady state—The steady-state temperatures associated with 100%, 50%, and 25% load are to be established, both with and without the high-pressure (HP) feedwater heaters being bypassed.
- Global stresses due to top-to-bottom temperature differentials.
- Thermal transients
 - Normal (cold) start. Based on EPRI research for economizer cracking, multiple spikes occur on startup in the feedwater going to the economizer so it is reasonable to expect that similar spikes will occur in the FW going from the economizer to the drum.
 - Hot start. There are likely to also be multiple spikes associated with hot starts.
 - Normal shutdown.
 - Emergency shutdown.
 - Cycle from full load to 25% load, maintain load, and return to full load to simulate weekend turndown.
 - Cycle from full load to 50% load, maintain load, and return to full load to simulate turndown following daily peak loads.
 - Remove a bank of FW heaters.
 - Restore a bank of FW heaters.
 - Top off from low drum level or empty drum while offline using DA tank fluid.
 - Two-shifting operation (off every evening, on again in morning) to simulate older plants that have been relegated only to peaking operation during worst summer and winter months.

While treatment of the above comprehensive list was viewed as desirable, available funding required that the analyses be substantially restricted; therefore, the following conditions were analyzed as reported in subsequent sections of this report:

- Pressure only.
- Normal (cold) start, continued to steady-state at 100% load, followed by normal shutdown. This analysis also captured the effect of top-to-bottom temperature differentials.
- Step change in FW temperature such as occurs with removal and restoration of a bank of FW heaters or when topping off the drum with cold FW from the deaerator.

2.3 Materials

All of the pressure boundary materials used in the steam drum selected for this project were carbon steels. The drum shells and heads were formed from carbon steel plate made to ASME SA-212 Grade B, and the feedwater and downcomer nozzles were ASME SA-105 forgings. The drum cylinders were rolled to half sections and joined by longitudinal welds. The drum was built in halves that were joined together by a girth weld located mid-length.

2.3.1 Plates

SA-212 Grade B carbon steel plate was almost always made to coarse grain (CG) practice. The material had minimum specified tensile strength of 70 ksi (482.63 MPa) and minimum specified yield strength of 38 ksi (262.00 MPa). The SA-212 Grade B specification was discontinued in 1967 and replaced by SA-515 Grade 70 (CG practice) and SA-516 Grade 70 fine grain (FG) practice.

The issue of CG practice or FG practice requires some clarification. All of the pressure vessel steel plate specifications reference ASME SA-20 [2-3], which contains the general requirements for plate that delineate the metallurgical structure and melting practice comprising CG and FG practice. When a CG austenite grain size is specified, the steel has an American Society for Testing and Materials (ASTM) grain size in the range of 1 to 5 (higher numbers are finer). The average grain diameter for ASTM Number 1 is 0.0098 in. (0.25 mm) and for Number 5, 0.0025 in. (0.064 mm) [2-4].

When a FG austenite grain size is specified, aluminum is usually used as the grain refining element during melting, and the requirement is for an ASTM Number 5 or finer. FG practice typically produces a grain size of ASTM Number 7 with an average grain diameter of 0.0012 in. (0.031 mm). The aluminum content for FG practice should be in excess of 0.020% total, or alternatively, 0.015% acid soluble aluminum.

The effect of FG practice is to lower (improve) the ductile-to-brittle transition temperature, giving the material higher fracture toughness, or stated differently, higher absorbed energy in a Charpy V-notch test. This improvement in fracture toughness is especially important for the hydro test, particularly when performed at 1.5 times design pressure. There have been a few

instances of drum failures during hydrostatic testing due to inadequate fracture toughness for the test temperature employed.

The importance of fracture toughness and the influence of melting and deoxidation practice emerged during World War II with the breakup of Liberty ships in the cold waters of the North Atlantic. These ships had previously been made of riveted hulls, and the improvement in productivity from a change to all-welded hulls was a resounding success until the unexplained fractures appeared. In the two decades following WW II, the science of fracture mechanics matured and impacted the fabrication of all steel structures, including pressure vessels [2-5]. While ASME Section I (Power Boilers) still has no formal requirements for fracture toughness, the major OEMs have generally integrated such considerations into their material procurement and fabrication methods. This observation is borne out in relation to the B&W practice for drum material as follows [2-6]:

Carbon steel plate is the primary material used in drums. SA-299, a 75,000 psi (515 MPa) tensile strength material, ordered to fine grain melting practice for improved toughness, is used for heavy section drums, those more than about 4 in. (100 mm) in thickness. SA-516 Gr 70, a fine grained 70,000 psi (485 MPa) tensile strength steel, is used for applications below this thickness, down to 1.5 in. (38 mm) thick shells. SA-515 Gr 70, a coarse grain melting practice steel, is used for thinner shells. Only in rare cases, where crane lifting capacity or long distance shipping costs are important considerations, are higher strength steels used.

2.3.2 Forgings

Drum nozzles are made from carbon steels, and specifications for tubes, pipes, or forgings are typically utilized, depending on size and application. The strength of nozzle material includes a lower range than is typical for plates for two reasons. First, the quantities and weights of materials for nozzles are much lower, and the need to minimize weight is not a major issue. Second, the compensation rules in design permit the reinforcement to be either in the plate, the nozzle, or shared between the two. Therefore, the use of lower strength levels in the nozzles is not a design impediment. Nozzle materials have a minimum specified room temperature tensile strength of 60 to 75 ksi (413.69 to 517.11 MPa) and a minimum specified room temperature yield strength from 30 to 40 ksi (206.84 to 275.79 MPa).

The discussion of FG versus CG melting practice for plates and the associated effect on fracture toughness in the previous section, while theoretically applicable, is much less relevant to nozzle materials for two reasons. First, the sizes and thicknesses are smaller, and the size constraint results in stress states that are less likely to result in brittle fracture. Second, the large metal working reductions used to produce these wrought products are likely to promote recrystallization to a FG size that will persist unless there is a subsequent austenitization at a very high temperature, resulting in grain growth.

Forgings are often viewed as the premier wrought product because of the substantial amount of working reduction and the usually favorable alignment of inclusions in the forged part. Forgings often are completed to near final shape and size, thus requiring little or no machining to complete the part. For cylindrical hollow shapes, solid forgings can be produced and bored to the desired inside diameter. A final heat treatment is usually required to achieve the desired mechanical properties.

It is difficult to generalize on the sizes of forgings because of the myriad possibilities. Maximum weights of 10,000 lbs (4535.92 kg) are typical of forgings specifications used for boiler drum nozzles.

The ASME General Specification for forgings is SA-788 [2-7]. In contrast to SA-20 for plates, this general specification contains no mandatory limits for residual elements such as Cu, Ni, Cr, Mo, V, and Cb in carbon steels, but it does contain supplementary requirements that can be invoked by the purchaser to restrict such residuals.

2.4 Mechanical Properties and Chemical Composition

Table 2-1 shows the specification mechanical properties for the SA-212 Grade B plate and the large SA-105 nozzle forgings used in construction of the CE drum.

Table 2-1
Requirements for Mechanical Properties and Chemical Composition for Plates and
Nozzles Used in the CE Drum

| Item | SA-105 Forging | SA-212 Grade B Plate |
|---------------------------------|----------------|----------------------|
| Spec. Tensile Strength (ksi) | 70 min. | 70–85 |
| Min. Spec. Yield Strength (ksi) | 36 | 38 |
| Min. Elong. in 2 in. (%) | 22 | 22 |
| Min. Red. of Area (%) | 30 | |
| Max. Hardness (Brinell) | 187 | |
| C (max.) | 0.37 | 0.35 |
| Mn | 0.60–1.05 | 0.90 max. |
| Si | 0.35 max. | 0.13–0.33 |
| P (max.) | 0.040 | 0.035 |
| S (max) | 0.050 | 0.04 |
| Cu (max.) | 0.43 | |
| Ni (max.) | 0.43 | |
| Cr (max.) | 0.34 | |
| Mo (max.) | 0.13 | |
| V (max.) | 0.04 | |
| Cb (max.) | 0.03 | |
| (Cu+Ni+Cr+Mo) (max.) | 1.00 | |
| (Cr+Mo) (max.) | 0.32 | |

Notes: (1) In PW-5.2, Section I prohibits the use of carbon or alloy steel with carbon in excess of 0.35% in welded construction; this restriction supersedes the material specification.

1 in. = 25.4 mm
 1 ksi = 6.895 MPa

2.5 References

- 2-1. *Thermal Fatigue of Fossil Boiler Drum Nozzles*. EPRI, Palo Alto, CA: 2005. 1008070.
- 2-2. *ASME Boiler and Pressure Vessel Code: An Internationally Recognized Code, Section I, Rules for Construction of Power Boilers, 2004 Edition*. American Society of Mechanical Engineers, New York, NY 2004.
- 2-3. *ASME Specification SA-20, Specification for General Requirements for Steel Plates for Pressure Vessels, Section II, Part A, Ferrous Materials Specifications*. American Society of Mechanical Engineers, New York, NY 2004.
- 2-4. George E. Dieter. *Mechanical Metallurgy, Second Edition*. McGraw-Hill, New York, NY 1976, pp. 198–199.
- 2-5. T. L. Anderson. *Fracture Mechanics: Fundamentals and Applications, Second Edition*. CRC Press, New York, NY 1995.
- 2-6. S. C. Stultz and J. B. Kitto, Eds. *Steam, Its Generation and Uses, 40th Edition*. Babcock & Wilcox Co., Barberton, OH 1992.
- 2-7. *ASME Specification SA-788, Steel Forgings, General Requirements, Section II, Part A, Ferrous Materials Specifications*. American Society of Mechanical Engineers, New York, NY 2004.

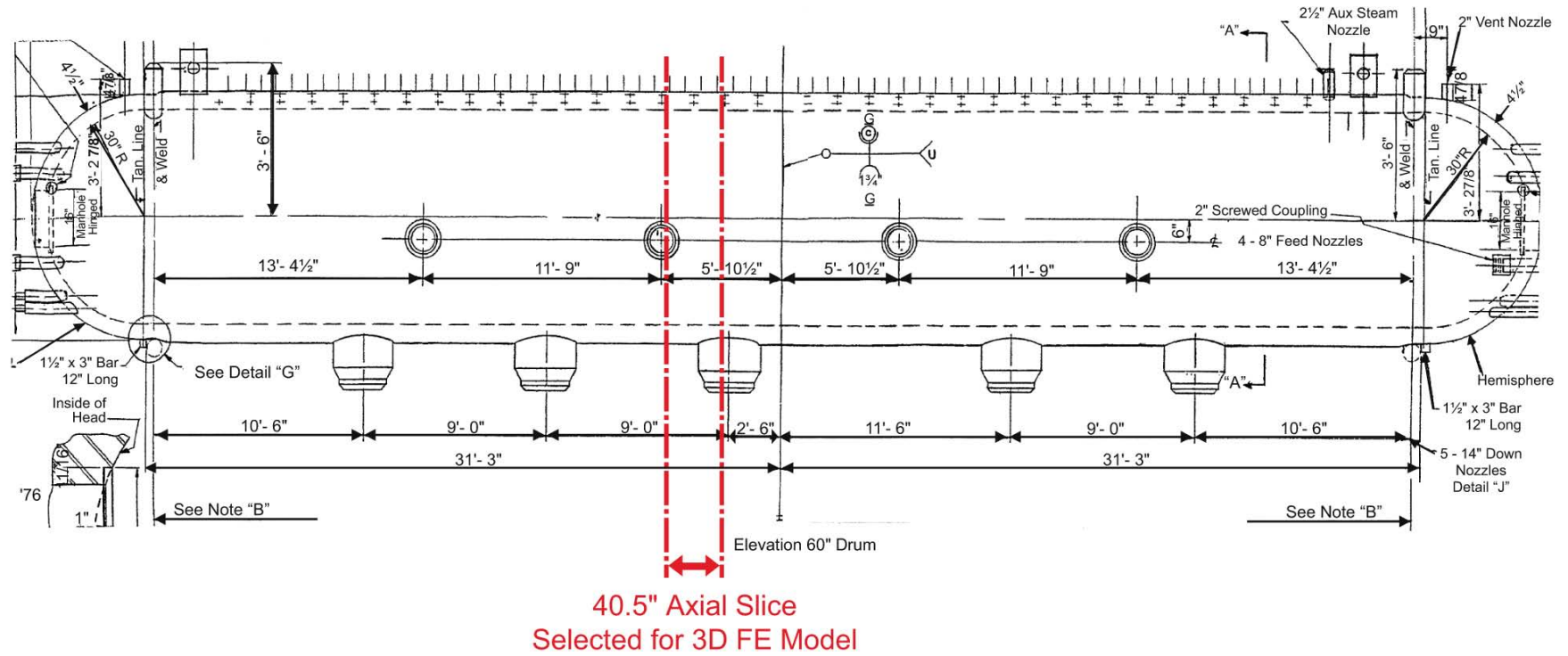
3

FINITE ELEMENT STRESS ANALYSIS

The objective of the finite element (FE) modeling and analysis was to more accurately quantify pressure and thermal stresses during operation that contribute to crack initiation and propagation. Based on research completed on this project to date [3-1], three principal areas of concern were identified: the feedwater inlet nozzles, the downcomer nozzles, and drum global stresses due to top-to-bottom temperature differentials. The FE analyses performed to address these issues will be described in this section.

3.1 Finite Element Model

A front elevation of the CE drum (see Figure 3-1) shows the 40.5-inch long axial slice selected for detailed three-dimensional FE modeling. This axial slice was selected because it includes all three principal areas of concern mentioned above: the feedwater inlet nozzle, the downcomer nozzle, and a complete (360°) section of the drum to capture the effects of top-to-bottom temperature differentials.



1 in. = 25.4 mm

Figure 3-1
Drum Elevation Showing Axial Slice Selected for Modeling

Eight-noded 3D “brick” elements were used to construct the FE model, shown in Figure 3-2, with appropriate mesh refinement at areas of interest. Note that the riser (inlet) tubes and steam outlets at the top of the drum were also included in the FE model for completeness. In no instance were the stresses in these areas as high as elsewhere in the drum; therefore, no results will be presented for these nozzles. From the standpoint of pressure and thermal stresses in the pressure parts, incorporation of drum internals was deemed to be unnecessary. However, the annulus between the drum ID and the shroud (see Figure 2-1) was considered in establishing the heat transfer coefficients discussed later. Details of the inlet nozzle and thermal sleeve, previously shown in Figure 2-3, were incorporated in the FE model section of this region as shown in Figure 3-3.

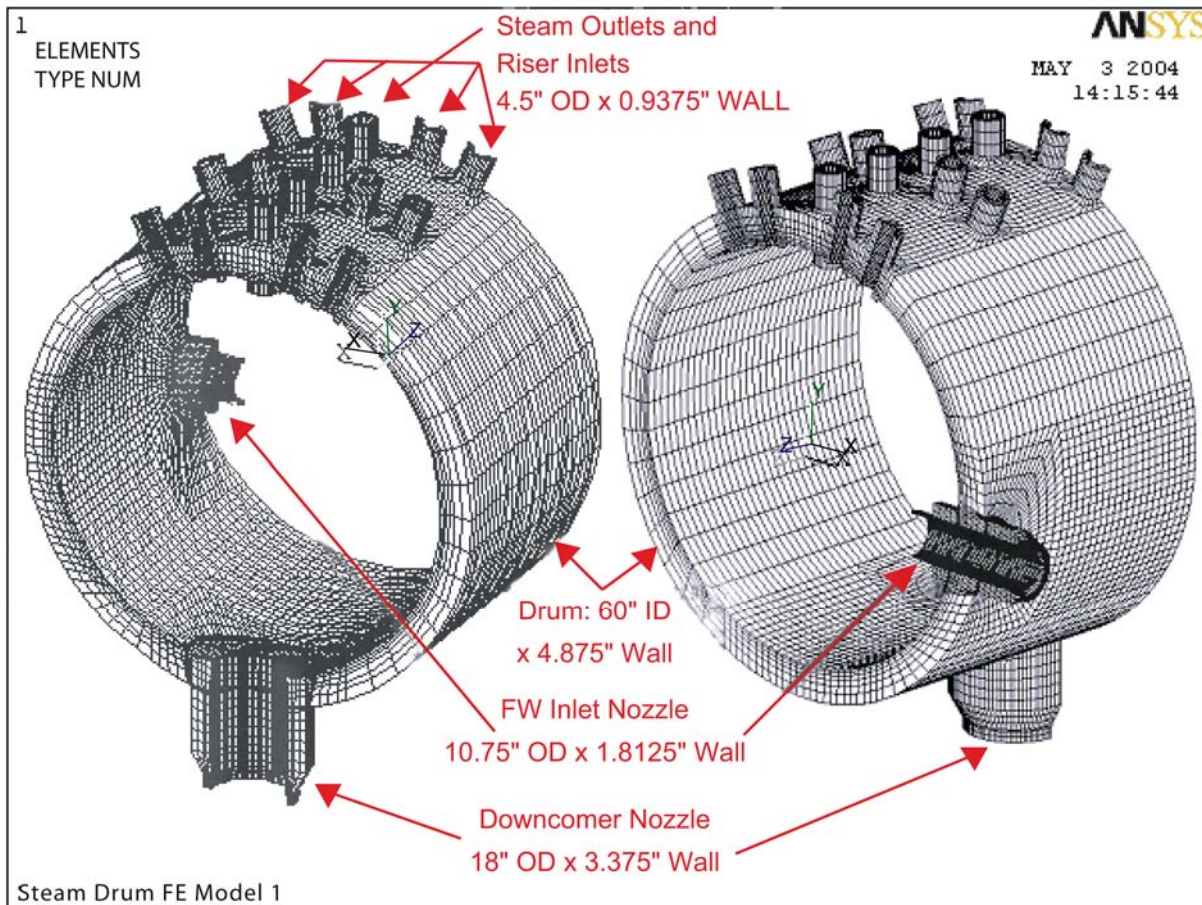
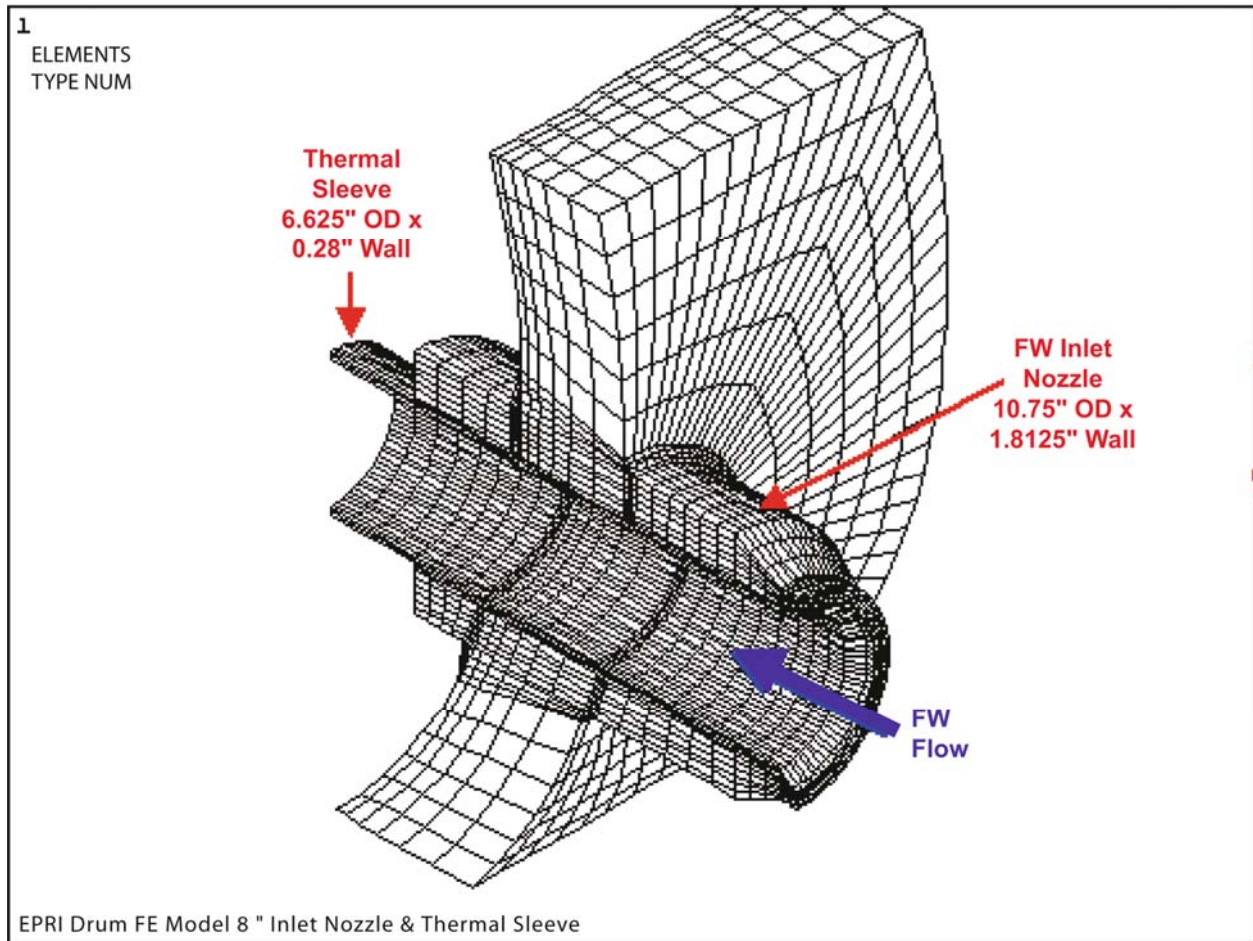


Figure 3-2
3D FE Model of the CE Drum



1 in. = 25.4 mm

Figure 3-3
Close-Up of Inlet Nozzle and Thermal Sleeve Region of the FE Model

3.2 Loading and Boundary Conditions

3.2.1 Loading

Two types of loading were simulated: internal pressure and transient thermal effects due to changes in temperature and heat transfer convection coefficients on the inside surface of the drum. The superposition of pressure and thermal loads yields total stresses in the drum during operation.

Important drum operating conditions identified in prior work on this project [3-1] included normal startup/steady-state/shutdown, thermal shock due to loss of feedwater heaters, topping off a hot drum with colder feedwater, load following and daily/weekly turndown, and emergency shutdown due to unit trip. Based on discussions with EPRI personnel regarding budgetary

constraints for the current phase of this project, the following load cases, representing a critical subset of the many possible operational scenarios that could be analyzed, were selected for detailed FE analysis:

- Internal pressurization—to separate the contribution of pressure to the total stress state
- Thermal shock—to determine the response to a unit thermal shock load due to loss of feedwater heaters or topping off a hot drum with colder feedwater
- Normal startup, steady state, shutdown—representing the typical variation in stress experienced during normal startup and shutdown

Details regarding each of these load cases are provided in subsections that follow.

3.2.2 Boundary Conditions

As shown in Figure 3-4, boundary conditions applied on the axial ends of the FE model consisted of defining a symmetry boundary at one end by fixing all axial displacements ($UZ=0$) at this end and one plane-strain boundary at the other end by coupling the displacement of all nodes at this location. These boundary conditions, which were applied for both pressure and thermal loading, simulate the large (global) axial constraint of the rest of the steam drum on the relatively small axial slice selected for modeling and evaluation, and were based on iterative studies of other possible approximations to account for these global constraints on a local model.

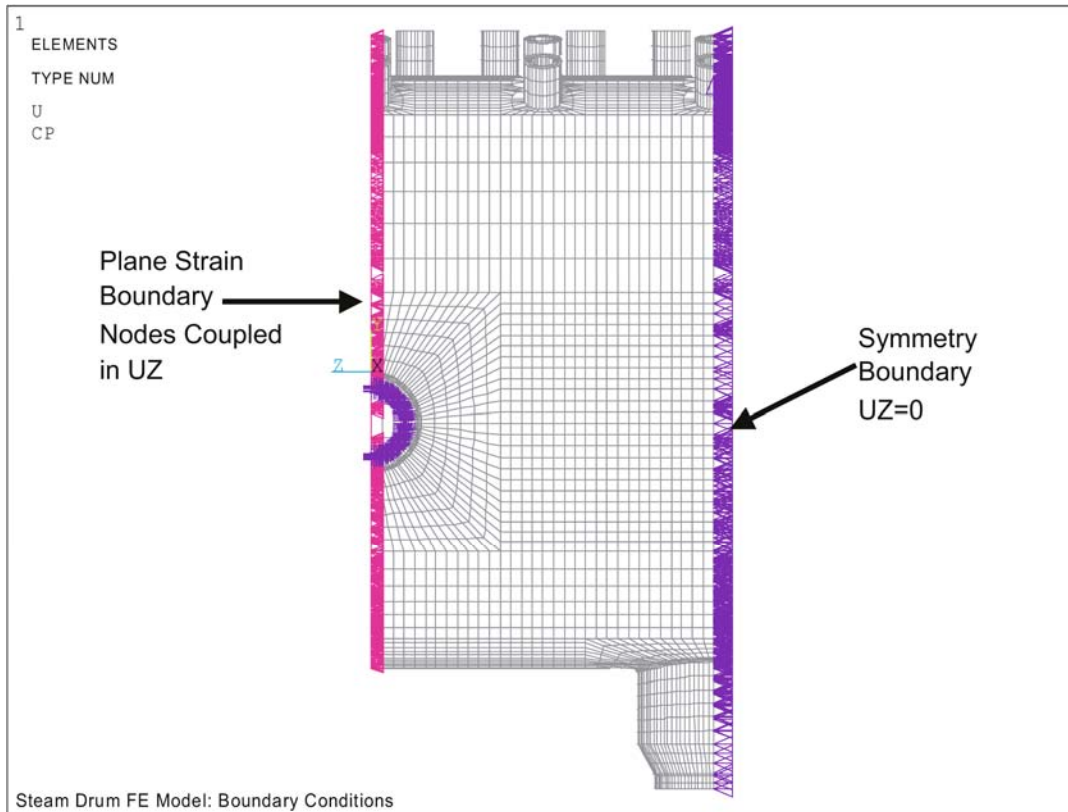


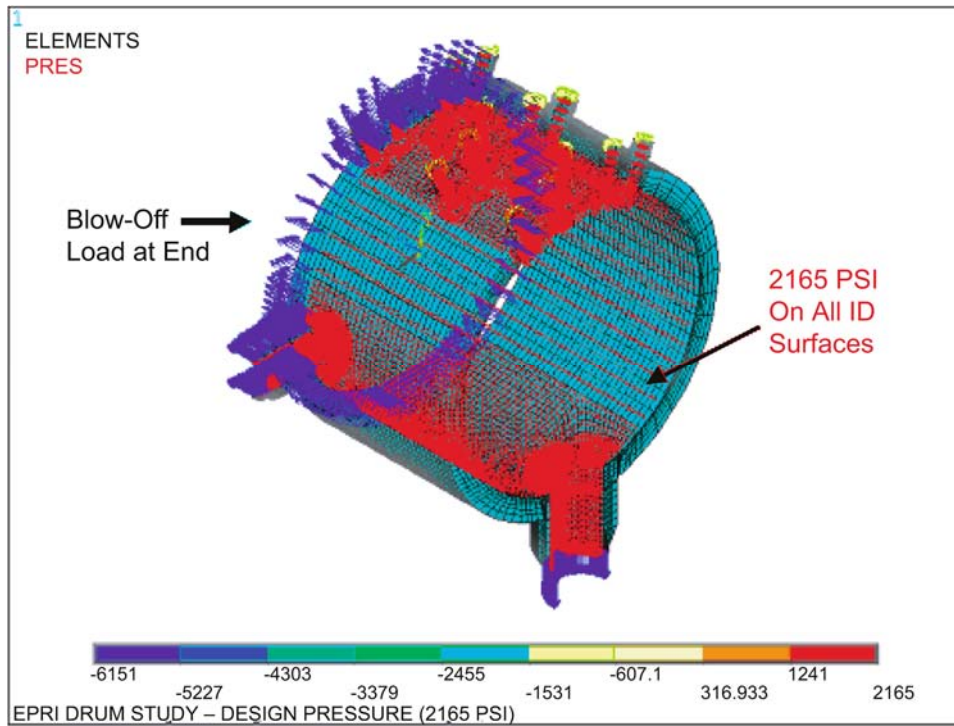
Figure 3-4
Boundary Conditions Imposed on Drum 3D FE Model

3.3 Internal Pressure Analysis

This load case was evaluated to determine the contribution of stress due to internal pressurization to the total stress state. A nominal internal pressure of 2165 psig (149.31 bars) was applied to all inside surfaces of the drum, as shown in Figure 3-5, with appropriate end (blow-off) loads at the section without symmetry boundary conditions, at the ends of the inlet and downcomer nozzles, and riser/outlet tubes.

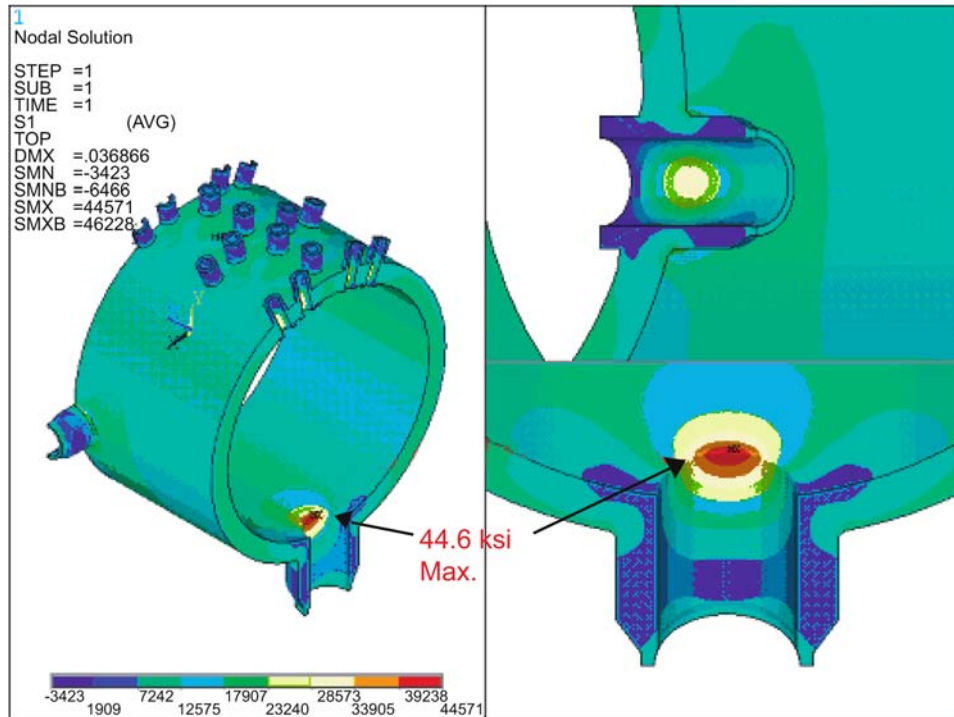
Resulting first principal (σ_1) stresses and stress intensities, as used in the ASME design-by-analysis codes (Sections III and VIII, Div. 2), are shown in Figures 3-6 and 3-7, respectively. For combined (multiaxial) stress states, the stress intensity provides a convenient basis to compare to the usual uniaxial material properties and is the underlying basis for fatigue analysis. A maximum first principal stress of 44.6 ksi (307.51 MPa) with an equivalent stress intensity of 46.4 ksi (319.92 MPa) was predicted at the downcomer bore intersection with the drum ID surface (a corner location), due to the concentration of hoop stress at this location. Maximum stresses on the inlet nozzle ID surface are approximately 20% lower than the downcomer because of the stick-through configuration of the nozzle, which provides additional reinforcement area to resist pressure stresses. These stresses exceed the expected material yield strength, and local yielding is expected to occur on first pressurization. However, the stress range

for pressurizing/depressurizing does not exceed twice the yield strength, so the stresses shake down early in life, and fully elastic behavior is anticipated in subsequent pressurization cycles.



1 psi = 6.89 MPa

Figure 3-5
2165 psig (149.30 bars) Internal Pressure Loading



1 ksi = 6.895 MPa

Figure 3-6
First Principal Stresses (psi) due to 2165 psig (149.30 bars) Internal Pressure

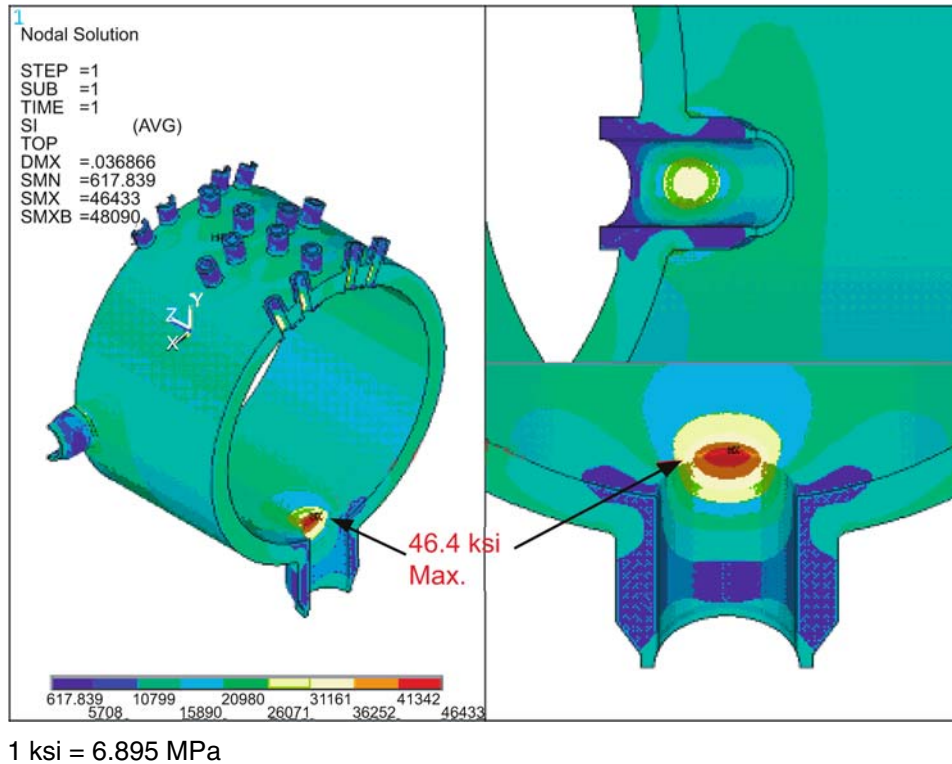


Figure 3-7
Stress Intensities (psi) due to 2165 psig (149.30 bars) Internal Pressure

3.4 Thermal Shock Analysis

This load case was evaluated to determine the response to a unit thermal shock load due to an operational event such as the loss of feedwater heaters or topping off the drum with colder feedwater.

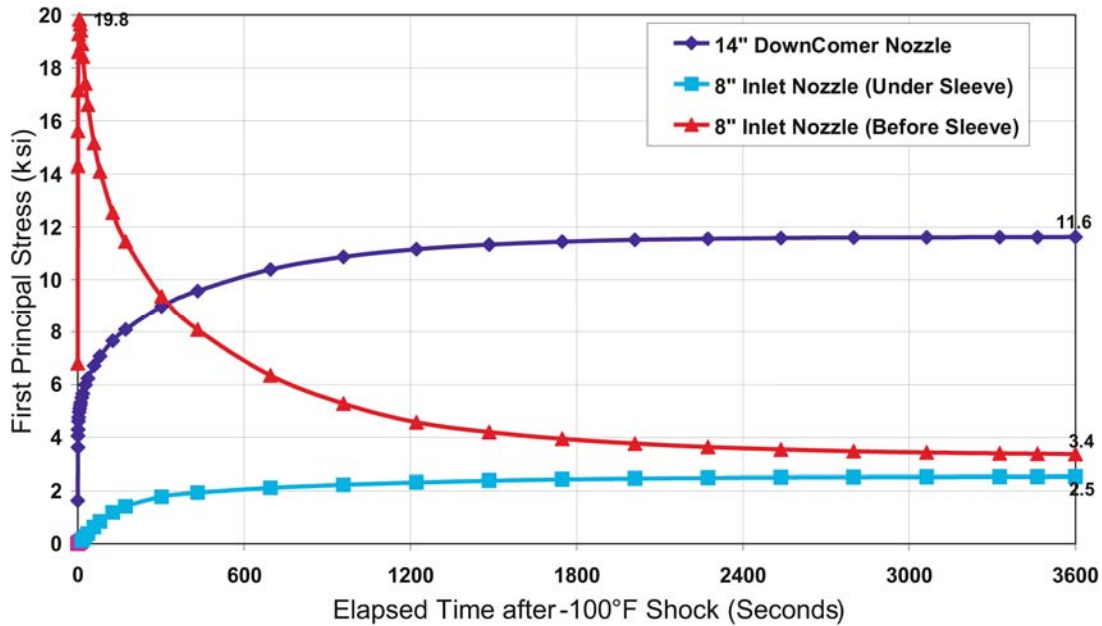
Operational data relevant to the loss of feedwater heaters extracted from a boiler circulation study performed by ABB CE Services and TVA in 1991–1992 [3-2] is presented in Table 3-1. This indicates that the cold shock at the drum inlet is in the range of 112°F to 168°F, (62°C to 93°C) corresponding to a load range of 19% to 100%. For convenience, a unit cold shock of 100°F (56°C) was selected for the FE analysis. Elastic stresses resulting from this 100°F (56°C) cold shock can then be linearly scaled up or down to yield resulting stresses for a cold shock event of a known magnitude. The equivalent cold shock at the 60° arc at the bottom of the drum in contact with subcooled liquid and the downcomer was estimated to be 25°F (13.8°C) for a 1:4 mixing ratio of cold to hot fluids, based on the data from the TVA study [3-2].

**Table 3-1
Data on Cold Shock due to Loss of Feedwater Heaters [3-2]**

| % Load | KW | Vac. | Flow (lb/hr) | % Flow | All Temperatures in °F | | | | | |
|-------------------------|--------|------|--------------|--------|------------------------|----------|----------|---------------------|--------------|-----------|
| | | | | | BFP out | Htr3 out | Htr2 out | Htr1 out (Econ. In) | | Econ. Out |
| | | | | | T1 | T2 | T3 | T4 | ΔT_FW | |
| 107% | 295449 | 1.5 | 1,993,600 | 109% | 341.3 | 367.6 | 453.9 | 509.2 | 167.9 | |
| 100% | 276659 | 1.5 | 1,828,800 | 100% | 335.7 | 360.9 | 446.7 | 500.1 | 164.4 | 555 |
| 90% | 248405 | 1.5 | 1,606,000 | 88% | 326.9 | 351.8 | 435.1 | 487.0 | 160.1 | |
| 72% | 199579 | 1.5 | 1,271,900 | 70% | 311.0 | 336.2 | 415.1 | 463.5 | 152.5 | 535 |
| 64% | 177006 | 1.5 | 1,103,200 | 60% | 301.8 | 327.2 | 403.0 | 450.9 | 149.1 | |
| 46% | 127248 | 1.5 | 788,800 | 43% | 281.7 | 305.0 | 375.9 | 420.0 | 138.3 | 510 |
| 19% | 51786 | 1.5 | 352,900 | 19% | 242.0 | 257.4 | 318.0 | 354.3 | 112.3 | |
| 0 | | | | 0 | 220.0 | | | | | |
| | | | | | | | | Min= | 112.3 | |
| | | | | | | | | Max= | 167.9 | |
| 100% to 19% Load Change | | | | | | | | 145.8 | 52.1 | |

°C = °F x 5/9

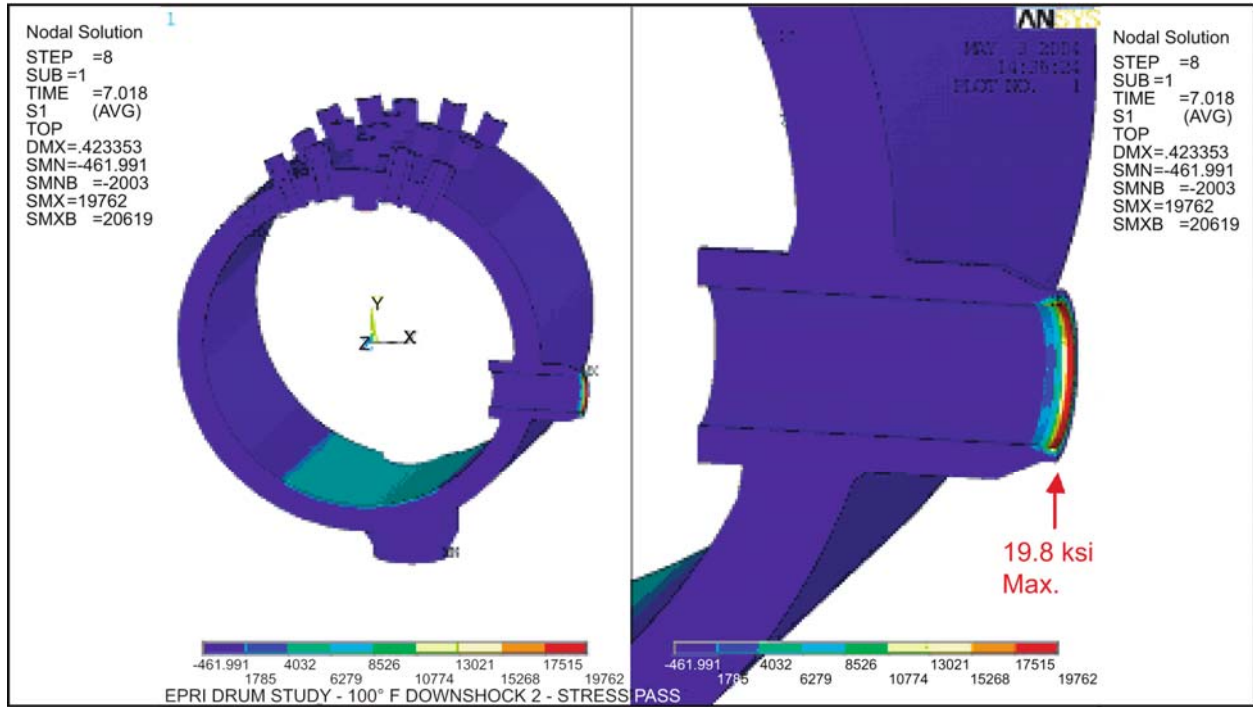
The transient stress response due to the -100°F (-56 °C) step change (downshock) at the inlet is shown in Figure 3-8 for three locations: the maximum stress location at the downcomer ID surface, the ID surface of the inlet nozzle protected by the thermal sleeve, and the ID surface of the inlet nozzle just upstream of the thermal sleeve, which is unprotected by the sleeve.



1 in. = 25.4 mm
 1 ksi = 6.895 MPa
 $^{\circ}\text{C} = ^{\circ}\text{F} \times 5/9$

Figure 3-8
Transient Stress Response to -100°F (-56°C) Cold Shock at the Drum Inlet

The unprotected nozzle ID response upstream from the thermal sleeve is typical of a step change in ID surface temperature with a peak of 19.8 ksi (136.52 MPa) occurring just 7 seconds after the initial thermal shock, eventually decaying to a steady-state value of 3.4 ksi (23.44 MPa). The thermal stress at the nozzle ID surface protected by the sleeve increases very slowly, eventually reaching a low steady-state value of 2.5 ksi (17.24 MPa). The ID surface stresses at the downcomer also increase slowly, eventually reaching a steady-state value of 11.6 ksi (79.98 MPa). Detailed color contours of first principal thermal stresses at the time of the maximum nozzle ID stress (7 seconds) and at steady state (1 hour after initial shock) are shown in Figures 3-9 and 3-10, respectively. At steady state (Figure 3-10) the maximum ID surface stress of 11.7 ksi (80.67 MPa) was predicted at the downcomer/drum ID intersection at circumferential locations consistent with the concentration of axial stresses at the downcomer hole. These axial stresses are generated because the colder drum tends to restrain contraction of the relatively narrow axial strip along the bottom of the drum, which is 25°F (13.8°C) colder than the rest of the drum.



1 ksi = 6.895 MPa
°C = °F x 5/9

Figure 3-9
Transient Stress Response at 7 Seconds After the Initial 100°F (-56°C) Cold Shock

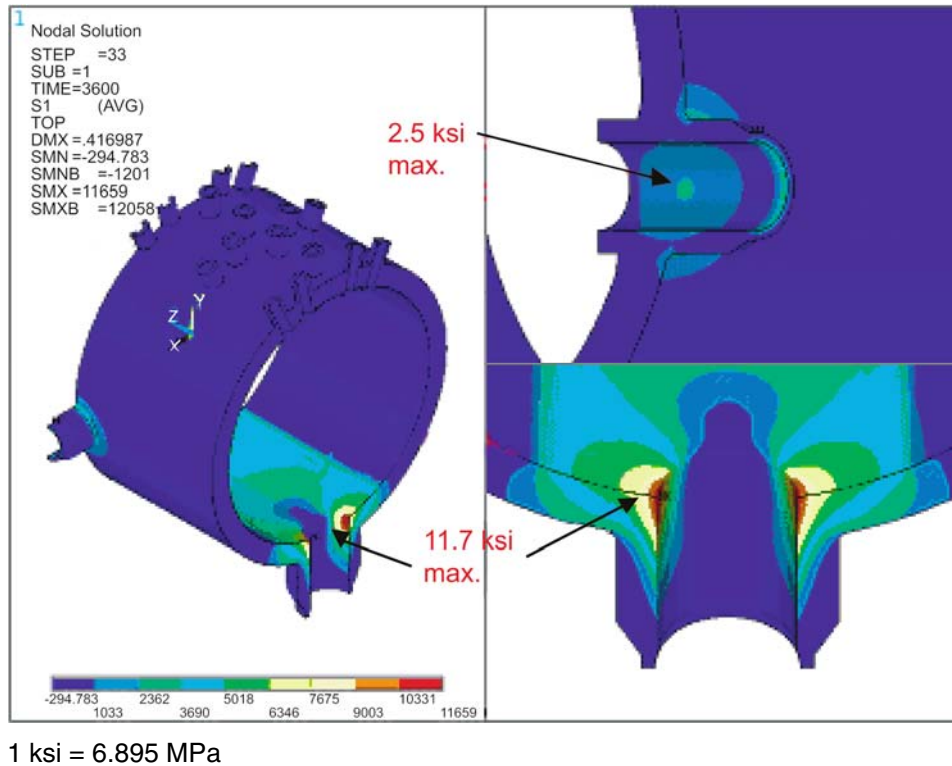


Figure 3-10
Steady-State Stress Response 1 Hour After Initial 100°F (-56°C) Cold Shock

3.5 Normal Startup, Steady-State, Shutdown Analysis

This load case was evaluated to determine stresses in the drum during a typical startup, steady-state operation at full load, and shutdown.

Two data sources were used to compose a “typical” startup/steady state/shutdown: a boiler circulation study performed by ABB and TVA in 1991–1992 [3-2] and operating data provided by TVA for the two 275 MW sister units with nominal 2000 psig drums built by CE [3-3].

3.5.1 Boiler Circulation Study

A tabular summary of critical data from the boiler circulation study is shown in Table 3-2.

Circulation ratio is the ratio of the mass flow rate of the steam-water mixture entering the drum through the riser tubes (equals downcomer flow) to the mass flow rate of steam exiting the drum. The inverse of the circulation ratio equates to the steam quality entering the drum through the riser tubes. For the 50% to 100% load range, the downcomer flow rate remains fairly constant with a higher circulation ratio (8 to 9) at 50% load and a lower circulation ratio (4.5 to 5) at full load. Feedwater inlet (economizer outlet) temperatures are 130°F to 90°F (71°C to 50°C) colder than steam saturation (outlet) temperatures for the 50% to 100% load range, while downcomer fluid temperatures are only 10°F to 15°F (5.5°C to 8.3°C) colder than steam saturation

temperatures for the same load range. The top-to-bottom drum temperature differential is therefore not expected to exceed 15°F (8.3°C) for the 50% to 100% load range. This is a very low differential and indicates that there is little concern for the “humping” phenomenon in this drum.

3.5.2 Operating Data

Data captured by the plate data acquisition system from two 275 MW units operated by TVA was downloaded to Microsoft Excel spreadsheets using DataWare software at 10- to 15-minute intervals. A tabular summary of selected data sets representing normal shutdowns followed by cold starts, warm starts, and a turbine-generator trip is provided in Table 3-3.

Plots of temperatures, pressures, and flow rates relevant to the drum evaluation, along with generator load (MW), are shown in Figures 3-11 and 3-12 for a typical startup and shutdown with periods of steady-state operation. In some instances instrumentation from certain transducers malfunctioned on one unit, but there was backup from the other unit to sort out the anomaly.

One typical startup, steady-state, shutdown transient composed from a review of the preceding plant operating data and boiler circulation study was distilled and is shown in Figure 3-13. The following is a summary of operating variables for the drum analysis and a description of how they were composed:

- Drum inlet (T_1 , P_1 , h_1): Drum inlet temperature (T_1) was not directly reported by TVA for normal operation [3-3] and was therefore estimated from economizer inlet temperatures using the results of the boiler circulation study [3-2]. Inlet pressure (P_1) was simulated from measured drum pressure. Heat transfer coefficient (h_1) was calculated corresponding to inlet temperature and pressure with the flow rate through one inlet nozzle equal to one-fourth of the total boiler feed pump flow rate.
- Downcomer (T_2 , P_2 , h_2): Downcomer temperature (T_2) was not directly reported by TVA for normal operation [3-3] and was therefore estimated to be 10°F to 15°F (5.5°C to 8.3°C) colder than drum saturation temperatures using the results of the boiler circulation study [3-2]. Downcomer pressure (P_2) was simulated from measured drum pressure. Heat transfer coefficient (h_2) was calculated corresponding to the estimated temperature and pressure, with the flow rate estimated from the circulation ratio (4.5 to 9 times inlet flow rate) as a function of load from the boiler circulation study [3-2].
- Drum bottom (T_3 , P_3 , h_3): The temperature (T_3) and pressure (P_3) for the 60° section at the bottom of the drum in contact with subcooled liquid were set equal to downcomer conditions. Heat transfer coefficient (h_3) was calculated corresponding to the estimated temperature and pressure with recirculation flow rate through the drum.
- Drum ID in contact with Steam (T_4 , P_4 , h_4): The temperature (T_4) and pressure (P_4) for the remaining 300° section of the drum ID surface in contact with saturated steam were set equal to drum saturation temperature at drum pressure. Heat transfer coefficient (h_4) was calculated corresponding to the saturation temperature and pressure with recirculation flow rate through the drum.

- Risers (T_5 , P_5 , h_5): The temperature (T_5) and pressure (P_5) for the riser ID surfaces in contact with saturated steam were set equal to drum saturation temperature at drum pressure. Heat transfer coefficient (h_5) was calculated corresponding to the saturation temperature and pressure with recirculation flow rate through the drum divided by the number of risers (144).
- Outlets (T_6 , P_6 , h_6): The temperature (T_6) and pressure (P_6) for the drum outlet ID surfaces in contact with saturated steam were set equal to drum saturation temperature at drum pressure. Heat transfer coefficient (h_6) was calculated corresponding to the saturation temperature and pressure with a flow rate equal to the total boiler feed pump flow rate divided by the number of outlets (72).

A tabular summary of these composed temperatures, pressures, and forced-convection heat transfer coefficients, estimated using Nusselt's equation for turbulent flow in pipes [3-4], is provided in Table 3-4.

Table 3-2
Data from 1991–1992 Boiler Circulation Study [3-2]

| Test # | Steam Flow Lbm/Hr | Percent of MCR | Drum Tsat °F | Econ Out °F | DC Temp. °F | Circ Ratio | No Pumps | DC Flow Lbm/Hr | Tsat Tec_out | [Top-Bot] Tsat TDC |
|--------|-------------------|----------------|--------------|-------------|-------------|------------|----------|----------------|--------------|--------------------|
| 20 | 1,894,105 | 96.64 | 647.9 | 554.9 | 633.5 | 4.55 | 3 | 8,618,178 | 93.0 | 14.4 |
| 21 | 1,925,580 | 98.24 | 648.2 | 556 | 633.6 | 4.47 | 3 | 8,607,343 | 92.2 | 14.6 |
| 23 | 1,916,369 | 97.77 | 648.2 | 556.6 | 633.5 | 4.49 | 3 | 8,604,497 | 91.6 | 14.7 |
| 22 | 1,920,954 | 98.01 | 648.2 | 556.3 | 635.7 | 4.95 | 4 | 9,508,722 | 91.9 | 12.5 |
| 5 | 1,848,509 | 94.31 | 647.7 | 554.4 | 635.4 | 5.12 | 4 | 9,464,366 | 93.3 | 12.3 |
| 16 | 1,879,528 | 95.89 | 647.9 | 554.7 | 633.3 | 4.58 | 3 | 8,608,238 | 93.2 | 14.6 |
| 17 | 1,847,067 | 94.24 | 647.9 | 555.6 | 633.6 | 4.74 | 3 | 8,755,098 | 92.3 | 14.3 |
| 18 | 1,858,433 | 94.82 | 647.9 | 555.3 | 633.4 | 4.65 | 3 | 8,641,713 | 92.6 | 14.5 |
| 19 | 1,888,074 | 96.33 | 647.9 | 555.3 | 633.5 | 4.58 | 3 | 8,647,379 | 92.6 | 14.4 |
| 6 | 1,409,127 | 71.89 | 644.2 | 535.7 | 631.8 | 6.09 | 3 | 8,581,583 | 108.5 | 12.4 |
| 3 | 1,428,076 | 72.86 | 643.8 | 534.8 | 633 | 6.67 | 4 | 9,525,267 | 109.0 | 10.8 |
| 7 | 1,390,576 | 70.95 | 644.1 | 535.7 | 631.8 | 6.21 | 3 | 8,635,477 | 108.4 | 12.3 |
| 8 | 1,392,304 | 71.04 | 644.1 | 534.9 | 631.6 | 6.2 | 3 | 8,632,285 | 109.2 | 12.5 |
| 9 | 1,385,938 | 70.71 | 644.1 | 534.5 | 631.6 | 6.29 | 3 | 8,717,550 | 109.6 | 12.5 |
| 10 | 1,381,968 | 70.51 | 644.1 | 534 | 631.4 | 6.25 | 3 | 8,637,300 | 110.1 | 12.7 |

$^{\circ}\text{C} = (^{\circ}\text{F} - 32) \times 5/9$

1 Lbm/hr = 0.0075 kgs/hr

Table 3-2 (cont.)
Data from 1991-1992 Boiler Circulation Study [3-2]

| Test # | Steam Flow Lbm/Hr | Percent of MCR | Drum Tsat. °F | Econ Out °F | DC Temp. °F | Circ Ratio | No Pumps | DC Flow Lbm/Hr | Tsat Tec_out | [TOP-BOT] Tsat TDC |
|--------|-------------------|----------------|---------------|-------------|-------------|------------|----------|----------------|--------------|--------------------|
| 2 | 959,372 | 48.95 | 641.1 | 509.4 | 631.6 | 8.97 | 3 | 8,605,567 | 132.0 | 9.8 |
| 11 | 950,494 | 48.49 | 642 | 512.3 | 629 | 7.24 | 2 | 6,881,577 | 129.7 | 13 |
| 1 | 1,029,120 | 52.51 | 641.5 | 509 | 633 | 9.24 | 4 | 9,509,069 | 132.5 | 8.5 |
| 12 | 1,044,536 | 53.29 | 641.8 | 511 | 632 | 8.21 | 3 | 8,575,641 | 130.8 | 9.8 |
| 13 | 966,599 | 49.32 | 641.8 | 510.6 | 631.9 | 8.91 | 3 | 8,612,397 | 131.2 | 9.9 |
| 14 | 994,898 | 50.76 | 641.8 | 510.6 | 631.8 | 8.75 | 3 | 8,705,358 | 131.2 | 10 |
| 15 | 995,980 | 50.82 | 641.8 | 510.7 | 631.7 | 8.98 | 3 | 8,943,900 | 131.1 | 10.1 |
| | | | | | | | Max. | 9,525,267 | 132.5 | 14.7 |
| | | | | | | | Min. | 6,881,577 | 91.6 | 8.5 |
| | | | | | | | Avg. | 8,728,114 | 109.4 | 12.3 |

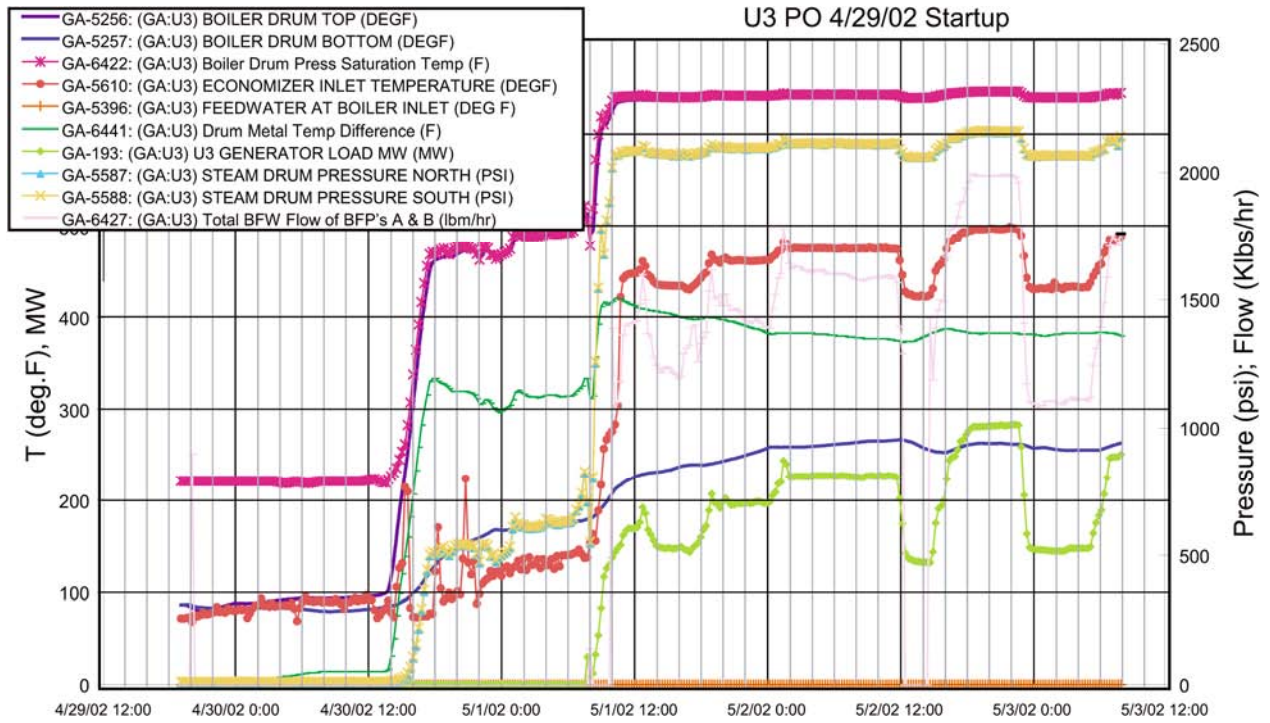
$^{\circ}\text{C} = (^{\circ}\text{F} - 32) \times 5/9$

1 Lbm/hr = 0.0075 kgs/hr

**Table 3-3
Operating Data Provided by TVA for Two 275 MW CE Drum Units [3-3]**

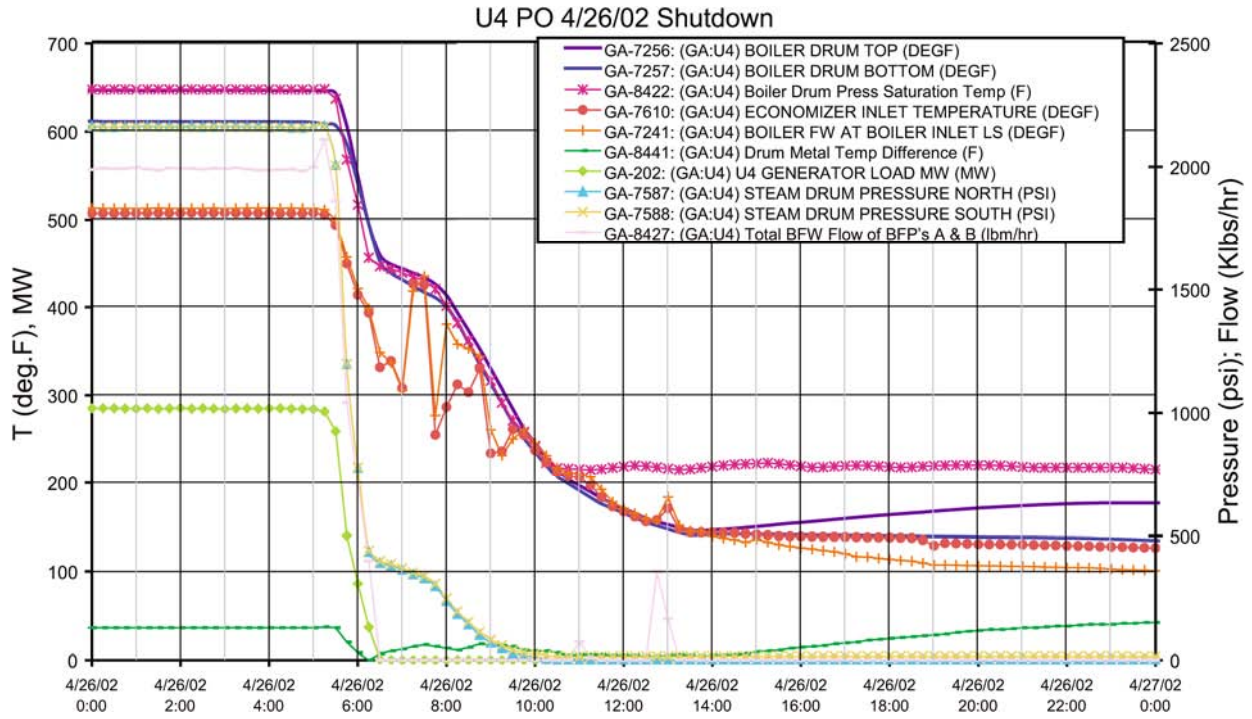
| Normal Shutdown and Cold Starts Following Long Shutdown Periods | | | | | | | | | | | | | | | | | | |
|--|------|----|------|-------------------------------|-------|----------------------------------|-------|---|----|-------|-----------------------|----------|-----------------------|------------|------------|------|-----------|---------|
| UNIT | TYPE | ID | GADS | START | START | END | END | HOURS | CC | MWWHL | EVENT DESCRIPTION | CAPACITY | VERBAL DESCRIPTION | RAMP RATES | | | DETA-T | |
| | | | | DATE | TIME | DATE | TIME | | | | | | | Tsat | Econ_In | Max | Tsat-Econ | TOP-BOT |
| CE DRUM UNIT# 3 | PO | | 1999 | 4/19/2002 | 10:26 | 5/1/2002 | 7:51 | 285.42 | P | 75921 | BOILER, MISCELLANEOUS | 266 | U3 PLANNED OUTAGE. | Tsat | 500 to 300 | <300 | 325 | 250 |
| | | | | Data Dump Period for Shutdown | | 4/17/2002 10:00 4/21/2002 10:00 | | | | | | | | | | | | |
| | | | | Data Dump Period for Startup | | 4/29/2002 19:00 5/3/2002 8:00 | | | | | | | | | | | | |
| CE DRUM UNIT# 3 | PO | | 1999 | 12/5/2003 | 11:04 | 12/14/2003 | 20:58 | 225.9 | P | 60089 | BOILER, MISCELLANEOUS | 266 | U3 PLANNED OUTAGE. | | | | | |
| | | | | Data Dump Period for Shutdown | | 12/3/2003 11:00 12/7/2003 11:00 | | | | | | | | | | | | |
| | | | | Data Dump Period for Startup | | 12/13/2003 8:00 12/16/2003 21:00 | | | | | | | | | | | | |
| CE DRUM UNIT# 4 | PO | | 1800 | 4/26/2002 | 6:22 | 5/24/2002 | 18:08 | 683.77 | P | 2E+05 | BOILER OVERHAUL (GENE | 266 | U4 PLANNED OUTAGE. | | | | | |
| | | | | Data Dump Period for Shutdown | | 4/24/2002 6:00 4/28/2002 6:00 | | | | | | | | | | | | |
| | | | | Data Dump Period for Startup | | 5/23/2002 6:00 5/26/2002 19:00 | | | | | | | | | | | | |
| CE DRUM UNIT# 4 | RS | | 0 | 9/12/2002 | 21:00 | 9/16/2002 | 6:38 | 81.63 | P | 21714 | RESERVE SHUTDOWN | 266 | | | | | | |
| | | | | Data Dump Period for Shutdown | | 9/10/2002 21:00 9/14/2002 21:00 | | | | | | | | | | | | |
| | | | | Data Dump Period for Startup | | 9/14/2002 18:00 9/18/2002 7:00 | | | | | | | | | | | | |
| Warm Starts Following a Shutdown Period of 20 to 40 Hours | | | | | | | | | | | | | | | | | | |
| UNIT | TYPE | ID | GADS | START | START | END | END | HOURS | CC | MWWHL | EVENT DESCRIPTION | CAPACITY | VERBAL DESCRIPTION | RAMP RATES | | | DETA-T | |
| | | | | DATE | TIME | DATE | TIME | | | | | | | Tsat | Econ_In | Max | Tsat-Econ | TOP-BOT |
| CE DRUM UNIT# 3 | U1 | | 1050 | 2/22/2003 | 23:13 | 2/23/2003 | 22:34 | 23.35 | P | 6211 | SECOND SUPERHEATER T | 266 | SECOND SH TUBE LEA | Tsat | 500 to 300 | <300 | 200 | 350 |
| | | | | Data Dump Period | | 2/21/2003 23:00 2/24/2003 23:00 | | | | | | | | | | | | |
| CE DRUM UNIT# 4 | U1 | | 1080 | 9/18/2002 | 7:53 | 9/19/2002 | 4:19 | 20.43 | P | 5435 | ECONOMIZER TUBE LEAKS | 266 | ECONOMIZER TUBE LEAK. | | | | | |
| | | | | Data Dump Period | | 9/17/2002 7:00 9/20/2002 5:00 | | | | | | | | | | | | |
| Warm Start Following a Shutdown Period of Less Than 10 Hours | | | | | | | | | | | | | | | | | | |
| UNIT | TYPE | ID | GADS | START | START | END | END | HOURS | CC | MWWHL | EVENT DESCRIPTION | CAPACITY | VERBAL DESCRIPTION | RAMP RATES | | | DETA-T | |
| | | | | DATE | TIME | DATE | TIME | | | | | | | Tsat | Econ_In | Max | Tsat-Econ | TOP-BOT |
| CE DRUM UNIT# 3 | RS | | 0 | 10/27/2002 | 22:00 | 10/28/2002 | 6:38 | 8.63 | P | 2296 | RESERVE SHUTDOWN | 266 | | Tsat | 500 to 300 | <300 | 350 | 410 |
| | | | | Data Dump Period | | 10/26/2002 22:00 10/29/2002 7:00 | | | | | | | | | | | | |
| Period Preceding and Following Turbine/Generator Trip | | | | | | | | | | | | | | | | | | |
| UNIT | TYPE | ID | GADS | START | START | END | END | HOURS | CC | MWWHL | EVENT DESCRIPTION | CAPACITY | VERBAL DESCRIPTION | RAMP RATES | | | DETA-T | |
| | | | | DATE | TIME | DATE | TIME | | | | | | | Tsat | Econ_In | Max | Tsat-Econ | TOP-BOT |
| CE DRUM UNIT# 4 | U1 | | 3620 | 2/14/2003 | 10:00 | 2/16/2003 | 3:05 | 41.08 | P | 10928 | MAIN TRANSFORMER | 266 | UNIT TRIPPED DUE TO | Tsat | 500 to 300 | <300 | 280 | 40 |
| | | | | Data Dump Period | | 2/13/2003 22:00 2/15/2003 10:00 | | Note:For this data dump use 10 minute intervals | | | | | | | | | | |

1 psia = 6.9 kPa



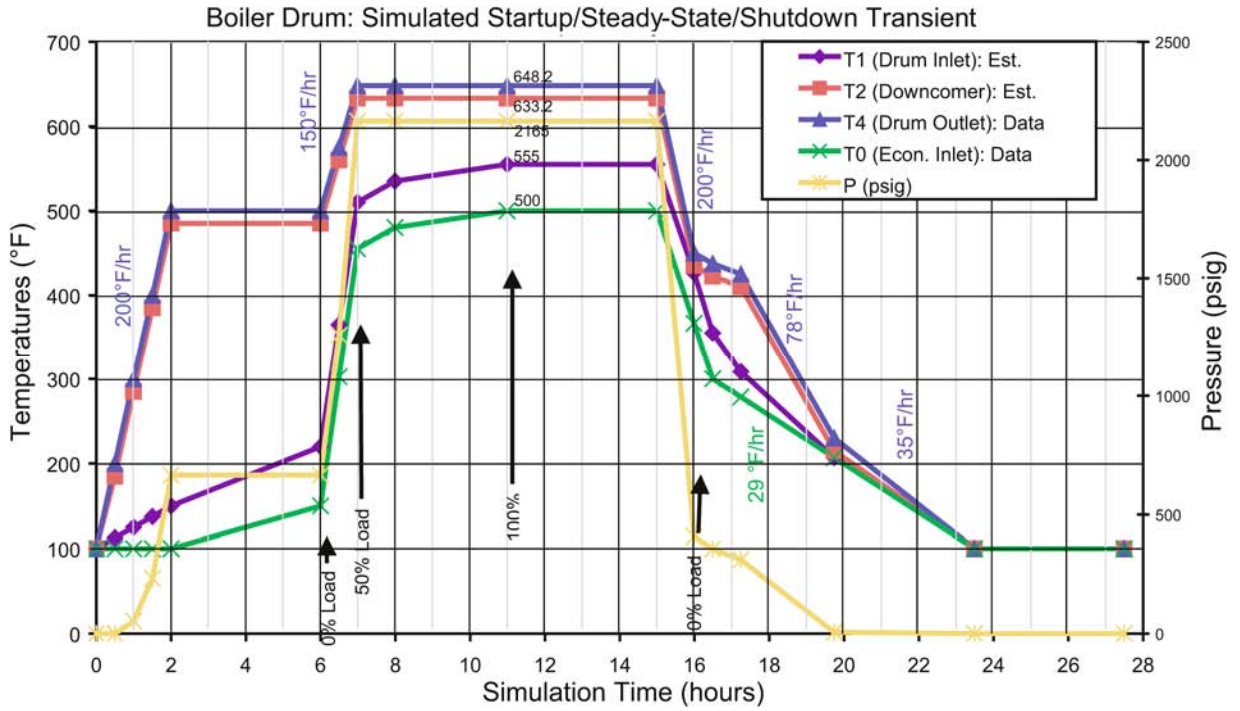
$^{\circ}\text{C} = (^{\circ}\text{F} - 32) \times 5/9$
 1 psi = 6.9 kPa
 1 lb/hr = 0.445 kg/hr

Figure 3-11
Temperatures, Pressures, Flow Rates, and MW for a Typical Startup



$^{\circ}\text{C} = (^{\circ}\text{F} - 32) \times 5/9$
 1 psi = 6.9 kPa
 1 lb/hr = 0.445 kg/hr

Figure 3-12
Temperatures, Pressures, Flow Rates, and MW for a Typical Shutdown



°C = (°F-32) × 5/9
 1 psig = 0.06896 bars

Figure 3-13
Composed Startup/Steady-State/Shutdown Transient for Drum FE Stress Analysis

**Table 3-4
Drum Temperatures, Pressures, and Heat Transfer Coefficients for Simulated Startup/ Steady-State/Shutdown Transient**

| | %Flow | time (hr) | °F/hr | P (psia) | P (psig) | Econ.In | Drum in | DC | Drum_Bot | Drum_Top | Riser Inl | Stm.Outl | Heat Transfer Coef. (Btu/hr/ft ² /°F) | | | | | | |
|----------|-------|-----------|--------|----------|----------|-----------------------|-----------|----------|----------------|-----------|-------------|-----------------|--|------|------|------|------|------|----|
| | | | | | | T0 (Ecor) | T1 (Drum) | T2 (Dov) | T3=T2 | T4 (Drum) | T5=T4 | T6=T4 | h1 | h2 | h3 | h4 | h5 | h6 | |
| Startup | | 0 | | 14.7 | 0 | 100 | 100 | 100 | | 100 | | | 185 | 3300 | 1500 | 1100 | 2800 | 65 | |
| | | 0.5 | | 14.7 | 0 | 100 | 112.5 | 185 | | 200 | | | 185 | 3300 | 1500 | 1100 | 2800 | 65 | |
| | | 1 | | 67 | 52 | 100 | 125 | 285 | | 300 | | | 185 | 3300 | 1500 | 1100 | 2800 | 65 | |
| | | 1.5 | | 247 | 232 | 100 | 137.5 | 385 | | 400 | | | 185 | 3300 | 1500 | 1100 | 2800 | 65 | |
| | | 2 | 200 | | 680 | 665 | 100 | 150 | 485 | | 500 | | | 185 | 3300 | 1500 | 1100 | 2800 | 65 |
| | 5% | 6.00 | | 680 | 665 | 150 | 220 | 485 | | 500 | | | 185 | 3300 | 1500 | 1100 | 2800 | 65 | |
| | 25% | 6.49 | | 1274.5 | 1260 | 302.5 | 365 | 560 | | 575 | | | 925 | 3300 | 1500 | 1100 | 2800 | 325 | |
| | 50% | 6.99 | 150 | 2179.7 | 2165 | 455 | 510 | 633.2 | | 648.2 | | | 1850 | 3300 | 1500 | 1100 | 2800 | 650 | |
| 75% | 7.99 | | 2179.7 | 2165 | 480 | 535 | 633.2 | | 648.2 | | | 2775 | 3300 | 1500 | 1100 | 2800 | 975 | | |
| SS | 100% | 10.99 | | 2179.7 | 2165 | 500 | 555 | 633.2 | | 648.2 | | | 3700 | 3300 | 1500 | 1100 | 2800 | 1300 | |
| | 100% | 14.99 | | 2179.7 | 2165 | 500 | 555 | 633.2 | | 648.2 | | | 3700 | 3300 | 1500 | 1100 | 2800 | 1300 | |
| Shutdown | 50% | 15.99 | | 422 | 407 | 367 | 427 | 435 | | 450 | | | 1943 | 3300 | 1500 | 1100 | 2800 | 683 | |
| | 5% | 16.49 | 133.3 | 371.5 | 357 | 300 | 355 | 422.5 | | 437.5 | | | 185 | 3300 | 1500 | 1100 | 2800 | 65 | |
| | | 17.24 | | 325.6 | 311 | 278.6 | 308.6 | 410 | | 425 | | | 185 | 3300 | 1500 | 1100 | 2800 | 65 | |
| | | 19.74 | | 20.8 | 6 | 207.1 | 207.1 | 215 | | 230 | | | 185 | 3300 | 1500 | 1100 | 2800 | 65 | |
| | | 23.49 | 28.6 | 14.7 | 0 | 100 | 100 | 100 | | 100 | | | 185 | 3300 | 1500 | 1100 | 2800 | 65 | |
| | | 27.49 | | 14.7 | 0 | 100 | 100 | 100 | | 100 | | | 185 | 3300 | 1500 | 1100 | 2800 | 65 | |
| | | | | | | T0= Economizer Outlet | | | | | | T6=Steam Outlet | | | | | | | |
| | | | | | | T1=Drum Inlet | | | | | | T5=Riser Inlet | | | | | | | |
| | | | | | | | | | T2=Downcomer | | T4=Drum Top | | | | | | | | |
| | | | | | | | | | T3=Drum Bottom | | | | | | | | | | |

°C = (°F-32) × 5/9
 1 psia = 6.9 kPa
 1 psig = 0.06896 bars
 1 Btu/hr/ft²/°F = 0.00568 kw/m²/K

3.5.3 Startup/Steady-State/Shutdown Stresses

Finite element stress results were reviewed and processed to determine the location and time at which the maximum stress occurred in the drum. Three critical locations were identified: the downcomer nozzle ID, the inlet nozzle ID, and the inlet nozzle OD. Maximum stress intensities at these locations, shown in Figures 3-14 and 3-15, include the combined effect of internal pressure and thermal transient stresses.

3.5.3.1 Downcomer Nozzle ID

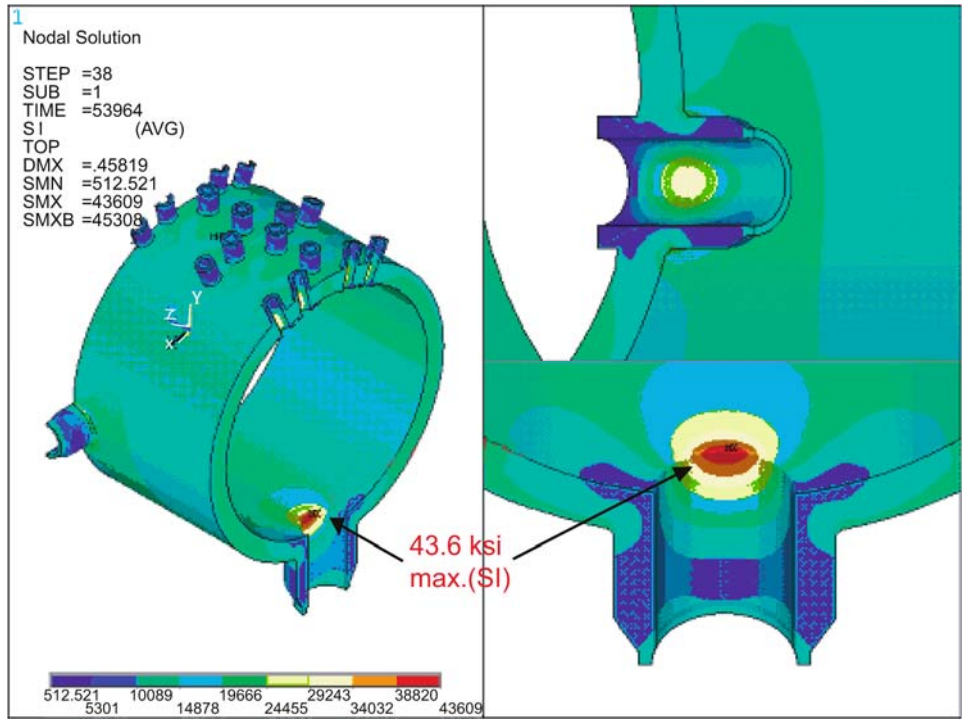
The maximum predicted stress of 43.6 ksi (300.61 MPa) at the downcomer nozzle ID (Figure 3-14) is predominantly due to internal pressure. Transient thermal stresses are out of phase with pressure stresses and tend to reduce the maximum stress of 46.4 ksi (319.92 MPa) due to pressure only (Figure 3-7). The variation in stress with time at this location, shown in Figure 3-16, illustrates this response.

3.5.3.2 Inlet Nozzle ID

The maximum predicted stress intensity at the inlet nozzle ID was 46.8 ksi (322.67 MPa) (Figure 3-15). The variation of total stress, thermal stress, and pressure stress with time at this location is shown in Figure 3-17. The maximum stress was predicted at the end of the startup (6.99 hours) with a pressure stress contribution of 78% and a thermal stress contribution of 22%. The nozzle ID location of maximum stress with respect to the drum corresponds to the OD of the drum. During startup, the drum ID surface heats up faster than the OD, resulting in tensile stresses at the drum OD. These tensile thermal stresses at the nozzle ID location, which is coincident with the drum OD, are additive to the pressure stresses.

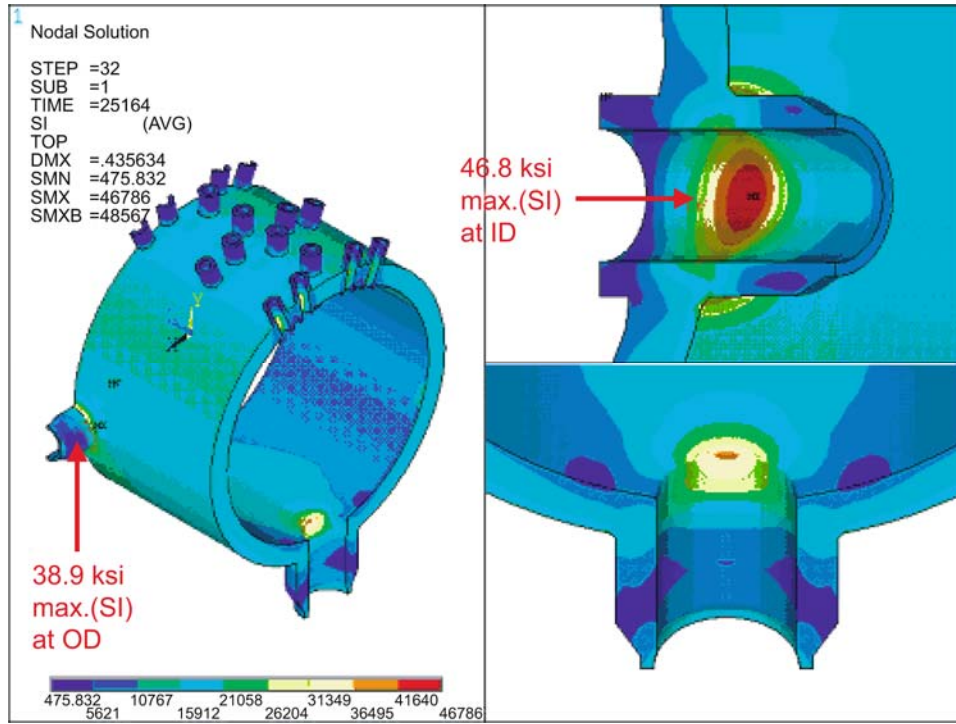
3.5.3.3 Inlet Nozzle OD

The maximum predicted stress intensity at the inlet nozzle OD was 38.9 ksi (268.21 MPa) (Figure 3-15). The variation of total stress, thermal stress, and pressure stress with time at this location is shown in Figure 3-18. The maximum stress was predicted at the end of the startup (6.99 hours) with a pressure stress contribution of 66% and a thermal stress contribution of 34%. The nozzle ID location of maximum stress with respect to the drum corresponds to the OD of the drum. During startup, the drum ID surface heats up faster than the OD, resulting in tensile stresses at the drum OD. These tensile thermal stresses at the nozzle OD location, which is coincident with the drum OD, are additive resulting in higher thermal stresses.



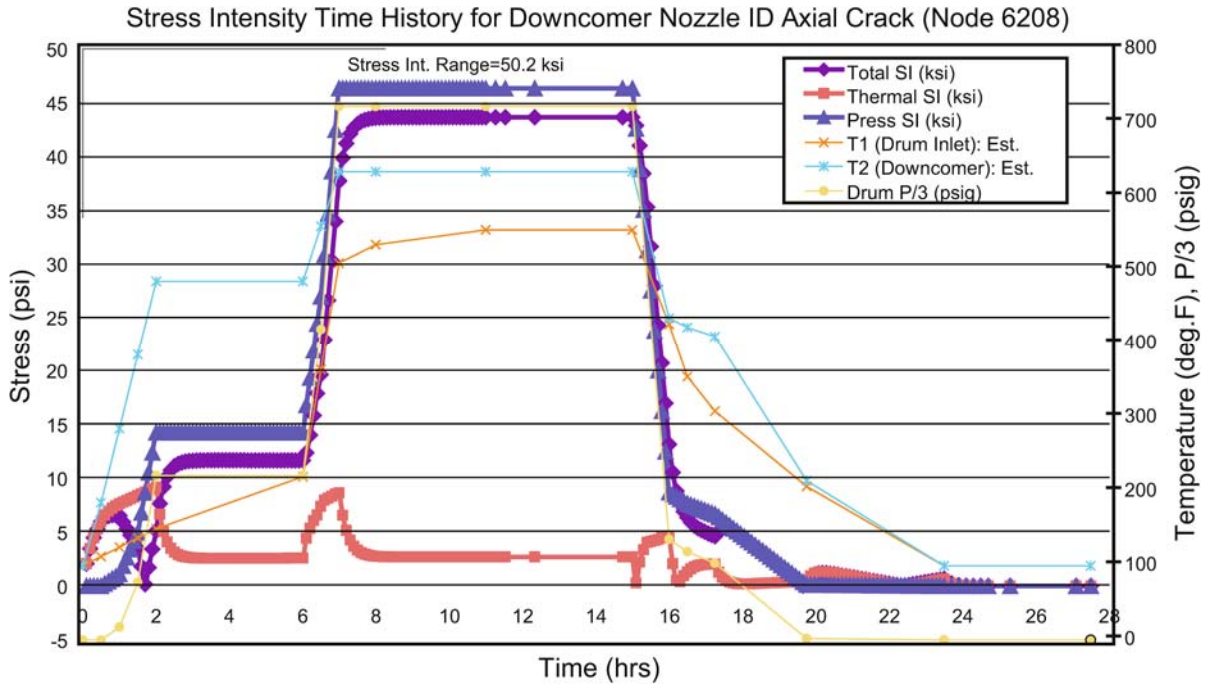
1 ksi = 6.895 MPa

Figure 3-14
Maximum Stress at Downcomer Nozzle ID During Startup/Steady-State/Shutdown Transient



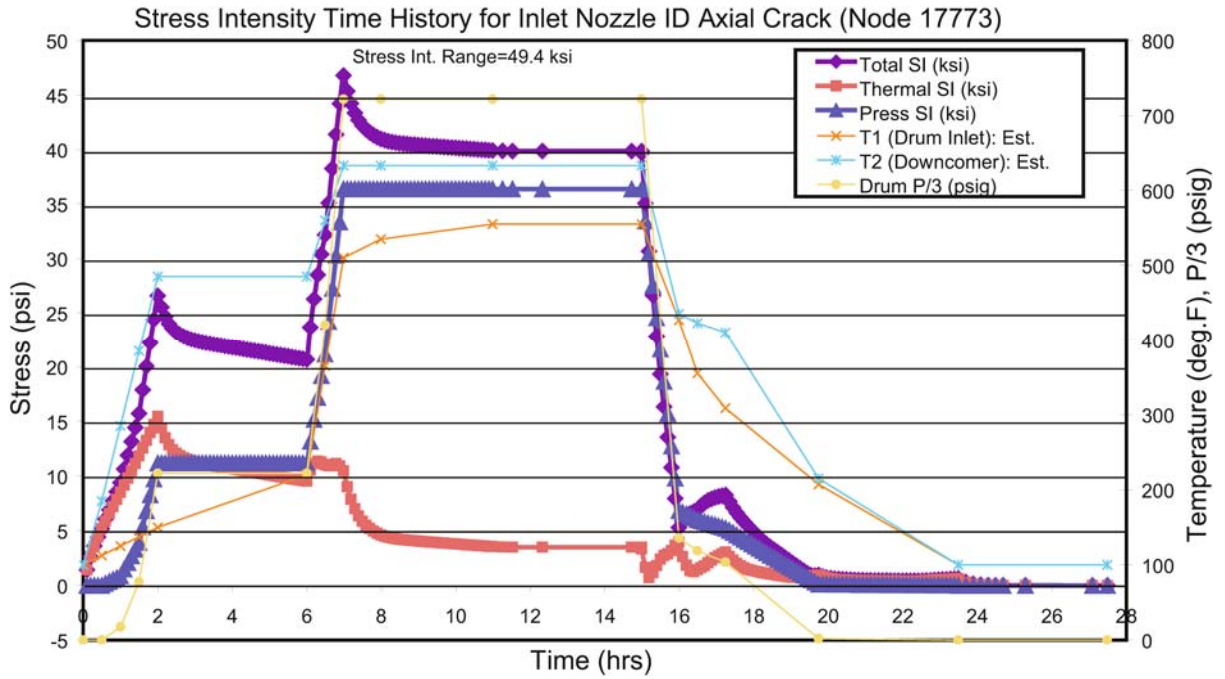
1 ksi = 6.895 MPa

Figure 3-15
Maximum Stress at Inlet Nozzle ID and OD During Startup/Steady-State/Shutdown Transient



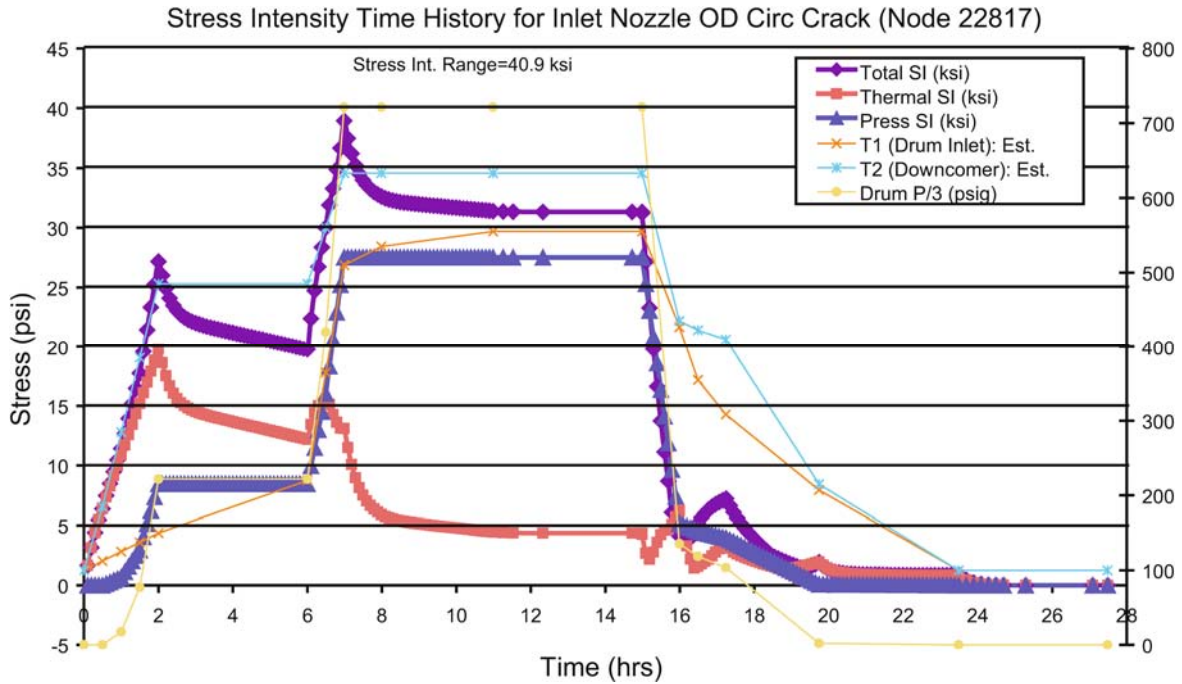
$^{\circ}\text{C} = (^{\circ}\text{F} - 32) \times 5/9$
 1 ksi = 6.895 MPa
 1 psi = 6.89 kPa
 1 psig = 0.06896 bars

Figure 3-16
Downcomer Nozzle ID Stress Response Versus Time



$^{\circ}\text{C} = (^{\circ}\text{F} - 32) \times 5/9$
 1 ksi = 6.895 MPa
 1 psi = 6.89 kPa
 1 psig = 0.06896 bars

Figure 3-17
Inlet Nozzle ID Stress Response Versus Time



$^{\circ}\text{C} = (^{\circ}\text{F} - 32) \times 5/9$
 1 ksi = 6.895 MPa
 1 psi = 6.89 kPa
 1 psig = 0.06896 bars

Figure 3-18
Inlet Nozzle OD Stress Response Versus Time

3.6 Discussion of Finite Element Stress Analysis

Principal conclusions from the FE stress analyses are as follows:

- For normal startup/shutdowns, the stress intensity range is dominated by pressure.
- The thermal stress contribution is minimal when the drum is at full pressure. The position of the maximum thermal stresses is 90° out of phase with pressure stresses for the downcomer nozzle ID, but in-phase with pressure stresses during heatup for the inlet nozzle ID and OD locations.
- The most significant thermal events at full pressure are the loss (bypass) of the string of three high-pressure feedwater heaters and topping off a partially full drum shortly after shutdown, which would result in a thermal stress intensity that would be additive to that due to pressure.

- The project was initiated on the premise that cracking of the large drum nozzles was mainly the result of thermal fatigue. Based on the magnitude of the thermal stresses from the FE stress analysis, these results appear to contradict that premise.
- The top-to-bottom temperature differentials are small for the situations analyzed, and there is no expectation that drum “humping” is an issue of concern.
- A fatigue analysis that attempts to quantify the effect of various types of operational cycles on the fatigue life of the drum is described in the next section of this report.

3.7 References

- 3-1. *Thermal Fatigue of Fossil Boiler Drum Nozzles*. EPRI, Palo Alto, CA: 2005. 1008070.
- 3-2. *Boiler Circulation Study for Tennessee Valley Authority Boilers*, Project No. 76010-A, ABB C-E Services, Inc., May 12, 1993.
- 3-3. Operating data from DataWare system provided by TVA for two 275 MW units with 2000 psig drums built by Combustion Engineering, Inc.
- 3-4. S. C. Stultz and J. B. Kitto, Eds. *Steam, Its Generation and Uses, 40th Edition*. Babcock & Wilcox Co., Barberton, OH 1992.

4

FATIGUE ANALYSIS

4.1 Fatigue Life Methodology

The fatigue life methodology used in this project follows the ASME design-by-analysis codes, Section III, and Section VIII, Div. 2. These codes use a Tresca-equivalent stress theory in which twice the shear stress, called the stress intensity (SI), is the basis for design. For ferritic steels there is a basic premise that the primary membrane stress is controlled to less-than or equal-to two-thirds of the yield strength, and that the primary plus secondary stress range is less-than or equal-to twice the yield strength, assuring shakedown to fully elastic behavior of the gross structure. Thus, only the areas of peak stress may repeatedly incur plasticity, which will be displacement controlled because of the limits imposed on the primary plus secondary stresses.

While components designed to Section I, a design-by-rule code, do not have an associated sophisticated stress analysis to formally classify stresses, it is almost certain that Section I components would fulfill the requirements of the design-by-analysis codes with regard to primary plus secondary stresses. This is particularly true for components designed prior to the late 1990s before the factor on tensile strength was lowered from 4.0 to 3.5. In that era, the allowable stresses for most ferritic steels in the time-independent region were controlled by tensile strength rather than yield strength.

4.1.1 Design Fatigue Curve and Adjustment to Account for Environmental Effects

The design fatigue curve used in this work is from ASME Section VIII, Division 2, Figure 5-110.1 which is applicable to carbon and low-alloy steels with a tensile strength of 80 ksi (551.58 MPa) or less at temperatures of 700°F (371°C) or less [4-1]. The design fatigue curve is based primarily on fully reversed (mean stress equals zero), strain-controlled fatigue tests of small polished specimens. A best fit to the experimental data was obtained by applying the method of least squares to the logarithms of the experimental values. The design stress values were obtained from the best-fit curves by applying a factor of two on stress or a factor of 20 on cycles, whichever was the more conservative at each point. These factors were intended to cover such effects as environment, size effect, and scatter of data; thus, it is not to be expected that a vessel will actually operate safely for 20 times its specified life. While the fatigue data are based on strain controlled tests, for convenience the strain amplitude has been multiplied by the modulus of elasticity and is shown as stress amplitude. Using this practice gives stress amplitudes that exceed the tensile strength in the low-cycle region of the curve, which is an artifact of converting strain amplitude to stress amplitude.

For several decades it has been recognized that the ASME design fatigue curve may not represent sufficient conservatism to account for the worst influence of aqueous environments or steam-water mixtures: the corrosion fatigue effect [4-2]. Corrosion fatigue occurs by the combined actions of cyclic loading and a corrosive environment. In boilers, corrosion fatigue occurs frequently on the water side of economizer tubes and headers; waterwall tubes and headers; and risers, downcomers, and drums, with a preference for regions with increased local stresses. While the mechanisms of crack initiation and growth are complex and not fully understood, there is consensus that the two major factors are strain and water-side environment. Strain excursions of sufficient magnitude to fracture the protective oxide layer play a major role. In terms of the water-side environment, high levels of dissolved oxygen and pH excursions from basic to acid are known to be detrimental. To minimize the potential adverse influence of corrosion fatigue in boiler water circuits, it is desirable to use “best practices” in:

- Design, by minimizing localized strain concentrations
- Control of water chemistry and during layup, by limiting dissolved oxygen and pH excursions
- Operation by conservative startup, shutdown, and turndown practices

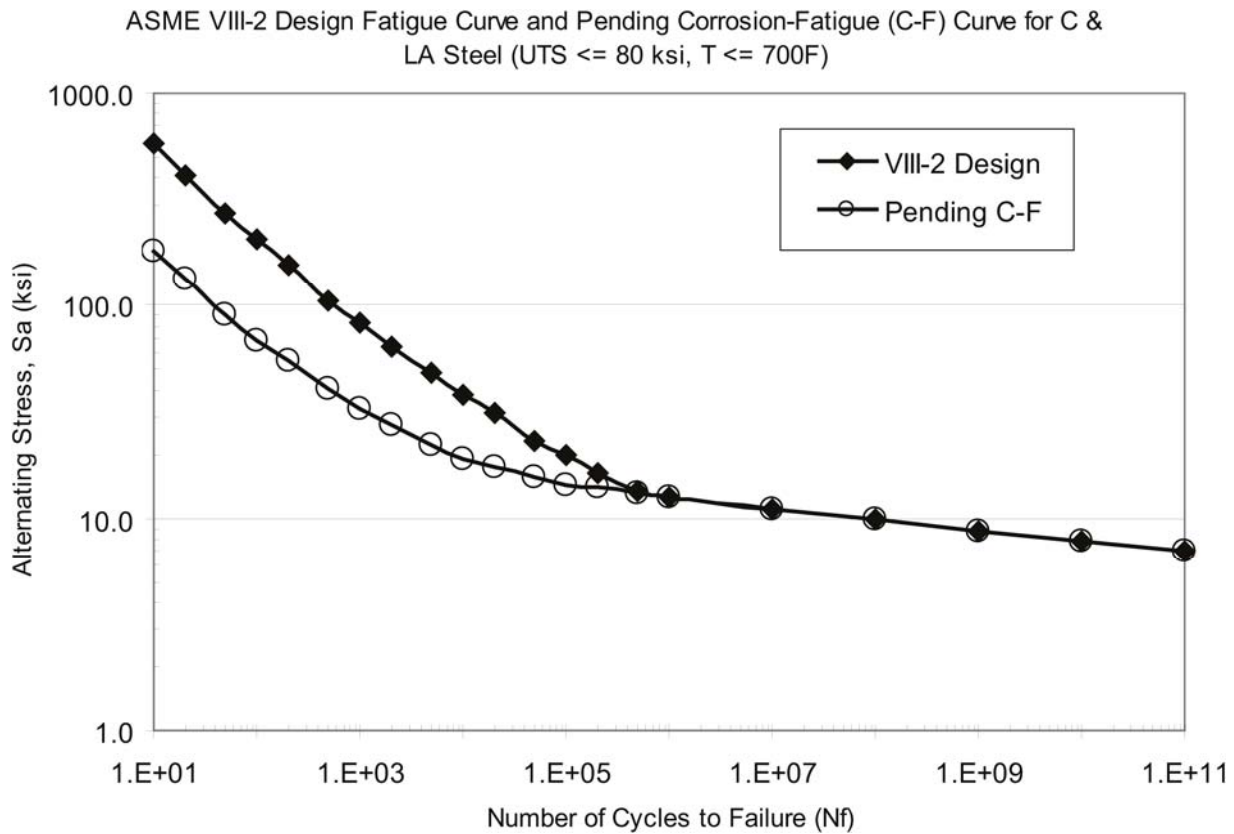
This role of corrosion fatigue is especially important for safe design of light-water nuclear reactor systems. In this regard, the ASME Subgroup on Fatigue Strength, which reports to the Subcommittee on Design, has concluded that the fatigue design curve is applicable under restricted conditions as follows:

- High strain rate ($\dot{\epsilon} \geq 1\%/sec$), or
- Low temperature [$T < 300^\circ F$ ($149^\circ C$)], and
- Low dissolved oxygen (≤ 0.04 ppm)

The emphasis in the research for light water nuclear reactor systems has been in the low cycle region of the curve ($< 1,000,000$ cycles). For very high strain rates the duration of the test is too short for the environment to exert a major influence, but as strain rate is lowered there is an increasing detrimental effect. Based on a review of the published literature [4-3], the Subgroup (SG) on Fatigue Strength has quantified the detrimental influence of decreasing strain rate and has concluded that, at low strain rates ($< \sim 0.0014\%/sec$), there is a saturation effect, and even slower strain rates do not continue to degrade the corrosion fatigue behavior. Thus, a “worst case” curve is being proposed as applicable to light water nuclear reactor systems where good chemical control is the expectation. Figure 4-1 shows the fatigue design curve for ASME Section VIII, Div. 2 and the pending worst case curve for light water nuclear reactor systems proposed by the SG-Fatigue Strength [4-1, 4-3]. The water chemistry practices in fossil power plants are likely to be less stringent than those of light water nuclear plants, and the worst case curve for light water nuclear reactors may still be too optimistic for some fossil power plant scenarios.

Figure 4-2 is based on the same information as that in Figure 4-1 but is shown as alternating stress versus fatigue life ratio (or life reduction factor), defined as the ratio of the number of cycles from the VIII-2 design curve to the number of cycles from the pending corrosion fatigue curve. It should be noted that, at a stress of 12.5 ksi (86.18 MPa), corresponding to 1,000,000

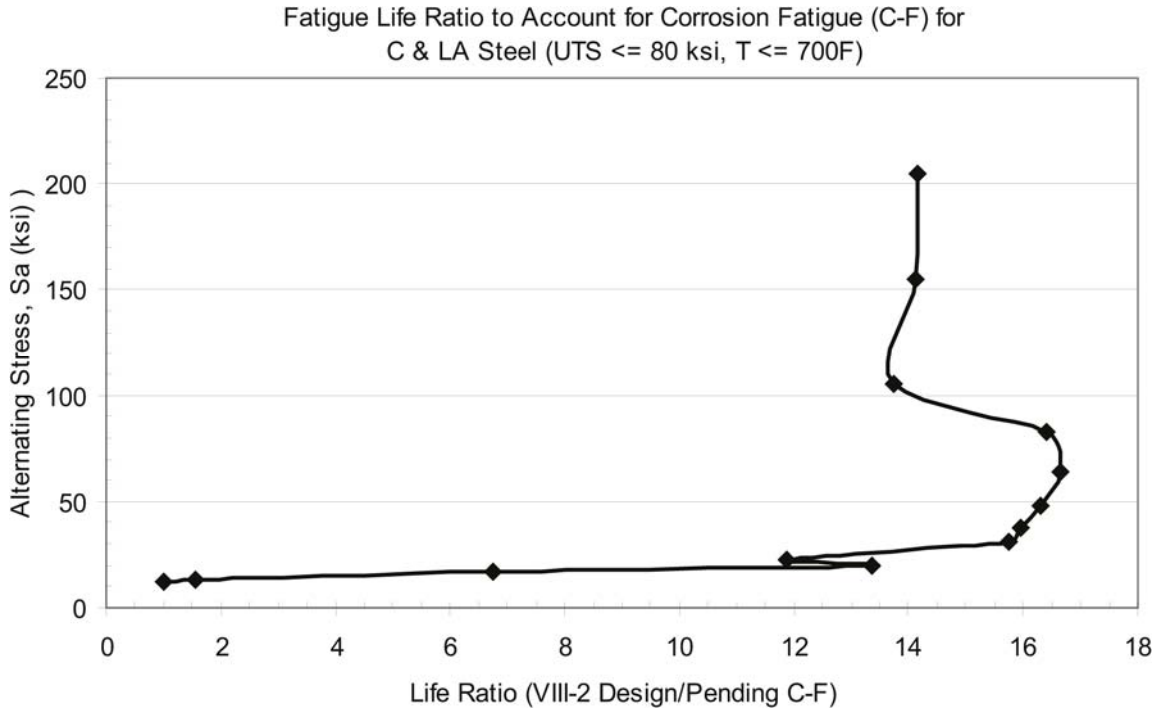
cycles, the two curves merge and the life ratio is 1. As stress increases, the life ratio rises rapidly until attaining values in the range of 14 to 16.7 above an alternating stress of about 27 ksi (186.16 MPa).



1 ksi = 6.895 MPa
 $^{\circ}\text{C} = (^{\circ}\text{F} - 32) \times 5/9$

Figure 4-1
Design Fatigue Curve from ASME Section VIII, Division 2 for Carbon and Low-Alloy Steels and Pending Curve Being Proposed by the Subgroup on Fatigue Strength to Account for Detrimental Effect of Corrosion Fatigue [4-1, 4-3]

If the simple cycle of zero to full pressure and back to zero is considered with the mean stress correction of Equation 4-1 (presented in the next section) using an ultimate tensile strength (UTS) of 70 ksi (482.63 MPa), UTS is essentially unchanged for carbon steels from room temperature to 700°F (371°C), and a maximum stress during the cycle of 39 ksi (268.90 MPa), a mean stress of 19.5 ksi (134.45 MPa), and an alternating stress of 19.5 ksi (134.45 MPa) is achieved. In older plants designed before the late 1990s, the allowable stress for carbon steel with a UTS of 70 ksi (482.63 MPa) was 17.5 ksi (120.66 MPa), giving a nominal operating stress of about 17.0 ksi (117.21 MPa). This leads to a stress concentration factor (SCF) of 2.3 (39/17) or higher as consistent with life reduction factors of 14 to 16.7 from corrosion fatigue. This is noteworthy because corrosion fatigue is generally associated with local areas of stress concentration.



1 ksi = 6.895 MPa
 $^{\circ}\text{C} = (^{\circ}\text{F} - 32) \times 5/9$

Figure 4-2
Fatigue Life Ratio (Life Reduction Factor) to Account for Corrosion Fatigue (CF) Effects in the Low-Cycle Fatigue Range (<1,000,000 Cycles) [4-1, 4-3]

4.1.2 Mean Stress Correction

The fatigue design curves are based on tests involving complete stress reversals, that is, the mean stress, S_m , equals zero. Since the presence of a mean stress component detracts from the fatigue resistance of the material, it is necessary to determine the “equivalent alternating stress” component for zero mean stress before entering the fatigue curve. This equivalent alternating stress, designated S_{aeq} , is the alternating stress component that produces the same fatigue damage at zero mean stress that the actual alternating stress component, S_a , produces at the existing value of mean stress. It can be produced graphically from the Goodman diagram (alternating stress as a function of mean stress) by projecting a line from the ultimate tensile strength, S_u , on the X-axis, through the point (S_m, S_a) to the Y-axis. It is usually easier, however, to use the simple formula [4-4]:

$$S_{aeq} = S_a / [1 - (S_m / S_u)] \quad \text{Eq. 4-1}$$

There is one nuance on correcting the calculated value of mean stress, S'_m , to the adjusted value of mean stress, S_m , herein simply called the mean stress, to correct the situation when the cyclic loading exceeds the yield stress, S_y , any time during the cycle. This correction was not made in the present work for simplicity because the results so obtained are conservative. But for completeness, a definition of the correction is included here [4-4].

$$\text{If } S_a + S'_m \leq S_y, S_m = S'_m \quad \text{Eq. 4-2}$$

$$\text{If } S_a + S'_m > S_y \text{ and } S_a < S_y, S_m = S_y - S_a \quad \text{Eq. 4-3}$$

$$\text{If } S_a \geq S_y, S_m = 0 \quad \text{Eq. 4-4}$$

The curves in Figure 4-1 are based on a room temperature modulus of elasticity of 30.0 E+03 ksi (207 E+03 MPa), and a correction must be made to the alternating stress to be used for life estimates by multiplying it by the ratio of the room temperature modulus to the modulus at the temperature used in the analysis.

4.2 Fatigue Life Estimates Based on the FE Stress Analyses

As discussed in Section 3, the objective of the FE modeling and analysis was to more accurately quantify pressure and thermal stresses that contribute to crack initiation and propagation during operation. Having established the detailed stress distribution for the feedwater inlet nozzles and the downcomer nozzles, this section will focus on the fatigue life estimates for three operating scenarios: (1) normal startup, steady state at full power, and shutdown; (2) bypassing all the high-pressure feedwater heaters at full power; and (3) topping off a full drum shortly after the unit is taken offline from a unit trip but remains at full pressure.

All the analyses use material properties for the nozzles as follows:

- Room temperature minimum specified yield strength = 36 ksi (248.21 MPa)
- Room temperature minimum specified tensile strength = 70 ksi (482.63 MPa)
- Estimated yield strength at 600°F (316°C) = 27.6 ksi (190.30 MPa)
- Estimated tensile strength at 600°F (316°C) = 70 ksi (482.63 MPa)
- Modulus of elasticity at room temperature = 30.0 E+03 ksi (207 E+03 MPa)
- Modulus of elasticity at 600°F (316°C) = 26.5 E+03 ksi (183 E+03 MPa)
- Elastic modulus temperature correction for fatigue curves = 1.132

4.2.1 Normal Startup, Steady-State, and Shutdown Fatigue Analysis

The stresses for this scenario were presented in Section 3.5. The three limiting areas were the downcomer ID, the FW inlet nozzle ID, and the FW inlet nozzle OD at the fillet junction with the drum shell. Note the time history of the stress intensity in Figures 3-16 to 3-18. There are some stress reversals in the time history, and a rigorous treatment of the cycle would require some sort of summation of each subcycle using a method such as “rainflow analysis” to accumulate the total fatigue damage. As a practical matter, the total strain range is one of the cycles in a rainbow analysis, and since it dominates the outcome, only the total strain range is considered in the present analysis. Table 4-1 shows the estimated fatigue lives for these three locations, and Figure 4-3 shows the location on the fatigue life curves.

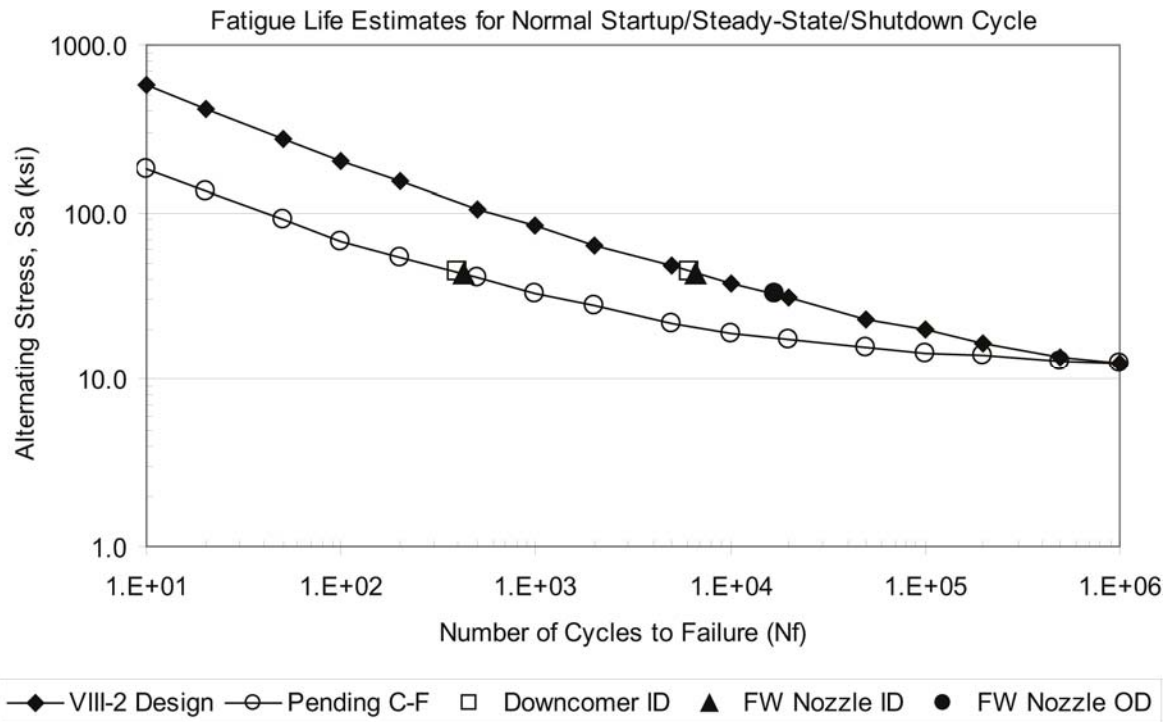
Table 4-1
Estimates of Fatigue Life for Normal Startup, Steady State, and Shutdown

| Item | Location | | |
|--|--------------|--------------------|------------------------------|
| | Downcomer ID | FW Inlet Nozzle ID | FW Inlet Nozzle OD |
| 3D FE Model Stress Intensities: | | | |
| Stress Range, ksi | 50.2 | 49.4 | 40.9 |
| Alt. Stress, S_a | 25.1 | 24.7 | 20.45 |
| Mean Stress, ksi | 25.1 | 24.7 | 20.45 |
| Mean Stress Correction | 1.559 | 1.545 | 1.413 |
| Final Alternating Stress With Modulus and Mean Stress Corrections | | | |
| Equiv. Alt Stress, S_{aeq} , ksi | 44.30 | 43.21 | 32.71 |
| Number of Cycles Based on Design Curve | 6,240 | 6,689 | 17,061 |
| Number of Cycles Based on Pending Corrosion Fatigue Curve | 395 | 426 | 17,061 (No Correction on OD) |

1 ksi = 6.895 MPa

It should be noted that the life estimates for the waterside locations (6240 and 6689 cycles), based on the design fatigue curve, are appreciably higher than expected in 30 years of operation, which is the anecdotal period reported for initial drum cracking. However, when environment is included by using the pending corrosion fatigue curve, life estimates of 395 and 426 cycles for the waterside locations equate to 13 to 14 normal startup and shutdown cycles annually, which is reasonably consistent with utility practices. The life reduction factor for the two waterside locations is 15.8 and 15.7 respectively. These are rather large “correction factors,” and there is

little basis on which to conclude whether a lower factor might be more appropriate. But it is encouraging that the life estimates based on the pending corrosion fatigue curve are nominally “in the ballpark” of reported experience.



1 ksi = 6.895 MPa

Figure 4-3
Fatigue Life Estimates for Normal Startup/Steady-State/Shutdown Cycles Shown on the Design Fatigue Curve and the Pending Corrosion Fatigue Curve

4.2.2 Bypassing a String of High-Pressure Feedwater Heaters at Full Load

In the EPRI research preceding this project [4-5], only three of the 51 units examined were designed to accommodate bypassing individual high-pressure feedwater heaters. In the remaining 48 systems, the high-pressure feedwater heaters have to be bypassed as a string of three heaters. Bypassing of feedwater heaters occurs during three types of operation:

- Performing heater maintenance while the unit is online
- Short-term peaking of megawatts resulting from full flow through the high-pressure turbine when there is no extraction flow
- During boiler trips caused by high or low drum level

During these periods when the feedwater heaters are bypassed, the feedwater temperature to the drum drops substantially, creating additional thermal stresses.

As discussed in Section 3, for convenience a -100°F (-56°C) downshock at the feedwater inlet nozzle, which was reduced by mixing to a -25°F (-14°C) downshock to the downcomer, was analyzed. Since the stresses are linear with the degree of downshock, stresses from other downshocks can be scaled up or down accordingly. As shown in Table 3-1, the severity of the downshock is dependent on the power level at which it occurs, the most severe case being a -164°F (-91°C) downshock at full load.

The stresses for the -164°F (-91°C) downshock are superimposed on those developed for the normal startup/steady-state/shutdown to get the combined effect. The same three locations as previously discussed for the startup/steady-state/shutdown cycle were considered. Table 4-2 shows the estimated lives for these three locations, and Figure 4-4 shows the location on the fatigue life curves.

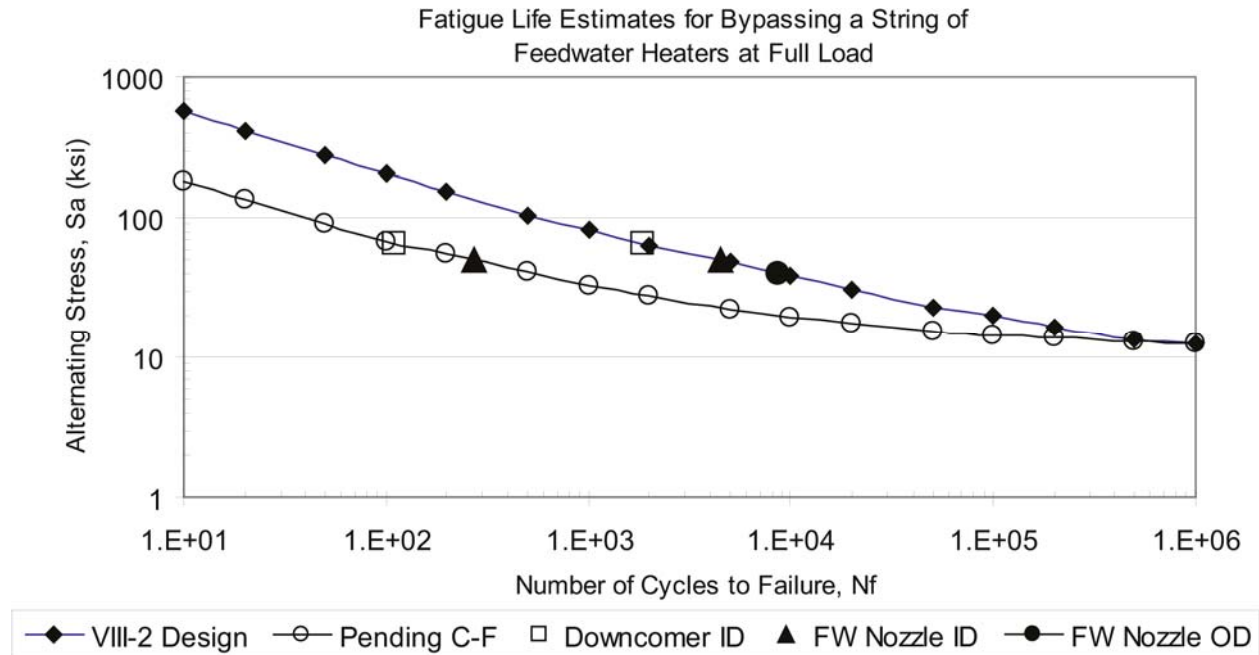
Table 4-2
Estimates of Fatigue Life for Bypassing the Feedwater Heaters at Full Load

| Item | Location | | |
|---|--------------|--------------------|--------------------------------|
| | Downcomer ID | FW Inlet Nozzle ID | FW Inlet Nozzle OD |
| 3D FE Model Stress Intensities with • T = -164°F for Bypassing FW Heaters: | | | |
| Stress Range (SU/SS/SD), ksi | 50.2 | 49.4 | 40.9 |
| Stress Range (FW Bypassed), ksi | 13.28 | 4.59 | 5.9 |
| Total Stress Range, ksi | 63.48 | 53.99 | 46.80 |
| Alt. Stress, S_a | 31.74 | 27.00 | 23.40 |
| Mean Stress, ksi | 31.74 | 27.00 | 23.40 |
| Mean Stress Correction | 1.830 | 1.628 | 1.502 |
| Final Alternating Stress With Modulus and Mean Stress Corrections | | | |
| Equiv. Alt Stress, S_{aeq} , ksi | 65.75 | 49.75 | 39.80 |
| Number of Cycles Based on Design Curve | 1,843 | 4,504 | 8,559 |
| Number of Cycles Based on Pending Corrosion Fatigue Curve | 111 | 273 | 8,559 (No Correction on OD) |

1 ksi = 6.895 MPa

• °C = °F x 5/9

It should be noted that the life estimates of 1843 and 4504 cycles for the waterside locations based on the design fatigue curve are substantially lower than those estimated for the startup/steady-state/shutdown cycle due to the severity of the downshock condition superimposed on normal operation. When environment is included by using the pending corrosion fatigue curve, life estimates of 111 and 273 cycles for the waterside locations are obtained. The life reduction factor for the two waterside locations is 16.6 and 16.5 respectively. These are rather large “correction factors,” and there is little basis to conclude whether a lower factor might be more appropriate. Bypassing of FW heaters is not a common operational event, and these life estimates indicate that it is nominally 1.5 to 3.6 times more damaging than a normal startup/steady-state/shutdown event. These results also indicate that when bypassing is performed, it should be done at part load rather than full load to minimize the severity of the downshock (see Table 3-1).



1 ksi = 6.895 MPa

Figure 4-4
Fatigue Life Estimates for a -164°F (-91°C) Thermal Downshock from Bypassing the Feedwater Heaters at Full Load Shown on the Design Fatigue Curve and the Pending Corrosion Fatigue Curve

4.2.1 Topping Off a Partially Full Drum Shortly Following Unit Trip

Operational events that can lead to low water levels in the drum include malfunctioning controls, massive tube ruptures in the waterwall circuit or superheater circuit, failure of boiler feed pumps, or abnormal recovery from a boiler trip. Events causing boiler trips include exceptionally high or low water level in the drum. If the drum gets dry or nearly so, prudent operation should necessitate a delay in filling the drum until it has cooled down substantially. Nevertheless, it is not an uncommon operational error to fill a dry drum with feedwater since retention of drum water level is critical to avoid overheating the waterwall tubes.

Shortly after an emergency shutdown, while the unit is at full pressure, the decreasing temperature of water in the drum causes a reduction in water level, which prompts topping off the drum to keep the level within the sight glass. Ideally, this action should be done slowly, using the lowest available flow from a single boiler feed pump (BFP). However, the assumption in this simulation is that a rapid fill occurs, causing a rapid thermal downshock at full pressure. The feedwater temperature exiting the BFP and entering the drum was assumed as that associated with 19% of full power from the heat balance diagrams; that is, it was assumed that there would be no heat pickup in the feedwater heaters of the economizer. From Table 3-1 it will be noted that the BFP exit temperature is 242°F (117°C) for this situation. It is additionally assumed that the entire drum comes to an equilibrium temperature of 648°F (342°C) at full pressurization of 2165 psig (149.30 bars) prior to the topping off event, giving a downshock of -406°F (226°C). As in the feedwater heater example, it was also assumed that mixing would reduce the severity

of the downshock to the downcomer to -101.5°F (-56°C). The final assumption was that the stress intensities preceding the downshock were those associated only with drum pressurization.

The stresses for the -406°F (-226°C) downshock are superimposed on those developed for the pressurization to get the combined effect. The same three locations previously discussed for the bypassing of feedwater heaters were considered. Table 4-3 shows the estimated lives for these three locations, and Figure 4-5 shows the location on the fatigue life curves.

Table 4-3
Estimates of Fatigue Life for Topping Off a Partially Full Drum Shortly Following Unit Trip

| Item | Location | | |
|---|---------------|--------------------|------------------------------|
| | Downcomer ID | FW Inlet Nozzle ID | FW Inlet Nozzle OD |
| 3D FE Model Stress Intensities (With • T= -406° F for Topping Off Drum): | | | |
| Stress Range (Pressurization), ksi | 46.4 | 36.5 | 27.5 |
| Stress Range (Topping Off), ksi | 32.88 | 11.36 | 14.61 |
| Total Stress Range, ksi | 79.28 | 47.86 | 42.11 |
| Alt. Stress, S_a | 39.64 | 23.93 | 21.06 |
| Mean Stress, ksi | 39.64 | 23.93 | 21.06 |
| Mean Stress Correction | 2.306 | 1.519 | 1.430 |
| Final Alternating Stress With Modulus and Mean Stress Corrections | | | |
| Equiv. Alt Stress, S_{aeq} , ksi | 103.46 | 41.16 | 34.09 |
| Number of Cycles Based on Design Curve | 522 | 7,708 | 14,837 |
| Number of Cycles Based on Pending Corrosion Fatigue Curve | 38 | 494 | 14,837 (No Correction on OD) |

1 ksi = 6.895 MPa

• °C = •°F x 5/9

It should be noted that the downcomer is by far the most critical of the three components. Additionally, the life estimate for the downcomer is unrealistically short when the environmental effect is included. This pessimism is largely the result of failure to include consideration of yield strength in the mean stress correction from Equations 4-3 and 4-4 and using the more conservative estimate from Equation 4-1. Topping off the drum water level as described is a relatively frequent operational event, and these life estimates indicate that for the downcomer it is approximately 10.4 times more damaging than a normal startup/steady-state/shutdown event.

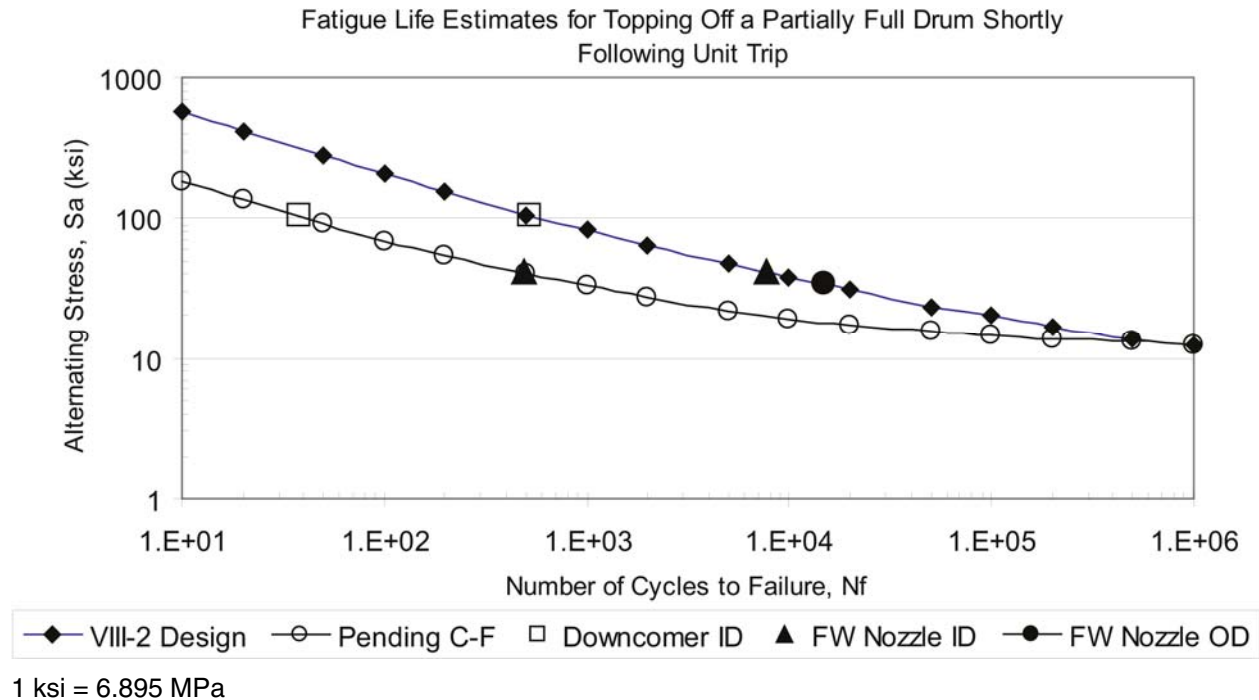


Figure 4-5
Fatigue Life Estimates for a -406°F (-226°C) Thermal Downshock from Topping Off a Partially Full Drum Shortly Following Unit Trip Shown on the Design Fatigue Curve and the Pending Corrosion Fatigue Curve

4.3 Discussion of Fatigue Analysis

In terms of component ranking, all three fatigue analyses showed a consistent ranking in which the downcomer ID was most critical, the FW inlet ID was second, and the FW inlet OD was least critical. This ranking is consistent with the experience reported in the original 2002 EPRI report for TransAlta Wabamun Unit 4, which was largely the basis for follow-up work. This consistency is likely confined to controlled circulation units in which there are a small number of large-diameter downcomers. The effectiveness of the feedwater nozzle thermal sleeve is validated by the substantially longer fatigue life estimates for that component.

The life estimates for a normal startup/steady state/shutdown based on the design fatigue curve were unrealistic in terms of the cracking typically observed after 30 or more years of service. However, application of a pending curve to account for corrosion fatigue provided life estimates that were reasonably consistent with experience.

The two thermal downshock scenarios (bypassing a string of high-pressure FW heaters and topping off a partially full drum) produced life estimates for the downcomer that appear to be unrealistically pessimistic, especially when using the pending corrosion fatigue curve to account for the environmental effect. This pessimism is largely the result of failure to include consideration of yield strength in the mean stress correction from Equations 4-3 and 4-4 and using the more conservative estimate from Equation 4-1.

Considering the number of cycles for the startup/steady-state/shutdown event for the downcomer ID location as unity, bypassing the FW heaters is equivalent to 3.6 times more cycles, and topping off the drum is equivalent to 10.4 times more cycles. Prudence should be exercised in operation to minimize the degree of downshock associated with these events.

While turndown was not analyzed in terms of thermal fatigue in the current project, the previous work [4-5] concluded that the “100% to 25% to 100%” load swing simulation was equivalent to 0.37 startup/steady-state/shutdown cycles; thus, it appears that the worst operating scenarios were covered in the current project.

Finally, regardless of the sophistication of the stress analysis, the estimated lives are critically dependent on corrosion fatigue, and life reduction factors on the order of 5 to 20 appear to be necessary to explain actual service experience in various components in fossil boilers. The pending corrosion fatigue curve developed by the ASME Subgroup on Strength [4-2, 4-3] is a step in the right direction and predicts factors from 14 to 16.7 in regions of appreciable stress concentration ($SCF = 2.3$). However, additional work is needed to validate the approach and to “hone in” on the factors appropriate to particular operating practices.

4.4 References

- 4-1. *ASME Boiler and Pressure Vessel Code: An International Code, Section VIII, Division 2, Alternative Rules for Construction of Pressure Vessels, 2004 Edition*. American Society of Mechanical Engineers, New York, NY 2004.
- 4-2. Personal communications between B.W. Roberts and Dr. William J. O’Donnell, Chair of ASME Subgroup on Fatigue Strength, May 26, 2005.
- 4-3. William James O’Donnell, William John O’Donnell, and Thomas P. O’Donnell, “Proposed New Fatigue Design Curves for Carbon and Alloy Steels in High Temperature Water.” Paper PVP2005-71410, 2005 ASME Pressure Vessel and Piping Conference, Denver, CO, July 17–21, 2005.
- 4-4. *Criteria of the ASME Boiler and Pressure Vessel Code for Design by Analysis in Sections III and VIII, Division 2*. ASME Press, New York, NY 1969.
- 4-5. *Thermal Fatigue of Fossil Boiler Drum Nozzles*. EPRI, Palo Alto, CA: 2005. 1008070.
- 4-6. *Thermal Fatigue Cracking of Boiler Drums*. EPRI, Palo Alto, CA: 2002. 1004614.

5

FRACTURE MECHANICS ANALYSIS

The objective of the fracture mechanics analysis was two-fold: to estimate critical crack size for normal operation and hydro test conditions, and to estimate the number of cycles required to propagate a known or suspected crack to critical size for typical pressure and thermal cyclic loads. Key elements of the fracture mechanics analyses—fracture toughness, crack models, crack tip stress intensity factors, and crack growth—will be described in this chapter.

5.1 Fracture Toughness

For the purpose of this study, the application of a linear elastic fracture mechanics (LEFM) approach will be demonstrated first because of its conservatism and suitability to address brittle fracture of typical 1950s-vintage drum materials during hydrostatic test conditions when temperatures are coldest and fracture toughness is at its lowest.

A detailed compilation of plane-strain fracture toughness (K_{Ic}) for materials typically used in drums is contained in the report for the first phase of this research project [5-1]. The fabrication material for the two 275 MW CE drums selected for this study was reported to be SA-212 Grade B carbon steel. Drum-specific fracture toughness data or grain refinement information was not available for these two units that went into commercial operation in 1959. Based on the vintage of these units, it is most likely that the melting practice of that era produced material of a coarse grain (CG) size, which has inferior toughness to materials produced with fine grain (FG) practice. The compilation of fracture toughness versus temperature data from EPRI report 1008070 [5-1] applicable to SA-212 Gr. B CG material is reproduced as Figure 5-1. A summary of K_{Ic} estimates for CG material at room temperature (70°F [21.11°C]) is given in Table 5-1.

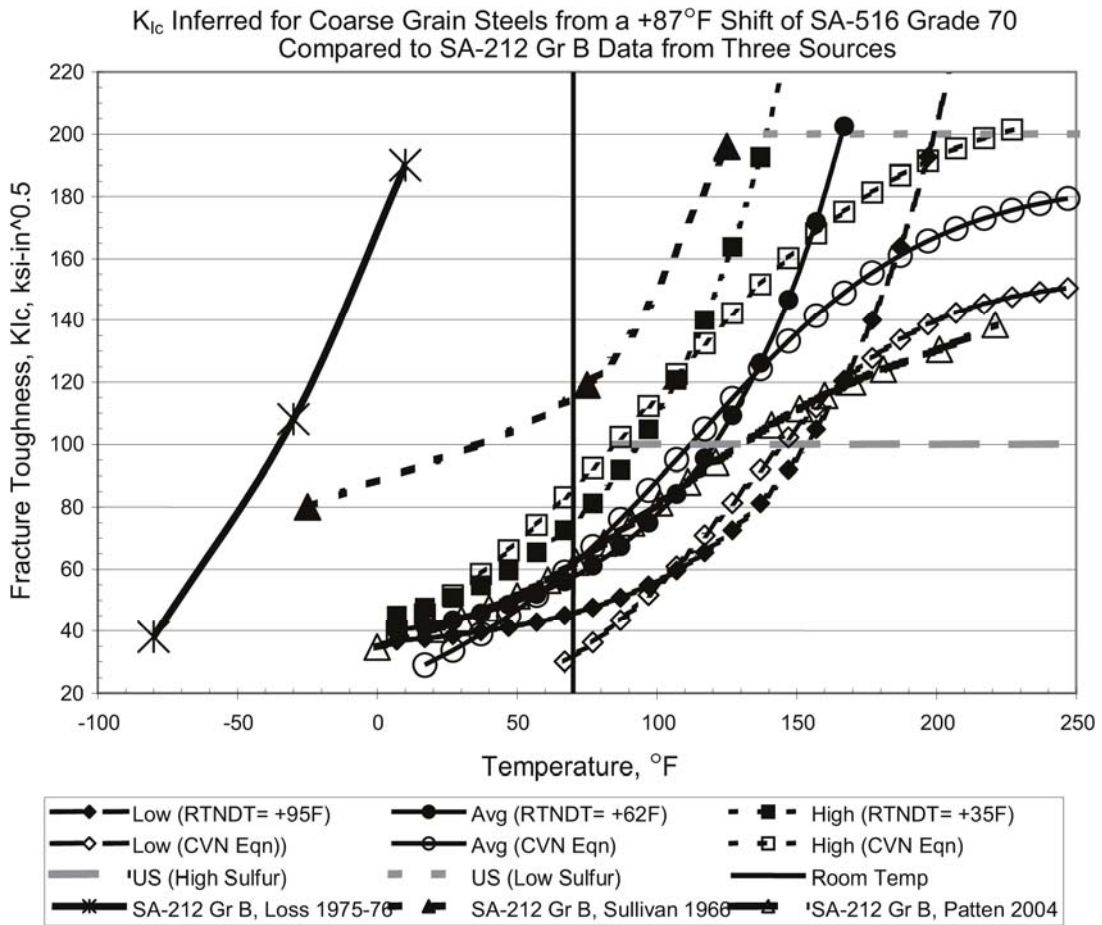
Table 5-1
Summary of Fracture Toughness Estimates, K_{Ic} , for Coarse Grain Carbon Steels at Room Temperature [5-1]

| Material and Melting Practice | K_{Ic} at 70°F (21.11°C), ksi√inch |
|--|--------------------------------------|
| CG Low (SA-516 Gr 70 +87°F [30.55°C]) | 45.8 |
| CG Low (SA-299 +87°F [30.55°C]) | 46.1 |
| CG Avg (SA-516 Gr 70 +87°F [30.55°C]) | 59.1 |
| CG Avg (SA-299 +87°F [30.55°C]) | 69.4 |
| CG High (SA-516 Gr 70 +87°F [30.55°C]) | 83.1 |
| CG High (SA-299 +87°F [30.55°C]) | 99.6 |

1 ksi√inch = 1.099 MPa√m

Based on these data, the lowest estimate for room temperature fracture toughness is 45.8 ksi√inch (50 x 10⁶ MPa√m). At normal drum operating temperatures, which are well in excess of 200°F (93.33°C), fracture toughness values are at the upper shelf. Upper-shelf fracture toughness values are primarily controlled by sulfur level, and it is recommended that the highest value be limited to 100 ksi√inch (109 MPa√m) for high sulfur steels and 200 ksi√inch (218 MPa√m) for low sulfur steels.

These fracture toughness estimates will be used in the determination of critical crack size for brittle failure.



1 ksi = 6.895 MPa

• °C = •°F x 5/9

Figure 5-1
Inferred Fracture Toughness for Coarse Grain Steel by a +87°F (48°C) Shift in Temperature of the SA-516 Grade 70 Steel with Independent Data for SA-212 Grade B CG Steel [5-1]

5.2 Crack Locations, Crack Models, and Stresses

5.2.1 Crack Locations

Based on the results of the FE stress analysis presented in Section 3, three potential crack initiation sites were identified for the fracture mechanics analysis. These locations are illustrated in Figure 5-2 and are summarized next.

Location 1: This location represents the most likely crack initiation site at the downcomer nozzle ID, which is oriented axially, normal to the direction of the maximum expected hoop stress due to internal pressure.

Location 2: This location represents a possible crack initiation site at the downcomer nozzle ID, which is oriented circumferentially, normal to the direction of the maximum expected axial stress due to thermal shock.

Location 3: This location represents the most likely crack initiation site at the inlet nozzle ID, which is oriented axially, normal to the direction of the maximum expected hoop stress dominated by internal pressure.

The inlet nozzle OD cracking location was not evaluated because there is no contact with two-phase steam-water fluid and corrosion fatigue is not expected at this location.

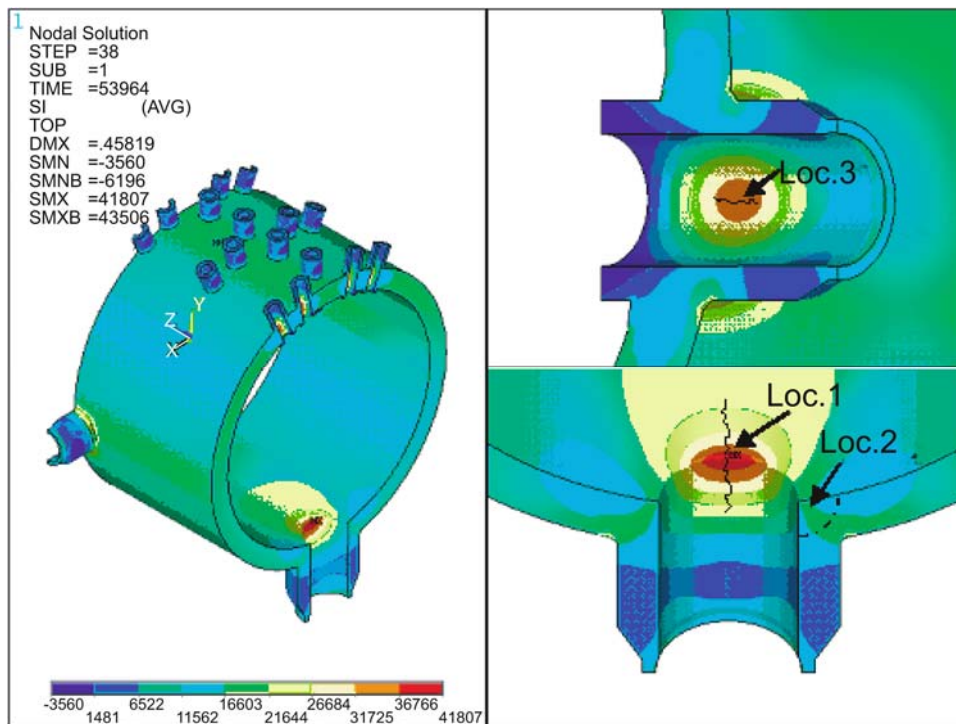


Figure 5-2
Crack Locations in Drum Identified for Fracture Mechanics Analysis

5.2.2 Crack Models

Two types of crack models were selected.

5.2.2.1 Part-Through-Wall Cracks

Part-through-wall crack models, shown in Figure 5-3, were selected to represent the early stages of crack propagation from the ID toward the OD. The quarter-elliptical nozzle corner crack model (Figure 5-3a) is a good representation of the downcomer nozzle ID cracks (Locations 1 and 2). The semi-elliptical axially oriented crack at the ID in a cylinder is applicable to longer ID surface part-through-wall cracks in the main drum body near the downcomer and at the inlet nozzle. Through-wall stress gradients for the part-through-wall cracks were extracted from the FE stress results presented in Section 3 and are shown in Figure 5-4.

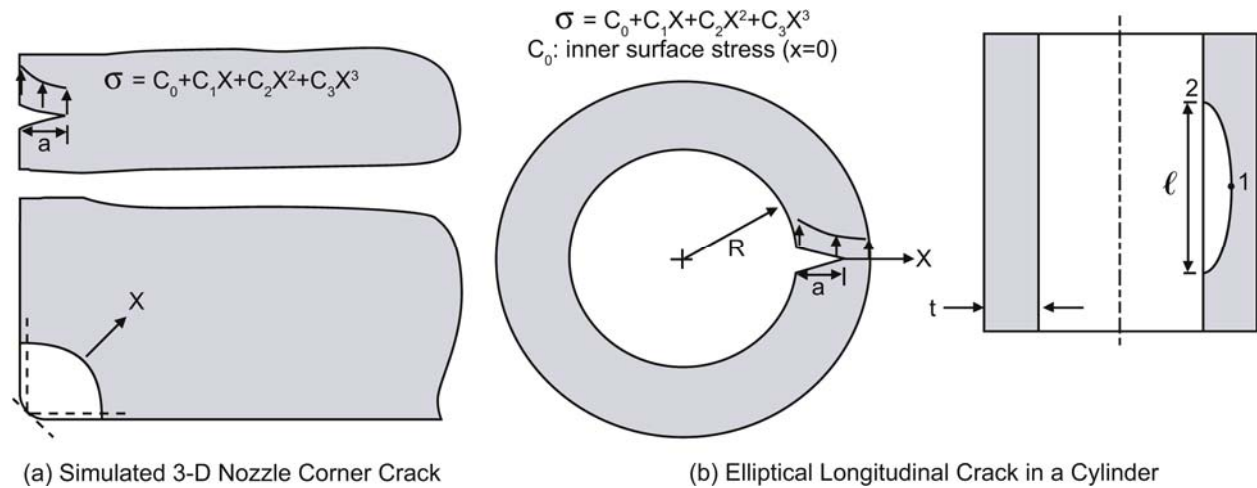
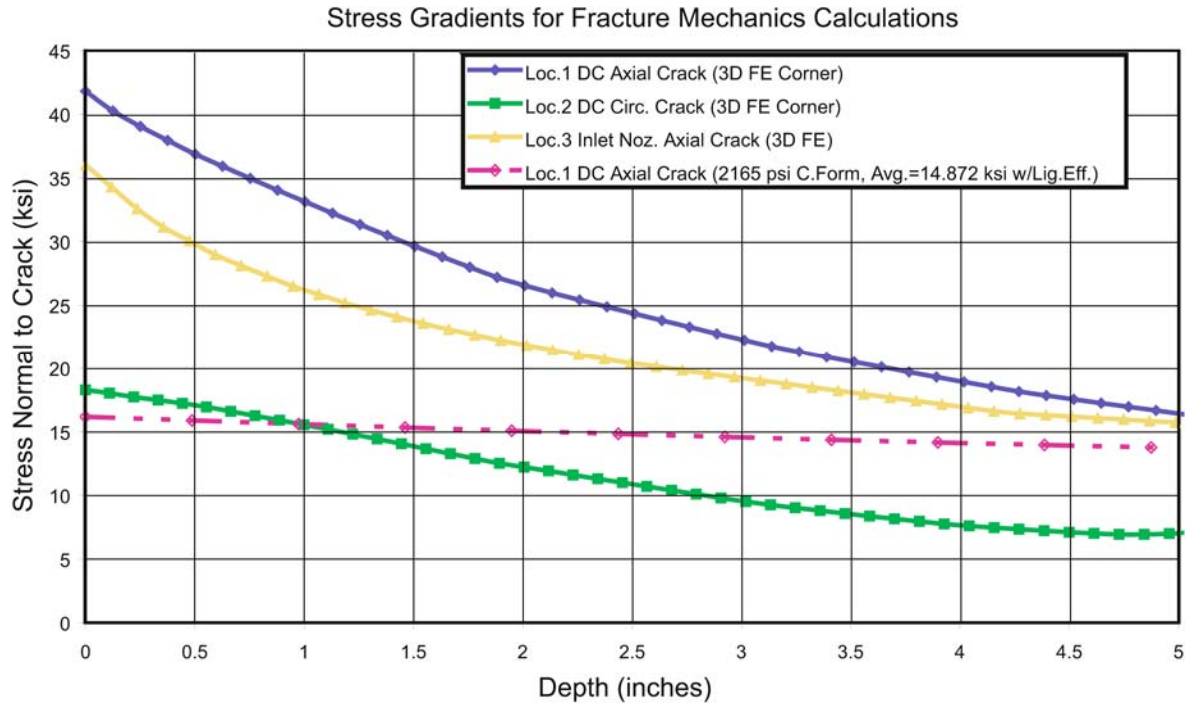


Figure 5-3
Part-Through-Wall Crack Models: (a) Quarter-Elliptical Nozzle Corner Crack, (b) Semi-Elliptical Crack at the ID of a Cylinder



1 in. = 25.4 mm
 1 ksi = 6.895 MPa
 1 psi = 6.89 kPa

Figure 5-4
Stress Gradients for Part-Through-Wall Crack Models

5.2.2.2 Through-Wall Cracks

The through-wall axial crack in a pressurized cylinder model (Figure 5-5) was used to assess the stability of a crack that has propagated through the drum wall resulting in a leak; that is, for a leak-before-break scenario. Only primary membrane stresses due to internal pressure are needed for input to this crack model. The average through-wall hoop stress was calculated as follows:

$$\sigma_{average} = \frac{pR_i}{t} = \frac{2165 \text{ psi} \times 30''}{4.875''} = 13.323 \text{ ksi} \quad \text{Eq. 5-1}$$

13.323 ksi = 91.9 MPa

Accounting for an axial ligament efficiency between downcomer nozzles $(108'' - 11.25'')/108'' = 89.6\%$ $([274.32 \text{ cm} - 28.58 \text{ cm}]/274.32 \text{ cm} = 89.6\%)$ yields an average through-wall ligament hoop stress of 14.872 ksi (102.54 MPa).

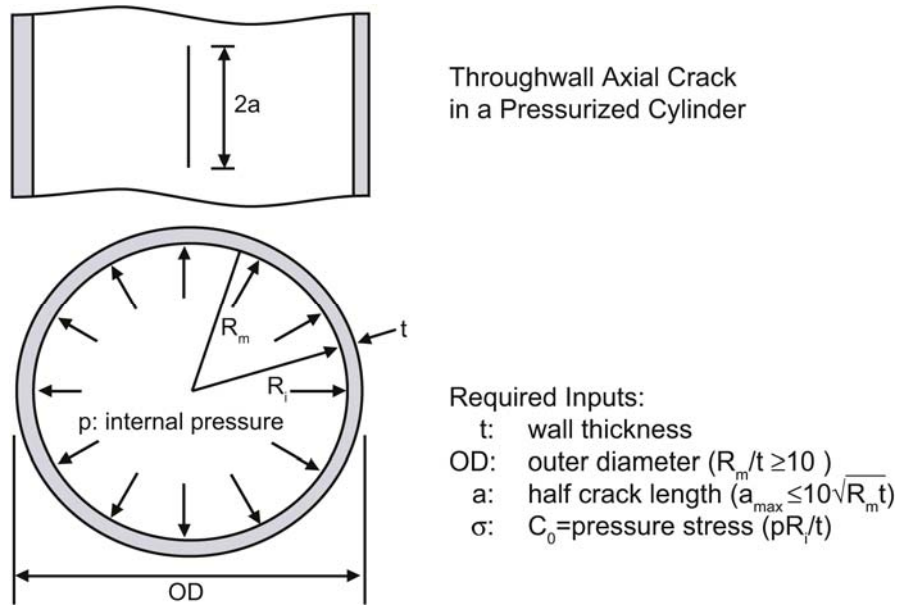


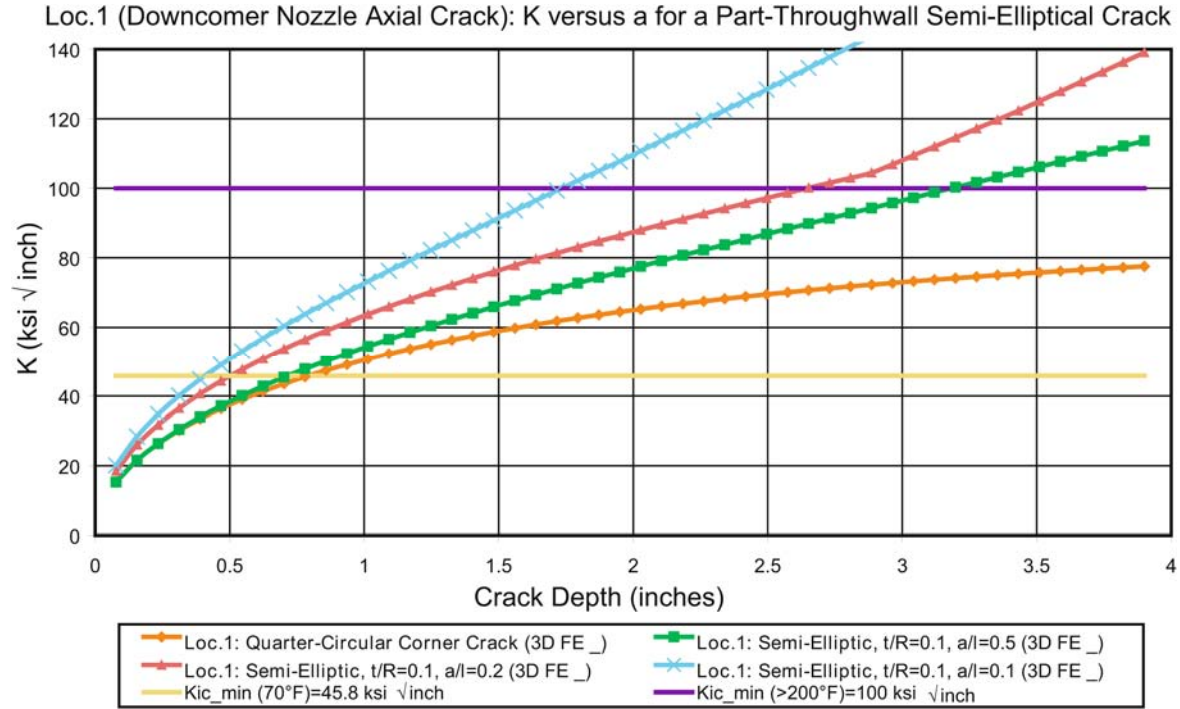
Figure 5-5
Through-Wall Axial Crack in a Pressurized Cylinder Model

5.3 LEFM Crack Tip Stress Intensity Factors and Critical Size

Crack tip stress intensity factors (K_I) versus crack size (a) for the crack models and stress distributions described earlier were calculated using Structural Integrity Associates' general purpose fracture mechanics software program, *pc-CRACK* [5-2]. Results are shown in Figures 5-6 through 5-9.

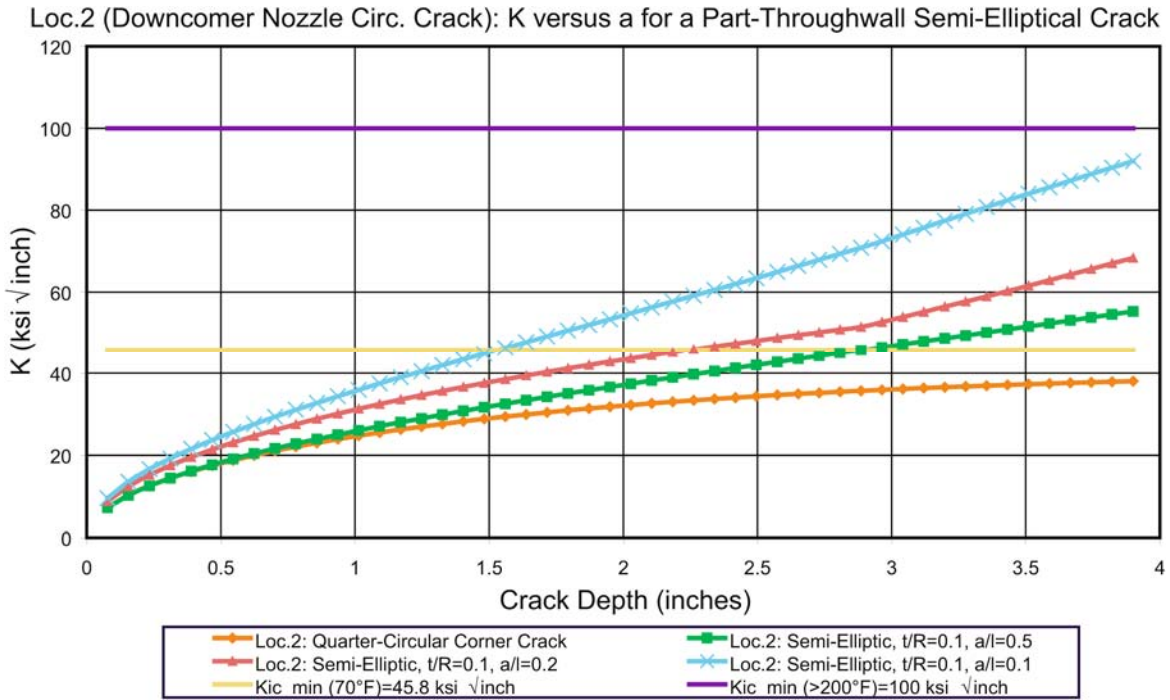
K_I versus a results for part-through-wall cracks (Figures 5-6, 5-7, 5-8) include a range of crack depth-to-length (a/l) ratios of 0.5 (semi-circular) to 0.1 (1:10). The quarter-circular corner crack model yields the lowest calculated K_I values because it does not include a correction for finite-width effects; it is therefore nonconservative for larger crack depths. The semi-elliptical crack in a cylinder model is conservative because the crack model formulation is for a thickness-to-inside-radius (t/R_i) ratio of 0.1, which is much lower than the actual drum geometry (t/R_i) ratio of 0.163 ($t=4.875$, $R_i=30"$ [76.2 cm]).

K_I versus a results for an axial through-wall crack (Figure 5-9) also includes the flat plate solution ($K_I = \sigma\sqrt{\pi a}$) to illustrate that this simple solution is nonconservative because it does not include shell curvature effects.



1 in. = 25.4 mm
 $^{\circ}\text{C} = (^{\circ}\text{F} - 32) \times 5/9$
 1 ksi√inch = 1.099 MPa√m

Figure 5-6
 Location 1 (Downcomer Axial Crack): KI versus a Results for a Part-Through-Wall Crack



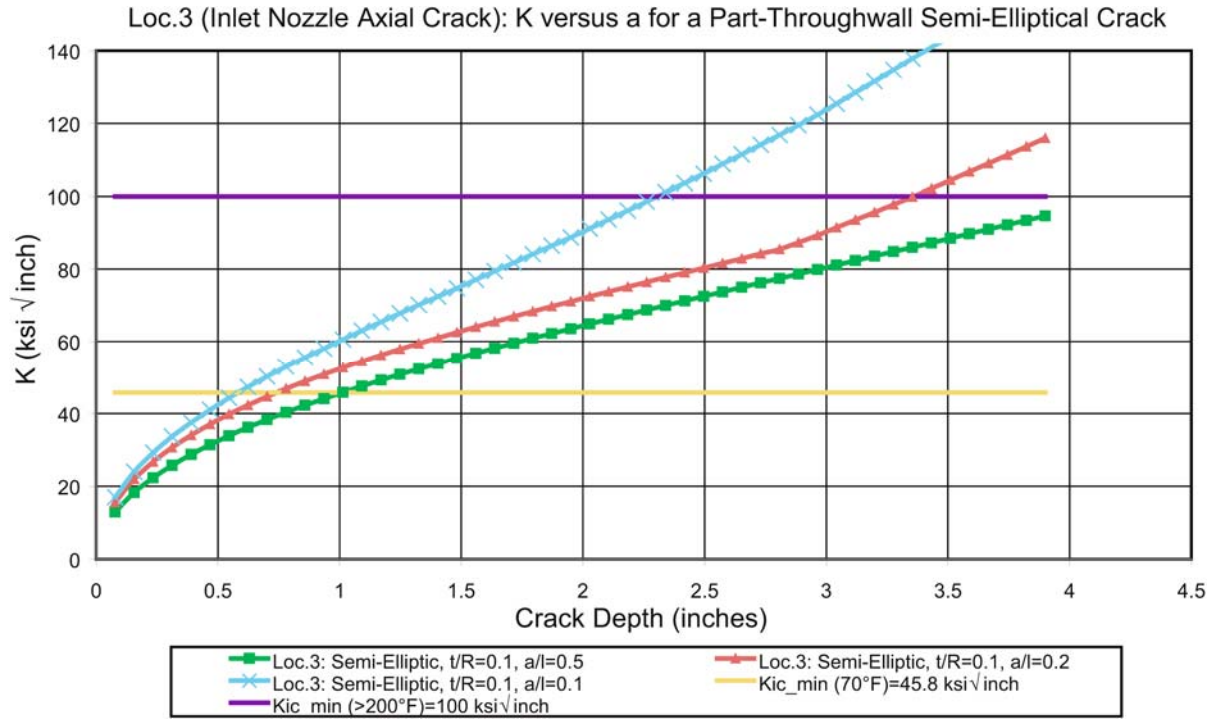
1 in. = 25.4 mm

°C = (°F-32) × 5/9

1 ksi√inch = 1.099 MPa√m

Figure 5-7

Location 2 (Downcomer Circ. Crack): K_I versus a Results for a Part-Through-Wall Crack



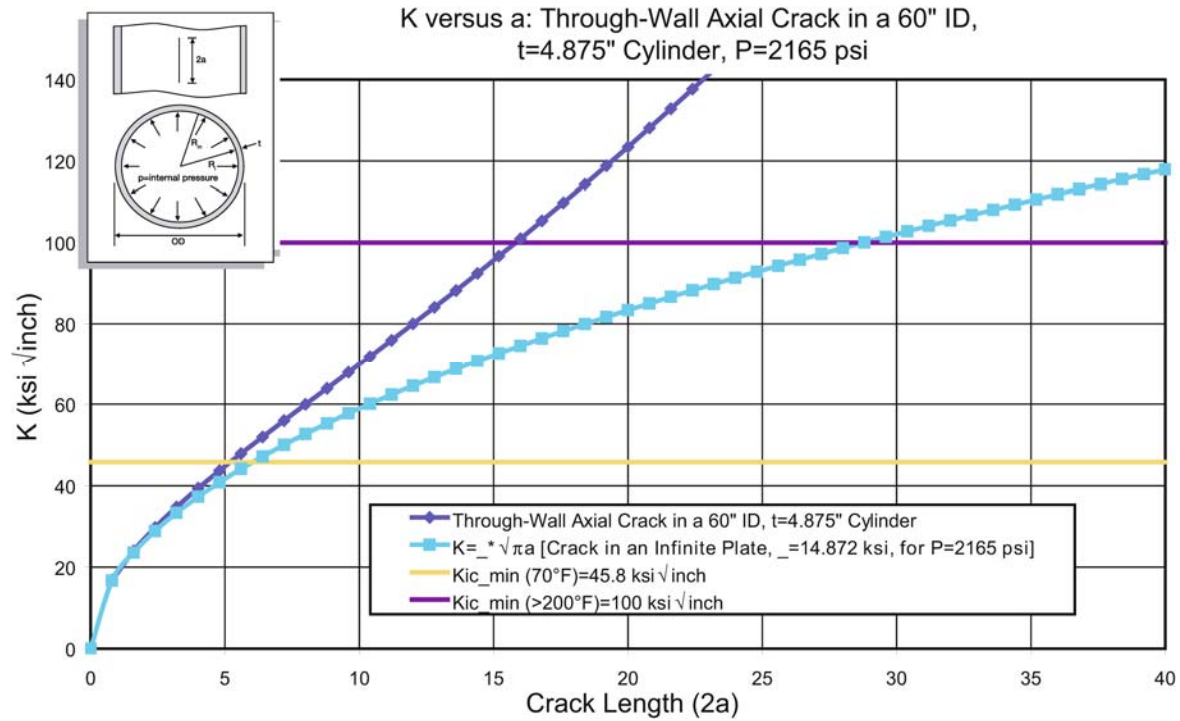
1 in. = 25.4 mm

$^{\circ}\text{C} = (^{\circ}\text{F} - 32) \times 5/9$

1 ksi√inch = 1.099 MPa√m

Figure 5-8

Location 3 (Inlet Nozzle Axial Crack): KI versus a Results for a Part-Through-Wall Crack



1 in. = 25.4 mm
 $^{\circ}\text{C} = (^{\circ}\text{F} - 32) \times 5/9$
 1 $\text{ksi}\sqrt{\text{inch}} = 1.099 \text{ MPa}\sqrt{\text{m}}$
 1 psi = 6.89 kPa

Figure 5-9
 K_I versus a Results for an Axial Through-Wall Crack in the Drum

Critical crack depths in Table 5-2 are applicable during normal operation when upper-shelf fracture toughness values in the range of 100–200 $\text{ksi}\sqrt{\text{inch}}$ (109–220 $\text{MPa}\sqrt{\text{m}}$) can be expected.

Table 5-2
Summary of Critical Crack Sizes (Inches) During Normal Operation for Upper-Shelf Fracture Toughness Values Ranging from 100–200 $\text{ksi}\sqrt{\text{inch}}$ (109–220 $\text{MPa}\sqrt{\text{m}}$)

| | K_{ic_min} (>200°F [93.33°C])=100 $\text{ksi}\sqrt{\text{inch}}$ (109 $\text{MPa}\sqrt{\text{m}}$) | | | | K_{ic_max} (>200°F [93.33°C])=200 $\text{ksi}\sqrt{\text{inch}}$ (220 $\text{MPa}\sqrt{\text{m}}$) | | | |
|--------------|--|-----------|-----------|--------------|--|-----------|-----------|--------------|
| | $a/l=0.5$ | $a/l=0.2$ | $a/l=0.1$ | Through-Wall | $a/l=0.5$ | $a/l=0.2$ | $a/l=0.1$ | Through-Wall |
| Loc. 1 | 3.184 | 2.647 | 1.733 | -- | >3.900 | >3.900 | >3.900 | -- |
| Loc. 2 | >3.900 | >3.900 | >3.900 | -- | >3.900 | >3.900 | >3.900 | -- |
| Loc. 3 | >3.900 | 3.359 | 2.307 | -- | >3.900 | >3.900 | >3.900 | -- |
| Through-Wall | -- | -- | -- | 15.821 | -- | -- | -- | 32.001 |

Critical crack depths in Table 5-3 are applicable to cold hydrostatic test conditions when fracture toughness values in the range of 45.8 to 100 ksi $\sqrt{\text{inch}}$ (50–109 MPa $\sqrt{\text{m}}$) at room temperature can be expected.

Table 5-3
Summary of Critical Crack Sizes (Inches) for a 1.5X Cold Hydro and Room Temperature Fracture Toughness Values Ranging from 45.8–100 ksi $\sqrt{\text{inch}}$ (50–109 MPa $\sqrt{\text{m}}$)

| | 1.5X Hydro K_{Ic} min (70°F [21.11°C])= 45.8 ksi $\sqrt{\text{inch}}$ (50 MPa $\sqrt{\text{m}}$) | | | | 1.5X Hydro K_{Ic} max (70°F [21.11°C])= 100 ksi $\sqrt{\text{inch}}$ (109 MPa $\sqrt{\text{m}}$) | | | |
|--------------|---|---------|---------|--------------|---|---------|---------|--------------|
| | a/l=0.5 | a/l=0.2 | a/l=0.1 | Through-Wall | a/l=0.5 | a/l=0.2 | a/l=0.1 | Through-Wall |
| Loc. 1 | 0.307 | 0.214 | 0.179 | -- | 1.497 | 1.129 | 0.851 | -- |
| Loc. 2 | >3.900 | 3.828 | 3.061 | -- | >3.900 | >3.900 | >3.900 | -- |
| Loc. 3 | 0.708 | 0.524 | 0.419 | -- | 3.340 | 2.879 | 1.918 | -- |
| Through-Wall | -- | -- | -- | 2.525 | -- | -- | -- | 9.352 |

5.3.1 Discussion

For a conservative (worst case) upper-shelf fracture toughness of 100 ksi $\sqrt{\text{inch}}$ (109 MPa $\sqrt{\text{m}}$) during normal operation, part-through-wall critical crack sizes (see Table 5-2) are greater than 3 inches (7.62 cm) (>60% of wall) for typical semi-circular cracks. For a very long (10:1) semi-elliptical axial crack at Location 1, the critical crack depth predicted was 1.733 inches (4.40 cm) (36% of wall). Through-wall axial crack lengths in the range of 15.8 to 32.0 inches (40.13 to 81.28 cm) can be tolerated before brittle failure. Therefore, the most likely scenario during normal operation is a leak before final failure.

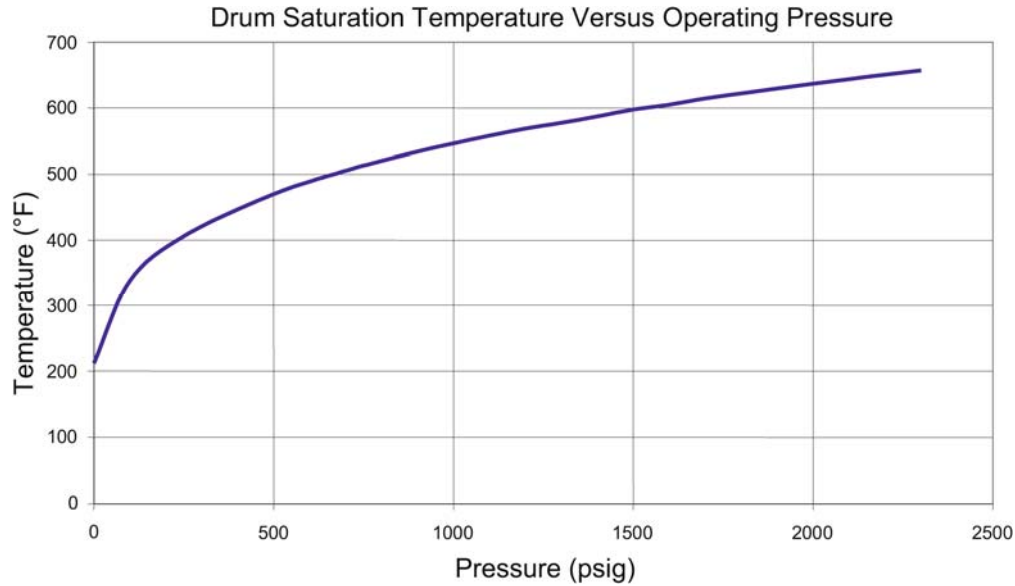
During a 1.5X cold hydro test (see Table 5-3), critical crack depths for a lower bound fracture toughness of 45.8 ksi $\sqrt{\text{inch}}$ (50 MPa $\sqrt{\text{m}}$) can be as low as 0.179 inch (4.54 mm) (3.7% of wall) for a part-through-wall crack. For the best-case scenario where fracture toughness at room temperature approaches 100 ksi $\sqrt{\text{inch}}$ (109 MPa $\sqrt{\text{m}}$), the minimum critical crack depth predicted was 0.851 inch (21.62 mm) (17% of wall). These small predicted critical crack depths indicate that the 1.5X cold hydro test is clearly the most significant threat to brittle fracture of the drum.

Larger critical crack sizes can be justified using an elastic-plastic fracture mechanics (EPFM) approach to take credit for ductile deformation at operating temperatures.

5.4 Critical Crack Sizes using EPFM

The preceding LFM critical crack size results provide a conservative estimate of critical size because they do not account for plastic deformation near the crack tip, which can be expected during normal operation. The following elastic-plastic fracture mechanics (EPFM) calculations illustrate the conservatism in the application of LFM for situations where higher ductility can be expected for materials such as carbon and low alloy steels operating at higher temperatures. Expected drum temperatures during normal operation corresponding to steam saturation

temperatures at pressure are shown in Figure 5-10. For a pressure of 500 psig (34.48 bars) which corresponds to less than 25% of full operating pressure and therefore a stress level less than 25% of the maximum stress, drum temperature is expected to be well above 400°F (204.44 °C). Significant ductility and upper-shelf fracture toughness behavior can be expected at this temperature.



$$^{\circ}\text{C} = (^{\circ}\text{F} - 32) \times 5/9$$

$$1 \text{ psi} = 6.89 \text{ kPa}$$

Figure 5-10
Drum Saturation Temperature Versus Operating Pressure

Analogous to the LFM crack-tip stress intensity factor (K_I), EPFM requires the computation of a crack-tip parameter called the J-integral (J_I), which characterizes the elastic-plastic stress-strain field in the vicinity of the crack tip. The onset of crack extension (tearing) is predicted when J_I exceeds the material ductile fracture toughness, J_{Ic} , as shown in Figure 5-11. Because of material ductility, stable crack extension can be expected beyond this point; that is, when J_I exceeds J_{Ic} . Unstable crack extension finally occurs when the material tearing resistance, known as the tearing modulus (T_{mat}) is exceeded, as illustrated in Figure 5-12. The applied tearing modulus (T) can be computed from the applied J_I versus crack size (a) relationship at a given stress level using the relationship:

$$T = \left(\frac{dJ}{da} \right) \times \frac{E}{\sigma_o^2} \tag{Eq. 5-2}$$

where E is the material modulus of elasticity and σ_o is the yield stress.

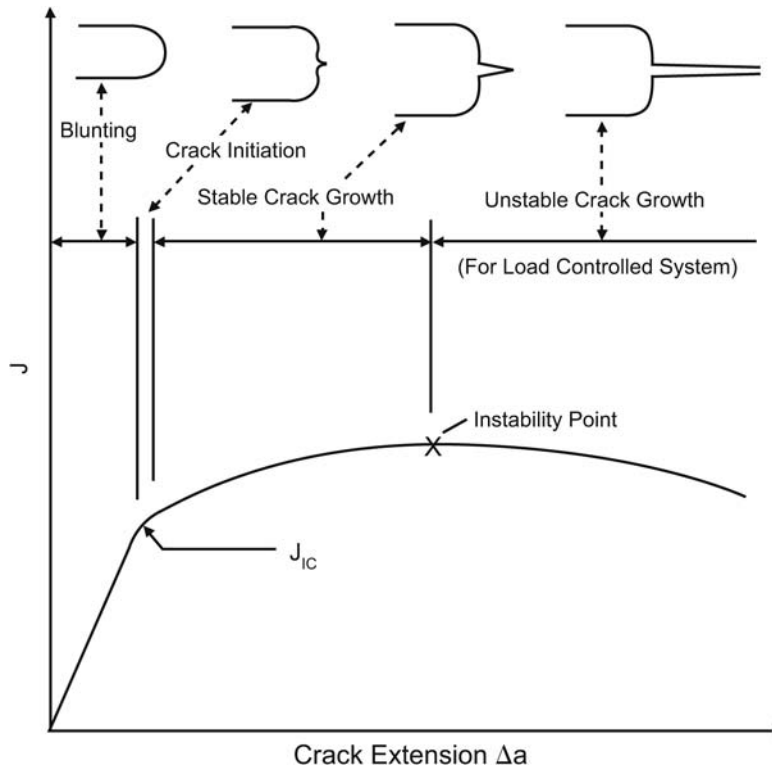


Figure 5-11
Typical Crack Growth Behavior of Ductile Materials

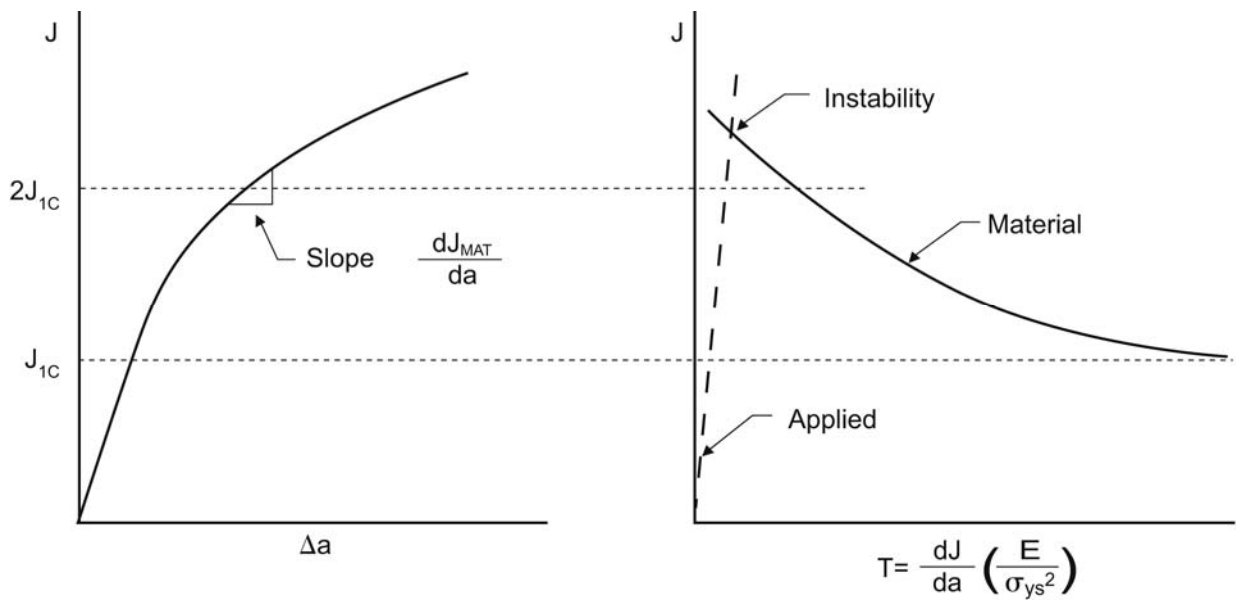


Figure 5-12
Tearing Modulus Concept for Stable Crack Growth

5.4.1 Crack Model

The same through-wall axial crack in a pressurized cylinder model shown in Figure 5-5 was selected to compare EPFM results with the LEFM results. The equivalent EPFM formulation for this model was obtained from a 1991 EPRI study [5-4]. The J-integral solution from this study is given as:

$$J = (8c\sigma_f^2 / \pi E) \times \ln[\sec(M\pi\sigma / 2\sigma_f)] \quad \text{Eq. 5-3}$$

where,

$$M = [1 + 1.2987\lambda^2 - 0.026905\lambda^4 + 5.3549 \times 10^{-4} \lambda^6]^{0.5}$$

$$\lambda = c / \sqrt{Rt}$$

$$\sigma = pR/t$$

p is internal pressure.

R and t are pipe mean radius and wall thickness.

c is crack half-length.

σ_f is flow stress usually defined as the average of yield and ultimate strengths.

J-resistance data from the EPRI study [5-4] is presented in the formula.

$$J = C_o + C_1(\Delta a)^n \quad \text{Eq. 5-4}$$

with the following data sets representing three different categories for a range of carbon steel base materials and welds:

Table 5-4
Different Categories for a Range of Carbon Steel Base Materials and Welds

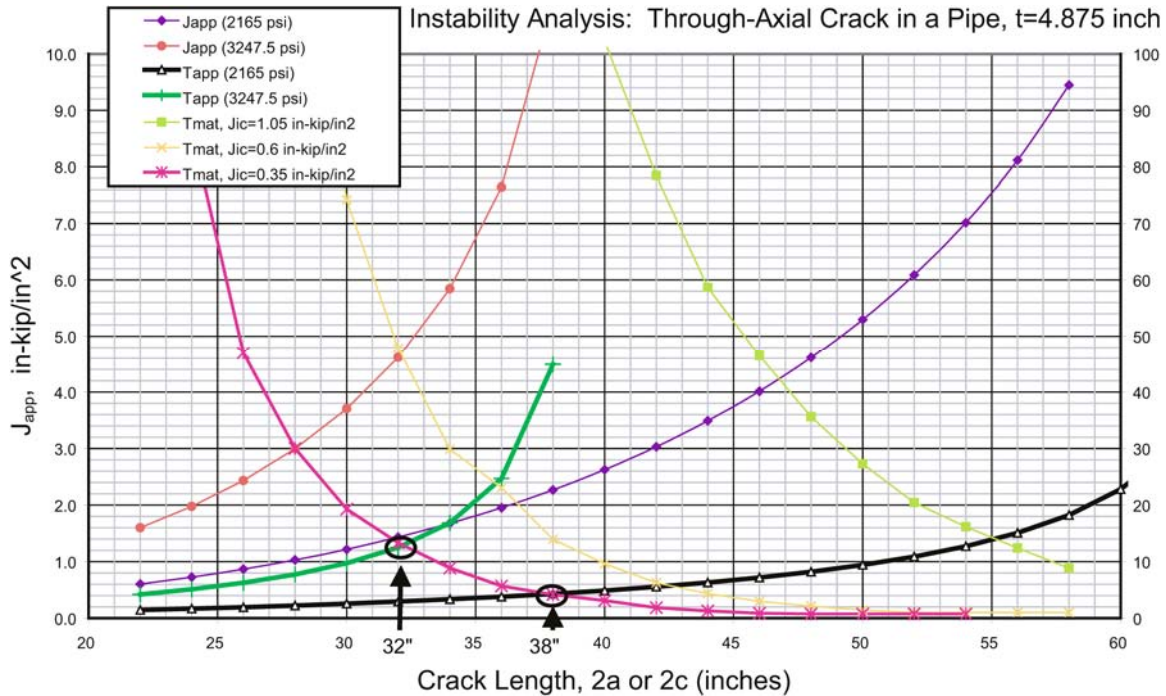
| Material | Temp. °F | J _i (in-lb/in ²) | C _o (in-lb/in ²) | C ₁ (in-lb/in ²) | n |
|----------|----------|---|---|---|-------|
| CS-1 | 550 | 350 (61.3 N/mm) | 0.0 | 1808 (317 N/mm) | 0.277 |
| CS-2 | 550 | 600 (105 N/mm) | 0.0 | 2563 (449 N/mm) | 0.274 |
| CS-1 | 550 | 1050 (184 N/mm) | 0.0 | 5400 (946 N/mm) | 0.344 |

$$^{\circ}\text{C} = (^{\circ}\text{F} - 32) \times 5/9$$

A material yield strength (at 550°F [287.77°C]) of 27.1 ksi (186.85 MPa), tensile strength of 60 ksi (413.69 MPa) and elastic modulus of 26×10^6 psi (179×10^3 MPa) were used in the calculations.

Applied J-integral (J_{app}), applied tearing modulus (T_{app}), and material tearing resistance (T_{mat}) versus crack size results are shown in Figure 5-13 for a normal operating pressure of 2165 psi (14.92 MPa) and 1.5x this pressure (3247.5 psi [22.39 MPa]). For the lowest J-integral fracture toughness of 350 in-lb/in² (61.3 N/mm), which equates to an equivalent plain strain fracture toughness of 100 ksi√inch (109 MPa√m), a through-wall critical crack length of 38 inches (96.52 cm) was predicted for an operating pressure of 2165 psi (14.93 MPa). This crack size is 2.4 times the predicted LEFM critical crack size of 15.8 inches (40.13 cm) shown in Table 5-2.

For the 1.5X hydro, a critical crack length of 32 inches (81.28 cm) was predicted using EPFM, compared with 9.352 inches (23.75 cm) using LEFM (see Table 5-3).



1 in. = 25.4 mm
1 kip/in² = 6.9 MPa

Figure 5-13
Applied J-integral (J_{app}), Applied Tearing Modulus (T_{app}) and Material Tearing Resistance (T_{mat}) Versus Crack Size for a Through-Wall Axial Crack in a Pipe

These results indicate that at least a factor of two on critical size can be realized using EPFM compared with LEFM for all normal operating scenarios where a reasonable amount of material ductility can be expected, with the exception of a cold hydrotest where brittle failure can occur.

Two significant brittle fractures of steam drums that occurred during initial hydrostatic testing are known. The first was in May 1966 at the Cockenzie Power Station of the Scotland Electricity Power Board [5-6]. The intended service pressure of the drum was 2775 psig (191.38 bars), and the failure occurred at a pressure of 3980 psig (274.48 bars) on the way to a final pressure of 4163 psig (287.11 bars). The drum was fabricated from quenched and tempered 5-9/16 inch (14.13 cm) thick Ducol W30 plate. The fracture origin was located in the bore of the drum at the toe of a downcomer thermal sleeve. Reportedly, the crack developed during the post-weld heat treatment cycle, likely a so-called stress-relief crack.

The other failure occurred at the Roxboro plant of Carolina Power and Light in 1971 [5-7]. As with the Cockenzie drum, the crack initiation site was a downcomer nozzle of stick-through design into which a water drainage slot had been flame cut on the stick-through end following final post-weld heat treatment. The untempered martensite from the flame cut would be very

brittle and capable of crack initiation. Other exacerbating factors included a high ductile-to-brittle transition temperature associated with exceptionally high normalizing temperatures used to form the plate in which there was no subsequent renormalization to refine the grain size.

These two examples are provided as evidence that avoidance of brittle fracture of the steam drum during the hydrostatic tests is not guaranteed and that serious consideration should be given to

- Materials of construction
- Fabrication practices
- Operational and maintenance history
- Hydrostatic test pressure
- Test temperature in establishing the hydro test practice for a given drum

In general, the repetition of a 1.5X hydro should be avoided for old units, and a hydro temperature higher than 70°F (21.11°C) should be evaluated based on the foregoing considerations.

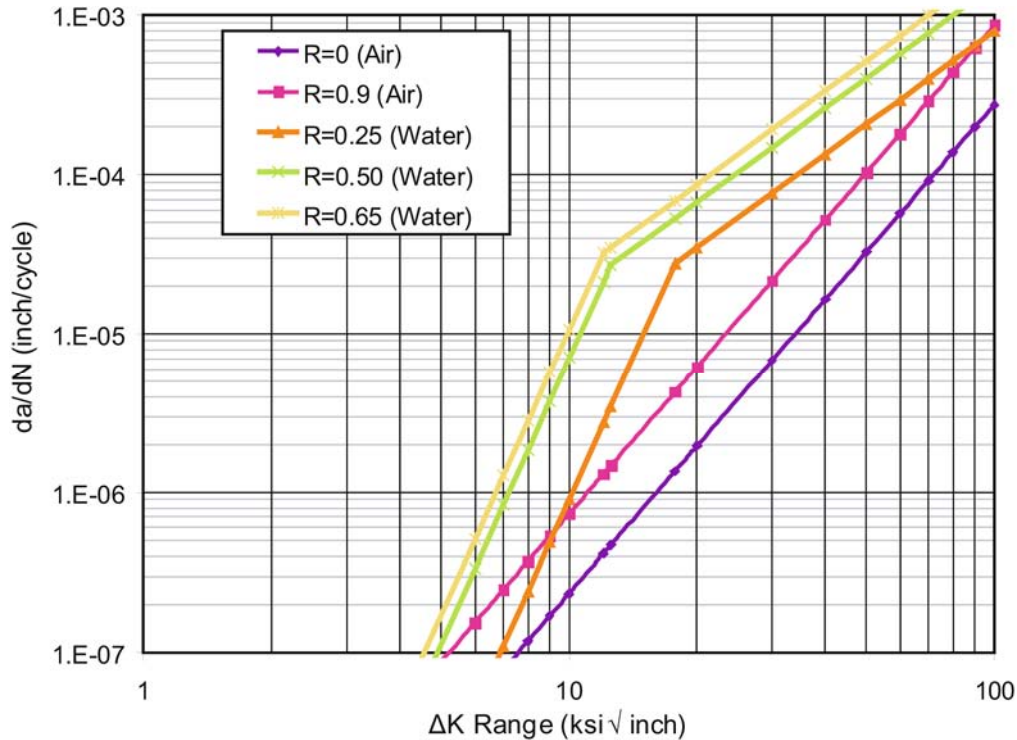
In summary, these two significant brittle fractures of steam drums during hydrotesting [5-1] confirm the preceding fracture mechanics critical crack size results which show that (a) failure is not expected during normal operation; and (b) brittle failure can occur during cold hydrostatic testing and is the most significant threat to drum integrity.

5.5 Crack Growth

Crack propagation calculations were performed to estimate the amount of crack propagation that can be expected during typical unit startups and shutdowns. The crack growth mechanism for water-touched components in the boiler has been documented to be corrosion fatigue [5-4]; that is, a synergy between cyclic stress and environment.

5.5.1 Corrosion Fatigue Crack Growth Rate

The material crack growth data in Section XI of the ASME Code for carbon and low-alloy ferritic steels in reactor water environment [5-5], as shown in Figure 5-14, was used as a starting point to simulate corrosion fatigue crack growth. EPRI data on corrosion fatigue crack growth rates in oxygenated water boiler environments [5-3] have indicated that corrosion fatigue crack growth rates under the most detrimental conditions may be in the range of 2 to 5 times greater than the ASME Section XI rates. Therefore, to conservatively bound expected crack propagation rates, crack growth predictions using the ASME Section XI data were multiplied by a factor of five.



1 in. = 25.4 mm
 1 ksi • in = 1.099 MPa•m

Figure 5-14
Fatigue Crack Growth Data from ASME Section XI for Carbon and Low-Alloy Ferritic Steels

5.5.2 Crack Growth Results

Crack growth results without and with corrosion fatigue factors of 5 on growth are shown in Figure 5-15 for a 10:1 (length:depth) part-through-wall crack having an initial depth of 0.08 inch (2.03 mm) at the downcomer ID (Location 1) and inlet nozzle ID (Location 3). The minimum predicted life with a corrosion fatigue factor of five was 1700 and 2400 cycles for Locations 1 and 3, respectively, for propagation through the wall of the drum. Additional cycles would be required to propagate these through-wall cracks to failure.

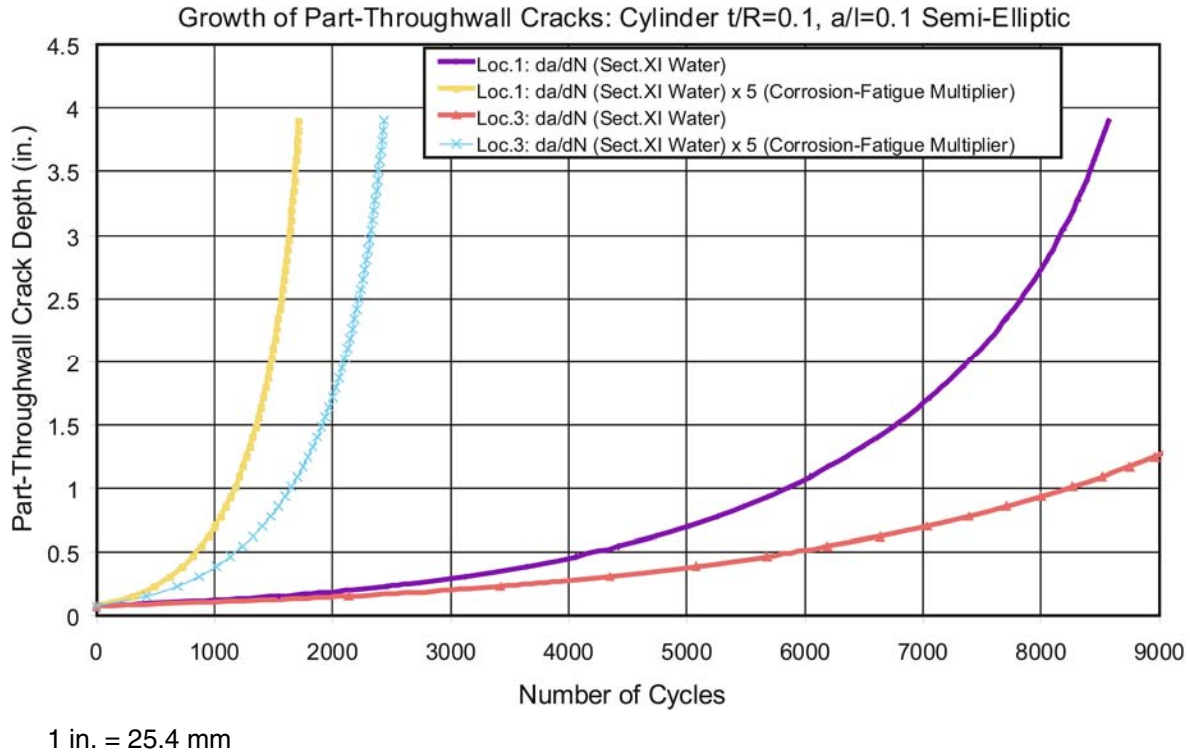


Figure 5-15
Fatigue Crack Growth Data from ASME Section XI for Carbon and Low-Alloy Ferritic Steels

5.6 Discussion of Fracture Mechanics Analysis

- The most significant threat to drum integrity is a 1.5X cold hydrostatic test when brittle failure could occur for through-wall critical crack sizes as small as 2.5 inches (6.35 cm). During normal operation, large through-wall crack sizes (> 30 inches [> 76.2 cm]) can be tolerated before failure occurs (a leak-before-break scenario).
- Fatigue crack growth data in water for carbon and low-alloy steels from ASME Sect. XI underpredicts expected growth rates; a corrosion fatigue multiplier of 2 to 5 has been suggested based on other EPRI studies.
- A minimum of 1700 normal start/stop cycles is required for through-wall propagation of a part-through semi-elliptical crack (with a corrosion fatigue multiplier of 5). Additional cycles would be required to grow a through-wall (leaking) crack to failure.
- Downcomer nozzle cracks are more life-limiting than the inlet nozzle cracks because of the effectiveness of the thermal sleeve.
- Remaining life assessment studies can provide utilities with a cost-effective alternative to immediate repair or replacement of aging drums with known or suspected cracking.

5.7 References

- 5-1. *Thermal Fatigue of Fossil Boiler Drum Nozzles*. EPRI, Palo Alto, CA: 2005. 1008070.
- 5-2. *pc-CRACK* for Windows, Version 3.1-98348, Fracture Mechanics Software Program, Structural Integrity Associates. 1998.
- 5-3. *Corrosion Fatigue Boiler Tube Failures in Waterwalls and Economizers, Volume 2: Laboratory Corrosion Studies*. Research Project 1890-05, EPRI, Palo Alto, CA: July 1992. TR-10045.
- 5-4. A. Zahoor. *Ductile Fracture Handbook*. Research Project 1757-69, EPRI, Palo Alto, CA: January 1991.
- 5-5. American Society of Mechanical Engineers, Boiler and Pressure Vessel Code, Section XI, "Rules for Inservice Inspection of Nuclear Power Plant Components," 1998, New York.
- 5-6. www.forgingexpert.com, website of Edward G. Nisbett, P.E., 2005.
- 5-7. Personal communication between Blaine W. Roberts and Dr. David N. French, 2005.

6

SUMMARY, CONCLUSIONS, AND FUTURE PLANS

6.1 Summary and Conclusions

The current project follows two earlier EPRI projects associated with cracking in fossil boiler steam drums [6-1, 6-2]. The first project resulted in the following conclusions:

- Utilities had experienced some drum cracking problems, but the cracking was seldom judged to be severe.
- There was no uniform practice by the utilities in dealing with cracking, and the approaches ranged from “do nothing” to removal by grinding or removal followed by weld repair.
- The time to initial cracking appeared to be about 30 years.
- Efforts for remediation of cracking met limited success, with recurrence of cracking reported in 24 to 48 months.
- Detailed stress and fracture mechanics analysis on one unit having drum cracks provided two conclusions: 1) the cracks in the large downcomers were thermally driven and would arrest at a nonthreatening depth if left undisturbed, whereas they would reinitiate if removed by grinding; and 2) the cracked drum satisfied a leak-before-break criterion; thus, a catastrophic failure was judged to be highly unlikely.

The second project was undertaken to develop a more definitive understanding of the role of unit operation in producing thermal fatigue cracking in drum nozzles. Using a simplified stress analysis, the following fatigue damage rankings were established for various operational events in relation to a normal startup/shutdown cycle for a unit with an economizer:

- Topping off a hot empty drum – 8.4 cycles
- Startup/shutdown of units with no economizer – 2.1 cycles
- Bypassing four high-pressure feedwater heaters – 1.8 cycles
- Topping off a hot half-empty drum – 1.1 cycles
- Startup/shutdown of units with economizers (reference case) – 1.0 cycles
- Bypassing three high-pressure feedwater heaters – 0.81 cycles
- Turndown 100% to 25% – 0.37 cycles
- Turndown 100% to 50% – 0.05 cycles

In the second project, in the absence of close riser tube spacing (that is, thin ligaments), the downcomer nozzles were identified as the most critical drum components for units operating with controlled circulation (pump assisted) in the waterwall circuits. The major additional work completed during the second project was related to fracture toughness issues that primarily impact steam drums during hydrostatic testing. In broad terms, drum steels are made either to fine grain (FG) or coarse grain (CG) melting practice. The FG steels have superior fracture toughness and are not likely to encounter brittle fracture during hydrostatic testing at room temperature. Work reported in the second project characterized the scatterband of fracture toughness properties for FG and CG melting practices and the associated critical crack sizes of concern during hydrostatic testing.

The second project left many questions unanswered, mainly due to the lack of sophistication in the areas of stress and fracture mechanics analysis, and provided the basis for this third project. The focus of this third project was to perform a detailed finite element stress analysis and associated fatigue life and fracture mechanics assessment on a steam drum in a Combustion Engineering 275 MW controlled circulation unit that began commercial operation in 1959. The three critical locations identified in the analysis were the ID of the downcomer nozzle, the ID of the feedwater inlet nozzle, and the OD fillet junction of the feedwater inlet nozzle to the drum shell. The major results were discussed in the concluding portions of Sections 3–5, and the relevant conclusions are summarized here.

6.1.1 Finite Element Stress Analysis

- For normal startup/shutdowns, the stress intensity range is dominated by pressure.
- The thermal stress contribution is minimal when the drum is at full pressure. The position of the maximum thermal stresses is 90° out of phase with the pressure stresses for the downcomer nozzle ID, but in phase with pressure stresses during heatup for the inlet nozzle ID and OD locations.
- The most significant thermal events at full pressure are the loss (bypass) of the string of three high-pressure feedwater heaters or topping off a partially full drum shortly after shutdown, which would result in a thermal stress intensity that would be additive to that due to pressure.
- The project was initiated on the premise that cracking of the large drum nozzles was mainly the result of thermal fatigue. Based on the magnitude of the thermal stresses from the FE stress analysis, these results appear to contradict that premise.
- The top-to-bottom temperature differentials are small for the situations analyzed, and there is no expectation that drum “humping” is an issue of concern.

6.1.2 Fatigue Analysis

Fatigue lives were estimated for the three critical components (locations) for three operational modes: (a) startup/shutdown; (b) bypassing a string of feedwater heaters; and (c) topping off a partially full drum shortly following a unit trip. The following conclusions were reached:

- All three fatigue analyses showed a consistent ranking in which the downcomer ID was most critical, the feedwater inlet ID was second, and the feedwater inlet OD was least critical.
- The effectiveness of the feedwater nozzle thermal sleeve is validated by the substantially longer fatigue life estimates for that component.
- The life estimates for a normal startup/shutdown based on the design fatigue curve were unrealistic in terms of the cracking typically observed after 30 or more years of service—6240 cycles for downcomer ID, 6689 cycles for feedwater inlet OD, and 17,061 for feedwater inlet OD.
- For the waterside locations, application of a pending curve to account for corrosion fatigue provided life estimates for startup/shutdown that were reasonably consistent with experience—395 cycles for downcomer ID and 426 cycles for feedwater inlet ID.
- No environmental adjustment is appropriate for the feedwater inlet OD location, which is in an air environment, and the 17,061 cycles may be reasonable since cracking has virtually never been reported to initiate at drum OD locations.
- For bypassing a string of high-pressure feedwater heaters, life estimates based on the design fatigue curve appeared unrealistically large for the waterside locations—1843 cycles for the downcomer ID and 4504 cycles for the feedwater inlet ID.
- For bypassing a string of high-pressure feedwater heaters, life estimates based on application of a pending corrosion fatigue curve appeared reasonable—111 cycles for the downcomer ID and 273 cycles for the feedwater inlet ID.
- For topping off the drum level, life estimates based on the design fatigue curve appeared reasonable for the waterside locations—522 cycles for the downcomer ID and 7708 cycles for the feedwater inlet ID.
- For topping off the drum level, life estimates based on application of a pending corrosion fatigue curve appeared unduly short for the downcomer ID—38 cycles, whereas the estimate for the FE inlet ID appear reasonable—494 cycles.
- Additional conservatism was introduced into the life estimates by a simplified method to account for the mean stress effect.
- Considering the number of cycles for the startup/shutdown event for the downcomer ID location as unity, bypassing the feedwater heaters is equivalent to 3.6 times more cycles, and topping off the drum is equivalent to 10.4 times more cycles. Thus, prudence should be exercised in operation to minimize the degree of downshock associated with these events.

- While turndown was not analyzed in terms of thermal fatigue in the current project, the previous work concluded that the “100% to 25% to 100%” load swing simulation was equivalent to 0.37 startup/shutdown cycles. Therefore, it appears that the worst operating scenarios were covered in the current project.

Regardless of the sophistication of the stress analysis, the estimated lives are critically dependent on corrosion fatigue, and life reduction factors on the order of 5 to 20 appear to be necessary to explain actual service experience in various components in fossil boilers. The pending corrosion fatigue curve developed by the ASME Subgroup on Strength is a step in the right direction and predicts factors from 14 to 16.7 in regions of appreciable stress concentration ($SCF > 2.3$). However, additional work is needed to valid the approach and to “hone in” on the factor appropriate to particular operating practices.

6.1.3 Fracture Mechanics Analysis

The fracture mechanics analyses examined both critical crack sizes and crack growth rates. The drum vintage (mid-1950s) led to the expectation that the material was produced to coarse grain melting practices, which provides poor fracture toughness. The following conclusions were reached:

- The most significant threat to drum integrity is a 1.5X cold hydrostatic test when brittle failure could occur for through-wall critical crack sizes as small as 2.5 inches (6.35 cm). During normal operation when the temperature is above 212°F (100°C), large through-wall crack sizes (>30 inches [> 76.20 mm]) can be tolerated before failure occurs (a leak-before-break scenario).
- Fatigue crack growth data in water for carbon and low-alloy steels from ASME Section XI underpredict expected growth rates. A corrosion fatigue multiplier of 2 to 5 has been suggested, based on other EPRI studies, as more consistent with experience.
- A minimum of 1700 normal start/stop cycles is required for through-wall propagation of a part-through semi-elliptical crack (with a corrosion fatigue multiplier of 5). Additional cycles would be required to grow a through-wall (leaking) crack to failure.
- Downcomer nozzle cracks are more life-limiting than the feedwater inlet nozzle cracks because of the effectiveness of the thermal sleeve.
- Remaining life assessment studies can provide utilities with a cost-effective alternative to immediate repair or replacement of aging drums with known or suspected cracking.

6.2 Future Plans

At the end of 2003, EPRI subscribers endorsed the detailed analysis of a limited number of steam drums. The project reported here was performed in 2004 on a Combustion Engineering steam drum. For 2005, a parallel detailed analysis has already begun for a Babcock & Wilcox drum.

Several possible projects are envisioned for 2006 and beyond including the following:

- Review/compilation of fracture toughness properties with statistical distributions that could be used in probabilistic assessments
- Review/compilation of fatigue initiation and fatigue crack growth rate data as affected by environment; for example, corrosion fatigue
 - Big unknowns in life estimation are:
 - The reduction in fatigue life due to corrosion fatigue, the effect on crack growth rate, and “ordering effects” to answer questions such as whether periods of “bad water chemistry” followed by “good water chemistry” can dramatically lower crack growth rates
 - The role of base metal composition, especially residual element content, on crack growth rates
- Focused project to use finite element analysis and fracture mechanics modeling for a variety of ligament configurations with development of software where utilities could input their ligament geometry and run scenarios on initiation, growth rate, and critical crack size along the lines of the EPRI BLESS, SAFER, and RRING codes
- Real-time monitoring of a “benchmark unit” for fatigue initiation and crack growth using the EPRI Creep-Fatigue Pro approach
- Improvements in the application of NDE to locate and size cracks, especially in the ligament area, mainly using OD probes
- Finite element analysis and fracture mechanics analysis of a mud drum
- Incorporation of a “drum assessment methodology” into user-friendly Windows software

6.3 References

- 6-1. *Thermal Fatigue Cracking of Boiler Drums*. EPRI, Palo Alto, CA: 2002. 1004614.
- 6-2. *Thermal Fatigue of Fossil Boiler Drum Nozzles*. EPRI, Palo Alto, CA: 2005. 1008070.

Export Control Restrictions

Access to and use of EPRI Intellectual Property is granted with the specific understanding and requirement that responsibility for ensuring full compliance with all applicable U.S. and foreign export laws and regulations is being undertaken by you and your company. This includes an obligation to ensure that any individual receiving access hereunder who is not a U.S. citizen or permanent U.S. resident is permitted access under applicable U.S. and foreign export laws and regulations. In the event you are uncertain whether you or your company may lawfully obtain access to this EPRI Intellectual Property, you acknowledge that it is your obligation to consult with your company's legal counsel to determine whether this access is lawful. Although EPRI may make available on a case-by-case basis an informal assessment of the applicable U.S. export classification for specific EPRI Intellectual Property, you and your company acknowledge that this assessment is solely for informational purposes and not for reliance purposes. You and your company acknowledge that it is still the obligation of you and your company to make your own assessment of the applicable U.S. export classification and ensure compliance accordingly. You and your company understand and acknowledge your obligations to make a prompt report to EPRI and the appropriate authorities regarding any access to or use of EPRI Intellectual Property hereunder that may be in violation of applicable U.S. or foreign export laws or regulations.

© 2005 Electric Power Research Institute (EPRI), Inc. All rights reserved.
Electric Power Research Institute and EPRI are registered service marks of the Electric Power Research Institute, Inc.

 Printed on recycled paper in the United States of America

The Electric Power Research Institute (EPRI)

The Electric Power Research Institute (EPRI), with major locations in Palo Alto, California, and Charlotte, North Carolina, was established in 1973 as an independent, nonprofit center for public interest energy and environmental research. EPRI brings together members, participants, the Institute's scientists and engineers, and other leading experts to work collaboratively on solutions to the challenges of electric power. These solutions span nearly every area of electricity generation, delivery, and use, including health, safety, and environment. EPRI's members represent over 90% of the electricity generated in the United States. International participation represents nearly 15% of EPRI's total research, development, and demonstration program.

Together...Shaping the Future of Electricity

Program:

Fossil Materials and Repair

1011916

ELECTRIC POWER RESEARCH INSTITUTE

3420 Hillview Avenue, Palo Alto, California 94304-1395 • PO Box 10412, Palo Alto, California 94303-0813 USA
800.313.3774 • 650.855.2121 • askepri@epri.com • www.epri.com